Review Article

Journal of Molecular Recognition

Received: 1 October 2010, Revised: 8 November 2010, Accepted: 9 November 2010, Published online in Wiley Online Library: 2011

(wileyonlinelibrary.com) DOI:10.1002/jmr.1117

A survey of the 2006–2009 quartz crystal microbalance biosensor literature

Bernd Becker[a] and Matthew A. Cooper[a]*

Since the publication of the original review of piezoelectric acoustic sensors in this series there has been a consistent, gradual expansion in the number of published papers using 'quartz crystal microbalances' (QCM). Between 2001 and 2009, the number of QCM publications per annum has increased from 49 to 273, with a two-fold increase in papers per annum between 2004 and 2008. Within the field, comparing the time covered by the current to the previous review, there are trends towards increasing use of QCM in the study of protein adsorption to surfaces (93% increase), homeostasis (67% increase), protein–protein interactions (40% increase) and carbohydrates (43% increase). New commercial systems have been released that are driving the uptake of the technology for characterization of binding specificities, affinities, kinetics and conformational changes associated with a molecular recognition event. This paper highlights theoretical and practical aspects of the principles that underpin acoustic analysis, then reviews exemplary papers in key application areas involving small molecular weight ligands, carbohydrates, proteins, nucleic acids, viruses, bacteria, cells and membrane interfaces. Copyright © 2011 John Wiley & Sons, Ltd.

Keywords: quartz crystal microbalance; label-free; biosensor; clinical analysis; membrane; self-assembled monolayer; protein adsorption; cell adhesion

INTRODUCTION

Acoustic biosensors have been employed in the label-free detection of a very broad range of analytes; from interfacial chemistries and lipid membranes through to small molecules and whole cells (Cooper and Singleton, 2007). They provide a unique method for observing *in situ* events involving 'soft matter', in which changes in contact mechanics, interfacial dynamics, surface roughness, viscoelasticity, density and mass can be monitored in real time (Thompson and Hayward, 1997; Janshoff *et al*., 2000; Cooper, 2003; Cote *et al*., 2003; Marx, 2003; Cooper, 2006b; Hook and Kasemo, 2006; Steinem and Janshoff, 2006; Hunter, 2009). In practice, most analytical platforms routinely used today use optics, with only a few of the more novel transducer modalities having transitioned from academic instrument prototypes to robust commercial platforms (Myszka and Rich, 2000; Cooper, 2002; Cooper, 2006a; Rich and Myszka, 2006; Rich and Myszka, 2007). However, over the last 5–10 years, there has been an increased recognition of the versatility and broad applicability of acoustic biosensors for the analysis of molecular recognition and associated phenomena. This level of information content goes beyond that produced by many more widely adopted optical label-free techniques that are used to analyse molecular changes occurring in biochemical processes. Acoustic sensor technology is thus highly interdisciplinary and has encompassed advances and improvements from electrical engineers through to cell biologists. This review seeks to impart an awareness of the theory and biological relevance of acoustic physics (in particular for BAW, TSM or QCM sensors), with a focus on the application areas of greatest relevance to biological and biochemical research. We examine 857 published applications of QCM to the analysis of chemical and biochemical systems over the period 2006–2009 and touch on the most recent developments that push the scope and depth of the field. Not reviewed are 83 papers published that specifically exploit electrochemical QCM, or 'EQCM', in which the QCM device is used as the working electrode of an electrochemical cell to study electron transfer processes in real time. For further information in this area the reader is referred to the excellent book chapter by Marx (Marx, 2006). Similarly, 108 papers that used QCM to characterize materials interfaces or non-biological modification of surfaces, such as polymer film deposition and response, surface wetting processes, and nano-structured surfaces are not reviewed.

Due to the rising popularity and commercial availability of acoustic biosensors QCM is increasingly used as a complimentary technique, for example, to confirm layer formation on surfaces that are then subject to a range of other studies. Although these publications will still be included in this review as far as publication statistics are concerned, they are not individually reviewed.

A detailed introduction to acoustic wave devices, biophysics and the application of QCM technology to liquid phase interactions has been published in the first of this series of reviews (Cooper and Singleton, 2007) and by others (Ferreira *et al*., 2009; Hunter, 2009). Briefly, acoustic transducers became of interest to physicists and chemists when it was demonstrated that there was a linear relationship between mass adsorbed to the surface and the resonant frequency of the crystal in air or a

* *Correspondence to: M. A. Cooper, Institute for Molecular Bioscience, University of Queensland, 306 Carmody Rd., St Lucia, Qld 4072, Australia. E-mail: m.cooper@uq.edu.au*

a *B. Becker, M. A. Cooper*
Institute for Molecular Bioscience, University of Queensland, St Lucia, Queensland, Australia

vacuum (Sauerbrey, 1959). Application to biological samples became possible when suitable oscillator circuits for operation in liquids were developed (Nomura and Okuhara, 1982). These can be combined with specific interfacial chemistries for target immobilization and macro- or micro-fluidic liquid delivery systems that enable controlled contact of a solution of analyte with its receptor.

PUBLICATION TRENDS

The number of research articles and reviews that involve QCM in the analysis of biological systems continues to increase year on year, with near-linear growth from 2003 to 2007 (Figure 1).

This trend has been driven by an increasing number of commercially available systems (Table 1) and a growing recognition of the versatility and analytical capability of acoustic biosensors. In addition, system sensitivity continues to improve and a number of suppliers now offer multi-channel systems that enable referencing against control surfaces or receptors and direct comparison of binding specificity.

Analysis of the application area of studies using the technique reveals that the vast majority of scientists use QCM to analyse the interaction of proteins with surfaces (Figure 2A). Binding or physisorbtion of proteins to surfaces was also the fastest growing area (93% increase), although there was significant growth in the use of QCM in the analysis of homeostasis (67%), protein–protein (40%), carbohydrates (43%) and interactions with whole cells and membranes (40 and 22%, respectively; (Figure 2B). For the first time, the number of fundamental studies on interactions of acoutic waves on biological materials and synthetic polymers decreased, whilst standard antigen-antibody immunoassays were flat (Figure 2B). There was a notable increase (albeit from a very low base) in papers on homeostasis and novel implementation of modified acoustic wave devices and QCM design.

BACTERIA

In systems using surface plasmon resonance, the penetration depth of the sensing evanescent wave is in the order of hundreds of nanometres, as defined by the interrogating light wavelength and metal film used to generate plasmons. As described in the introduction, the penetration depth of a thickness shear mode acoustic wave can be varied as a function of the fundamental frequency of resonance and overtone order sampled. This means that many researchers have found the QCM a versatile tool for both sensitive detection of micron sized bacteria, and characterization of bacterial adhesion mechanisms and the formation and morphology of microbial biofilms.

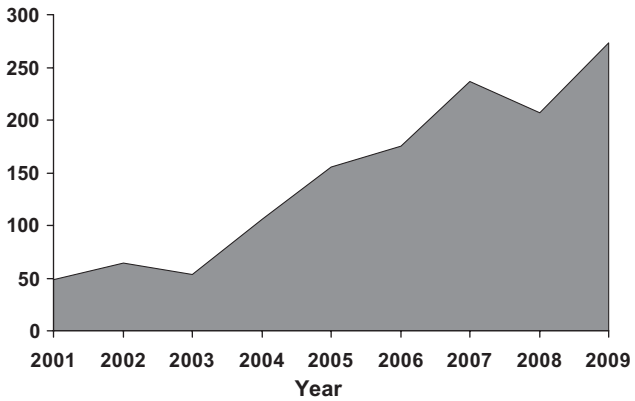

Figure 1. Number of publications per year referenced by a combined search of US National Library of Medicine PubMed and ISI Thompson Web of Science® using the terms 'quartz crystal microbalance' or 'quartz crystal resonant sensor'. Results exclude those publications relating to electrochemical quartz crystal measurement.

Detection and quantification of bacteria

Salmonella typhimurium was detected by physically adsorbed affinity-selected filamentous phage (Olsen *et al.*, 2006). Approx 3×10^{10} phage particles/cm^2 could be irreversibly adsorbed after 1 h at room temperature to prepare working biosensors. Sensors possessed a rapid response time of $<$180 s, had a low-detection limit of 10^2 cells/ml, with a linear concentration-response range of 10^2–10^7 cells/ml. *Escherichia coli* W1485 was detected using a functional mannose self-assembled monolayer in combination with the lectin concanavalin A (Con A) which binds to the polysaccharide envelope of the bacteria (Shen *et al.*, 2007c); the linear range was from 7.5×10^2 to 7.5×10^7 cells/mL. *E. coli* O157:H7 was detected using specific antibodies (Wang *et al.*, 2008b) and a DNA sensor with nanoparticle amplification was used to detect *E. coli* O157:H7 down to concentrations as low as 10^{-12} M of synthetic oligonucleotide and 2.7×10^2 cfu/mL of bacteria (Mao *et al.*, 2006). The effect of the spacer on hybridization was also investigated for *E. coli* O157:H7 DNA detection (Wu *et al.*, 2007). Chen *et al.* utilized streptavidin for the detection of *E. coli* and determined the affinity of the cell-displayed Strep-tag II peptide (Chen *et al.*, 2009a) and Adányi *et al.* used anti-*E. coli* IgG for the detection of *E. coli* in food (Adányi *et al.*, 2006). The influence of contaminants on the detection of *Cryptosporidium parvum* was studied (Poitras *et al.*, 2009) and a study reported the effect of pH, conductivity and viscosity of the medium in broth and milk on the detection of *E. coli* in an attempt to develop a sensor for the continuous long-term detection of microbial populations during fermentation processes (Han *et al.*, 2009). Alava *et al.* developed a sensor for the parallel detection of two different types of bacteria, one virus and a protein using immobilized antibodies. The minimal detection thresholds for *E. coli* MRE 162, *Bacillus atrophaeus*, *Cydia pomonella granulosis* virus (CpGV) and ovalbumin were 2.4×10^7 cfu/mL, 1.4×10^6 spores/mL, 1.1×10^8 granules/mL and 1 μg/mL.

Improvements of immobilization methods and detection

A number of publications dealt with the improvement of immobilization techniques using various grafted surfaces and different bacteria. The surface chemistry for antibody immobilization for a *B. anthracis* binding assay was investigated (Hao *et al.*, 2009). Mixed self-assembled monolayers with a combination of 11-mercaptoundecanoic acid (11-MUA) and 6-mercaptohexan-1-ol (6-MHO) were found to give the best results. *Edwardsiella tarda* was bound to a sensor surface using a novel immobilization method (Hong *et al.*, 2009) that gave higher detection sensitivity and a sensor that was reusable 10 times; oxidized IgG was cross-linked to hydrazide formed on self assembled monolayer (SAM) and the results compared with three conventional methods. A study compared the sensitivity and

Table 1. Commercially available biosensor systems based on the principles of QCM

Manufacturer	Website	Product(s)	No. of channels	Frequency (MHz)
Antech	www.anttech.com.tw	ADS Plus	1	2–16
Attana	www.attana.com	Attana™ A100	1	10
		Attana™ 200	2	10
		Attana™ Cell200	2	10
Initium	www.initium2000.com	Affinix® QN Pro	1–4	27–81
		Affinix® QN μ	1–4	27
		Affinix® Q4	4	27
CH Instruments	www.chinstruments.com	400B		8
	www.qsense.com	Q-Sense E4 Auto	4	1–70
qsense		Q-Sense E4	4	1–70
		Q-Sense E1	1	1–70
Resonant Probes GmbH	www.resonant-probes.de	IQCM	2	10–180
Sierra Sensors	www.sierrasensors.com	QCMA-1	2	10–40 (20 default)
TTP Labtech	www.ttplabtech.com	RAPid	4	16.5

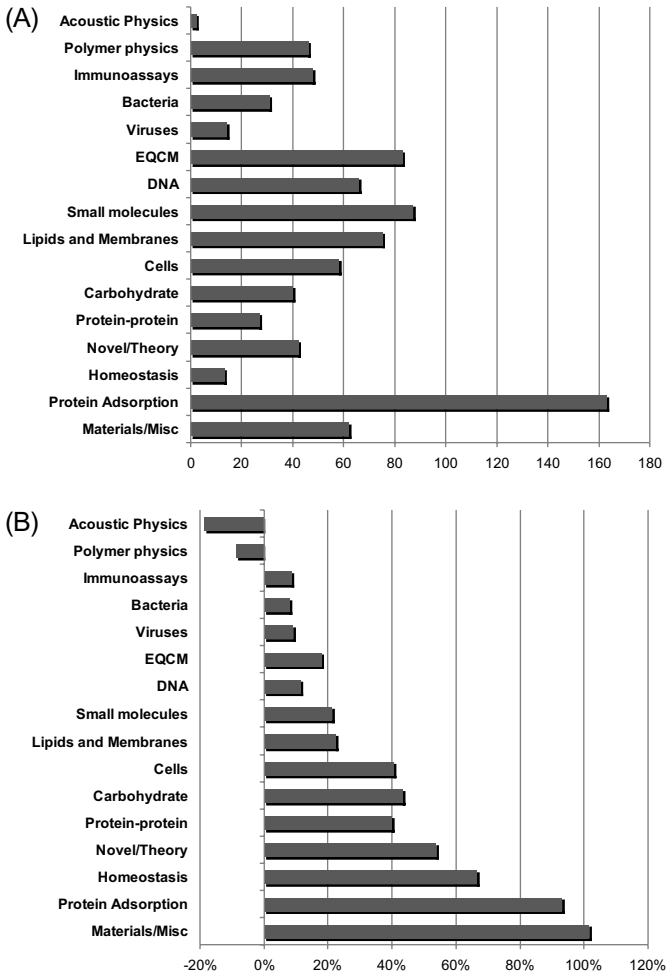

Figure 2. (A) Publications from Figure 1 classified by application area. The majority of applications studied remains the binding or physisorbtion of proteins to surfaces, with 158 papers in this area reported in the period. 'Novel/Theory' refers to a novel implimentation of QCM design in biosensing or a novel analytical method to derive new properties describing a biological 'soft matter' interactions; (B) Growth (or decline) in the number of papers in these application areas published during this review period (2006–2009) compared to the period previously reviewed (2001–2005).

accuracy of measuring saturating or equilibrium response levels against the use of the initial slope (dF/dt) for quantification of bacterial titres. A highly log-log linear response was obtained for detection of *E. coli* O157:H7 over a wide range of cell concentrations from 3×10^5 to 1×10^9 cells/mL (Poitras and Tufenkji, 2009). Measurements conducted over a broad range of bacterial cell concentrations showed that the optimal biosensor response is the initial slope of the dissipation shift as a function of elapsed time (D-slope).

Bacterial deposition on surfaces and biofilm formation

Bacterial adhesion to different types of surfaces was investigated in a number of different papers. This included polymer grafted stainless steel for orthopaedic implants (Ignatova *et al.*, 2006), artificial siderophores (Inomata *et al.*, 2007) and silica surfaces with determination of the deposition kinetics (Long *et al.*, 2009). Surface interactions of *Streptococcus salivarius* mutants, possessing various surface appendages of known lengths were investigated by Olsson *et al.* (2009). The magnitude of frequency and dissipation shifts was found to be influenced by the distance at which the cell body was held from the sensor surface by its surface appendages. The growth of biofilms of *Streptococcus* mutants was monitored (Schofield *et al.*, 2007; Tam *et al.*, 2007) using QCM, as well as *Pseudomonas aeruginosa* where the layer thickness was measured simultaneously using an optical method (Reipa *et al.*, 2006). Another laboratory study looked into the biofilm formation in water treatment systems (Sprung *et al.*, 2009).

HEMOSTASIS

The hemostatic system maintains vascular system integrity, and thrombosis (formation of a clot in a blood vessel) is one of the largest causes of morbidity and mortality in the western world. New clinical and research tools for characterizing the hemostatic system are hence of continued interest. The standard method for assessing surface induced blood coagulation often involves measurement of the soluble thrombin–antithrombin complexes via enzyme immunoassays, or substrates. In hospital laboratories citrated plasma held at 37°C is analysed using automated instrumentation. A platelet membrane substitute (phospholipid) and a factor XII activator is often added to the plasma, then an excess of calcium is added (thereby reversing the effects of citrate), enabling blood to clot. Clotting time can also be measured indirectly via electrical impedance or enzyme action on a peptide substrate; approaches that are suitable for near patient testing (e.g. Roche CoaguCheck and Hemosense INRatio). QCM provides an additional method for the determination of induced blood coagulation, since the fibrin formation can be detected *in situ* and in real time, and blood coagulation results in large changes in observed signal due to the viscosity-density contribution to frequency change.

The conversion of adsorbed fibrinogen to fibrin in the presence of the enzyme thrombin was studied using a number of different techniques. QCM showed that mass loss at the surface was consistent with fibrinopeptide release and the conversion to fibrin also resulted in the adsorbed layer becoming more strongly bound to the surface and more compact (Evans-Nguyen *et al.*, 2006). QCM was also used to study viscoelastic properties and morphology of fibrin as a function of the concentration of antithrombin III (AT) and the anti-coagulant heparin (Jung *et al.*, 2009b) and the binding of fibrinogen to different metal surfaces (Hulander *et al.*, 2009). The conversion of fibrinogen to fibrin was also monitored to evaluate the anticoagulant activity of some proteins, such as gastrodin (Liu *et al.*, 2006c) and a human recombinant endothelial cell-associated protein (Matsusaki *et al.*, 2008). QCM was also used in a study on complement activation by CpG, an oligonucleotide, in a human whole blood (Mangsbo *et al.*, 2009).

Sulfated or sulfonated polymers such as heparin play an important role as anticoagulants and their immobilization on cell surfaces using avidin-expressing binding sites was observed with QCM (Cabric *et al.*, 2008). Different types of sulfonated polymers, including polystyrenes with different sulfonation levels, various sulfonated polyethylene oxides, as well as sulfated chitosan were studied with regards to their antigolant activities by observing the binding to factor XII (FXII) (Chen *et al.*, 2007b) or antithrombin II (Jung *et al.*, 2009a). Platelet conformational changes (Fatisson *et al.*, 2008) and platelet aggregation (Ergezen *et al.*, 2007) were also studied using QCM and the selective sensitivity of this technique for the monitoring of platelet function and inhibition could be demonstrated (Figure 3). The interaction of thrombocyte vesicles with sensor surfaces of different lipophilicity was examined as a model for understanding the membrane properties of thrombocytes (Agmo Hernandez *et al.*, 2008).

A sensitive biosensor for detecting antithrombin III (AT III) was constructed based on in situ growth of nanogold on the gold electrode of a quartz crystal microbalance (Zhang *et al.*, 2008b). Heparin was used as the affinity ligand and immobilized onto the nanogold modified gold electrode. A flow injection analysis-quartz crystal microbalance (FIA-QCM) system was used to investigate the relationship between nanogold growth and the AT III response. Compared with the directly immobilized large nanogold particles, the in situ grown particles with the same size occupied more sensor surface, resulting in higher frequency shifts to AT III in the interaction study between heparin and AT III.

A setup for the analysis of glycated haemoglobin (HbA1c) in blood was reported by Pribyl and Skládal (2006). A combination of a piezoelectric biosensor for glycated haemoglobin based on a gold electrode with 3-aminophenylboronic acid (APBA) as a specific ligand and a flow-through photometric sensor for total haemoglobin (Hb) was used and the full range of HbA1c content (4–15%) in blood could be analysed (Pribyl and Skládal, 2006).

IMMUNOASSAYS

Protein immobilization

The immobilization of either antibody or antigen onto the surface of a sensor is a key step in the fabrication of most immunosensors, including those based on QCM. The density of bound antigen or antibody and the suppression of unspecific binding are essential to achieve high sensitivity for the analyte. The immobilization can occur via direct physical adsorption onto a gold surface or other surface, chemical immobilization via the formation of a new chemical bond, introduction of surfaces that allow electrostatic interactions and many other methods. The ease of fabrication and the reusability of the sensor are important factors for commercial applications. Therefore there is a strong interest in optimizing the binding to the sensor surface

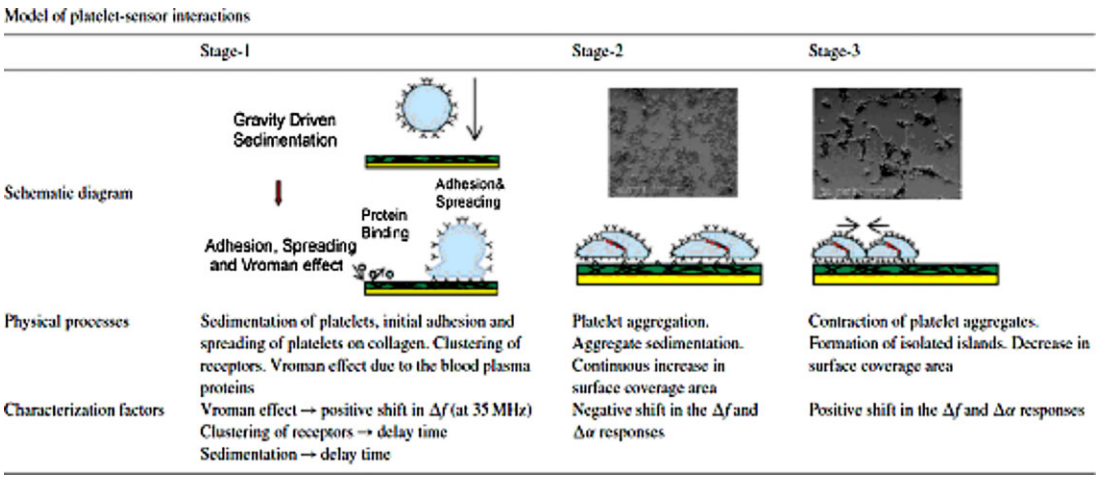

Figure 3. A piezoelectric thickness shear mode (TSM) biosensor was coated with collagen-I fibers to promote platelet activation and adhesion magnitude and frequency response of the sensor were monitored under static conditions at 37°C, using platelet-rich plasma, and PRP with adenosine diphosphate (ADP), a clinical aggregation inhibitor (abciximab), or a collagen binding inhibitor. Sensors loaded with PRP exhibited a 3-stage response: (i) no significant change in response for the first 20 min, (ii) followed by a larger drop in response and (iii) a gradual increase in response. Exogenous ADP stimulated an immediate Stage-2 response, while abciximab delayed and reduced the magnitude change of Stage-2. In the presence of collagen inhibitor, Stage-2 response was similar to that of control but was delayed by an additional 20 min. The obtained results were supported by epifluorescence and complementary SEM studies, and demonstrate the monitor platelet function and inhibition, particularly aggregation. From (Ergezen *et al.*, 2007), reprinted with permission.

and a number of publications have looked at different ways to immobilize proteins. Different methods were investigated for anti-C-reactive protein (CRP) monoclonal antibodies (Aizawa *et al.*, 2006), immunoglobulin G (IgG) (Caruso *et al.*, 1996; Sai *et al.*, 2006; Shen *et al.*, 2007b; Yang *et al.*, 2009b), BSA using a temperature controlled surface (Liu *et al.*, 2008), carcinoma antigen 125 (CA 125) onto gold nanowires (Tang *et al.*, 2008), aflatoxin B_1 antibody-functionalized magnetic core-shell composite nanoparticles (Wang and Gan, 2009) and other antibodies (Serizawa *et al.*, 2007). Ding *et al.* used poly-L-lysine/hydroxyapatite/carbon nanotube hybrid nanoparticles for the immobilization of carbohydrate antigen 19-9 (CA19-9) (Ding *et al.*, 2008) and Hirlekar Schmid *et al.* used a crosslinked layer of protein A to generate a uniform, stable and sterically accessible antibody coating (Hirlekar Schmid *et al.*, 2006). In general, those studies that employed polymeric or planar ethylene glycol self-assembled monolayer supports for directed immobilization of proteins gave the most reproducible results.

Clinical analysis

A synthetic peptide from the juxtamembrane region of IA-2 (a Type 1 Diabetes associated antigen) was used in the development of a diagnostic assay of autoimmune diseases (Ayela *et al.*, 2007). The auto-antibodies directed against wheat gliadin, a protein fraction of cereal gluten which is involved in celiac disease, were detected in human sera (Balkenhohl and Lisdat, 2007). A simplification of the conventional ELISA assay without multiple labelling and separation steps was achieved by using an QCM immunoassay utilizing antibodies against carcinoembryonic antigen (CEA) (Tang *et al.*, 2006; Chen and Tang, 2007). CEA together with tumour markers such as α-fetoprotein (AFP), prostate specific antigen (PSA) and carcinoma antigen 125 (CA125) was detected in a multi-array immunoassay device without cross-reactivity with other tumour markers (Zhang *et al.*, 2007a).

Rheumatoid arthritis (RA)-specific (cyclic citrulline-containing) peptide was immobilized to functionalized single-walled carbon nanotubes and deposited on crystal to generate a sensor that allowed detection in the femtomol range. The sensitivity of the nanotube-based sensor was higher than that of the established ELISA and microarray assay systems, detecting 34.4 and 37.5% more RA patients with anti-citrullinated peptide antibodies than those found by ELISA and microarray, respectively (Drouvalakis *et al.*, 2008). Microalbumin, α1-microglobulin, β2-microglobulin and IgG in urine as prognostic markers for diabetes nephropathy were detected using a QCM immunosensor array. Luo *et al.* showed that the immunosensor array was highly comparable to immunonephelometry (Luo *et al.*, 2006). A rapid, simple, portable and sensitive immunoagglutination assay that uses silica particles instead of the traditional latex microspheres and quartz crystal microbalance (QCM) for quantifying *Schistosoma japonicum* antibodies as an efficient test for the diagnosis of schistosomiasis was developed by Wang *et al.* (2006a). An immunosensor array for the rapid detection of HIV-1 and HIV-2 was developed by Wen *et al.* (2009). Clinical serum samples were used and the linear range for the measurement was 0.01–0.2 NCU/ml. Kim *et al.* developed a competitive assay for the detection of C-reactive protein (CRP), a cardiovascular biomarker, with a detection limit for CRP of 0.130 ng/mL (Kim *et al.*, 2009). QCM was also used to analyse binding kinetics and specificity of iron oxide nanoparticles for MRI imaging coated with human anti-VCAM1 antibodies (Amstad *et al.*, 2009).

Affinity studies

Antibody-modified liposomes were used to developed an assay for direct quantitative detection of human immunoglobulin G (hIgG) without the need for the immobilization of antigen or antibody on the quartz crystal surface (Chen *et al.*, 2007a). The assay was based on the specific agglutination of antibody-coated liposomes in the presence of the corresponding antigen, which was correlated with the frequency shift of a piezoelectric device. An ultrasensitive piezoelectric method for the detection of the

aflatoxin B_1 was developed based on the indirect competitive immunoassay and the biocatalysed deposition amplification utilizing the oxidation of 4-chloro-1-naphthol by hydrogen peroxide, generated by horseradish peroxidase, to yield the insoluble product benzo-4-chlorohexadienone on the surface of quartz crystal microbalance (Jin *et al.*, 2009). The proposed approach allowed the determination of aflatoxin in the range of 0.01–10 ng/mL. Various single-chain fragment variable antibodies (scFv) against cytrochrome P450 1B1 were used to develop an immunoassay with good sensitivity (detection limit 2.2 nM) and selectivity (Shen *et al.*, 2007d). A mercapto *Schistosoma japonicum* antigen was self-assembled onto the quartz crystal surface via a Au nanoparticle mediator monolayer to sense the *S. japonicum* antibody (SjAb) and coupled with a an amplification path based on an insoluble biocatalysed precipitation product generated by horsereaddish peroxidase (Wu *et al.*, 2006). The detection limit for the *S. japonicum* antibody was as low as 5 ng/ml. Other specific immunoassays were developed for the detection of matrix metalloproteinase-1 (MMP 1) (Soumetz *et al.*, 2009), oratoxin A (OTA) mycotoxin (Vidal *et al.*, 2009), mesothelin (Corso *et al.*, 2006), and immunoglobulin E (IgE) (Yao *et al.*, 2009a). Chu *et al.* developed a protocol for a doubly amplified immunoassay based on antibody-functionalized Au nanoparticles as the primary amplifying probe and a dendritic-type immunocomplex of protein A and antibody-modified Au nanoparticles as the secondary amplifying probe (Chu *et al.*, 2006).

CARBOHYDRATES

Cellulose and modified cellulose

Cellulose is the main structural component in the cell walls of algae and plants and is also secreted by some bacteria to assist in the formation of biofilms. Cellulose and modified celluloses have a number of industrial uses in the production of paper, cellophane and rayon to name just a few and increasingly in the production of biofuels such as cellulosic ethanol. The physical forms and the behaviour of cellulose and cellulose nanofibrils is of importance in many industries. In paper and pulp industrial research a study showed that immobilized cellulose nanofibers are excellent models for the pulp fiber surface (Ahola *et al.*, 2008a), while another study looked at the interaction between cellulose and lignin (Notley and Norgren, 2006). The activity of cellulose degrading enzymes has been studied using QCM by a number of groups (Ahola *et al.*, 2008b; Josefsson *et al.*, 2008; Turon *et al.*, 2008; Hu *et al.*, 2009a). Hu *et al.* used QCM to investigate cellulase activity on cellulose films and compared their results to the IUPAC dinitrosalicylic acid standard method and biccinchoninic acid and ion chromatography methods for the determination of cellulase activity (Hu *et al.*, 2009b). They found that the QCM technique provided results best correlated to those obtained by measuring the actual reducing sugars. Cellulose as well as modified celluloses have been used in polyelectrolyte adsorption studies (Hedin *et al.*, 2007; Amirkhani *et al.*, 2008; Enarsson and Wagberg, 2009) as well as in the construction of thin films (Notley, 2008) or multilayer films (Xing *et al.*, 2007; Aulin *et al.*, 2008; Hedin *et al.*, 2009).

Other polysaccharides

Polysaccharides are often used in the construction of mutilayer bio-compatible surfaces, amongst others these include chitosan, alginate and dextran derivatives. Alginate was the focus in the study of the self assembly and crosslinking of polyelectrolyte multilayer films of chitosan and alginate (Alves *et al.*, 2009) and the fabrication of adhesives composed of cross-linked alginate and polyphenols (Bitton *et al.*, 2007). Chitosan adsorption on model films was investigated (Indest *et al.*, 2008), as well as the immobilization of glucose oxidase (GOD) in films with alternating layers of chitosan made by layer-by-layer (LbL) fabrication (Caseli *et al.*, 2006a). Chitosan derivatives were also used to generate multilayer assemblies (Channasanon *et al.*, 2007). Of particular interest are chitosan sulfate and fucoidan sulfate as they have promising anticoagulant properties and represent an alternative to heparin treatment of vascular grafts (Indest *et al.*, 2009). Film formation and adsorption was studied for partially 2,3-*O*-methylated amyloses (Kida *et al.*, 2008), cationic starch (Kontturi *et al.*, 2008), and dextran (Kwon *et al.*, 2006). Covalently immobilized layers of carboxymethyl dextran were used in a study to investigate the fouling of dextran layers in cell culture medium, fibronectin, and serum solutions (Dubois *et al.*, 2009). QCM was also used to characterize the interaction of a protein-polysaccharide complex extracted from the mushroom *Agaricus blazei* Murill with a cell membrane model represented by a Langmuir monolayer of dimyristoyl phosphatidic acid (Schmidt *et al.*, 2009).

Mucins

Mucins are a family of heavily glycosylated proteins (glycoconjugates) of high molecular weight that occur in large aggregates that are produced by epithelial tissues in most metazoans and play a role in many biological interactions. Mucins could be immobilized onto different types of functionalized gold surfaces (Feldoto *et al.*, 2008). Bovine submaxillary gland mucin was immobilized and the mucoadhesive properties of hydrophobically modified derivatives of dextran and hydroxypropylcellulose were assed using QCM (Chayed and Winnik, 2007) Measurements revealed that a pre-adsorbed bovine salivary mucin layer stabilizes IgG through complexation on a polymeric model surface (Sandberg *et al.*, 2009a).

Interaction with carbohydrate-binding proteins

Carbohydrate-binding proteins are generally referred to as lectins. They are highly specific for certain carbohydrate moieties and play an important role in biological recognition phenomena involving cells and proteins. For example, some viruses use lectins to attach themselves to the cells of the host organism during infection. Mimicking the biological process specific interactions of plain (unmodified) and PEGylated, lectin-grafted liposomes with model membranes containing glycolipids were assessed under real-time flow conditions (Bakowsky *et al.*, 2008) using QCM. Using a novel method, monosaccharide-derivatized photoprobes were immobilezed on PEG surfaces and their interaction with the lectins concanavalin A (the agglutinin from *Canavalia ensiform*is, Con A), *Viscum album* agglutinin (VAA), *Ulex uropaeus* lectin I (UEA) and *Pisum sativum* agglutinin (PSA) was studied (Pei *et al.*, 2007). Different carbohydrates were immobilized onto a gold surface using alkyne-containing thiols carbohydrate azides and 'click-chemistry' and the interactions with different lectins determined (Zhang *et al.*, 2006; Norberg *et al.*, 2009). Huang *et al.* looked at the influence of surface rigidity on the binding (Huang *et al.*, 2007b). They created a polymer

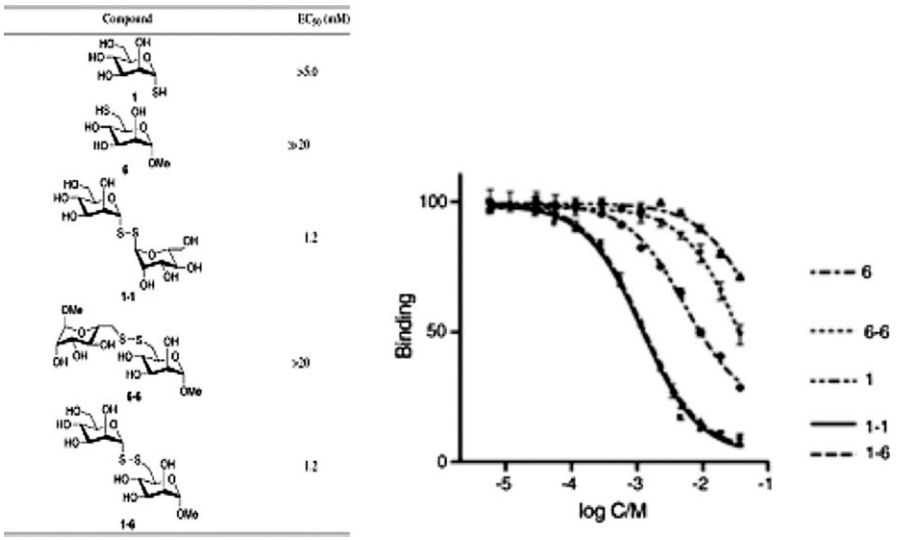

Figure 4. Estimation of EC_{50} values (50% inhibition of concanavalin A binding) for tested carbohydrate structures [left]. Inhibitory responses of Con A binding in presence of DCL constituents 1, 6, 1–1, 6–6. The curves were based on consecutively diluted concentrations of tested inhibitors included in the QCM-assay with Con A [right]. From (Pei *et al.*, 2006), reprinted with permission.

containing mannose and probed the interaction with Con A once immobilized to a gold surface via an alkanethiol substituent. Cross-linked polymer decreased the flexibility of the polymer backbone between the carbohydrate binding sites, and it was proposed that the cost of conformational entropy for multivalent binding was minimized. Binding constants of cross-linked polymer with Con A were significantly larger than with a carbohydrate self-assembled monolayer.

Mori *et al.* investigated the binding kinetics of concanavalin A (Con A) using biotinylated mannotriose (Man_3-bio) dispersively immobilized in the matrix of biotinylated lactose (Gal-Glc-bio) on a streptavidin-covered surface. The binding kinetics and affinities of Con A to Man_3-bio in the Gal-Glc-bio matrix could be obtained, with the affinity for the 1:2 binding observed to be ten-fold larger than that for the 1:1 binding, with a three-fold larger association rate constant (k_{on}) and a three-fold smaller dissociation rate constant (k_{off}). This is the first example to obtain separate kinetic parameters for the 1:1 and 1:2 bindings of lectins to carbohydrates on a surface (Mori *et al.*, 2009). Simonis *et al.* determined the kinetic constants of the binding of heparin and other sulfated polysaccharides to immobilized P-selectin (Simonis *et al.*, 2007b). They analysed six semi-synthetic glucan sulfates, with different degrees of sulfation, which imparts a strong influence on inhibitory activity. Kinetic data illustrated that the inhibitory capacity correlated well with the off-rate of these polysaccharides ($R = 0.99$) and that the association rate (k_{on}) affected activity to a lesser extent. A much slower dissociation of the inhibitors from the receptor than the physiological ligands was key for inhibitory capacity and highly charged compounds with a slow off-rate, such as heparin or glucan sulfates, appeared as potent candidates for P-selectin inhibition. The binding kinetics and affinity of the two low molecular weight heparins (LMWHs) enoxaparin and nadroparin, and of the unfractionated heparin Liquemin N to P- and L-selectin were also determined (Simonis *et al.*, 2007a).

The affinity of lectins for specific carbohydrates was also used for the direct detection of bacteria. Con A was immobilized using avidin-biotin and a detection limit of approximately 1.0×10^4 cfu/mL was achieved. An increase of detection was observed in the presence of free biotinylated ConA. Using Con A and lectin from *Arachis hypogaea*, different response profiles were achieved for *E. coli*, *Staphylococcus aureus* and *Mycobacterium phlei*, thus demonstrating the feasibility of this approach for the discrimination of different bacteria. (Serra *et al.*, 2008). QCM was also used to study the complex formation of Con A and the glycoprotein carboxypeptidase Y (Lebed *et al.*, 2006), to show that dermatan sulfate demonstrated a high level of binding activity to the receptor activator of NF-κB ligand (RANKL) and obstructed the binding of RANK to RANKL (Shinmyouzu *et al.*, 2007). Stablin is a small protein relating to the coagulation in arthropods and its binding constant to chitin was determined using QCM (Matsuda *et al.*, 2007). Other notable publications include determination of the affinity of various synthetic oligosaccharides to recombinant calreticulin (Takatani and Ito, 2006; Tatami *et al.*, 2007), the rapid identification of lectin inhibitors from a dynamic combinatorial library of glycosyldisulfides (Figure 4) (Pei *et al.*, 2006), and the identification of a trimannoside-recognizing peptide sequences from a T7 phage display (Nishiyama *et al.*, 2009).

OLIGONUCLEOTIDE INTERACTIONS

Oligonucleotide immobilization

A number of publications describe the improvement of existing methods or development of new methods for the immobilization of RNA or DNA. These consisted of covalent immobilization (Lee *et al.*, 2008a; Razumovitch *et al.*, 2009; Sato *et al.*, 2009) including a photochemical method (Nakano *et al.*, 2006), polycationic surfaces (Rawle *et al.*, 2007; Yang *et al.*, 2008a), inclusion in a layer-by-layer self-assembly system (Sultan *et al.*, 2009), natural organic matter (Nguyen and Chen, 2007; Nguyen and Elimelech, 2007a), adsorption directly to quartz (Nguyen and Elimelech, 2007b) and the use of biotinylated DNA on streptavidin (Yamasaki *et al.*, 2007). Surface morphology was shown to play an important role, leading to a three- to five-fold better sensitivity in an DNA detection assay where nanogold 'hollow' spheres where used instead of a flat gold

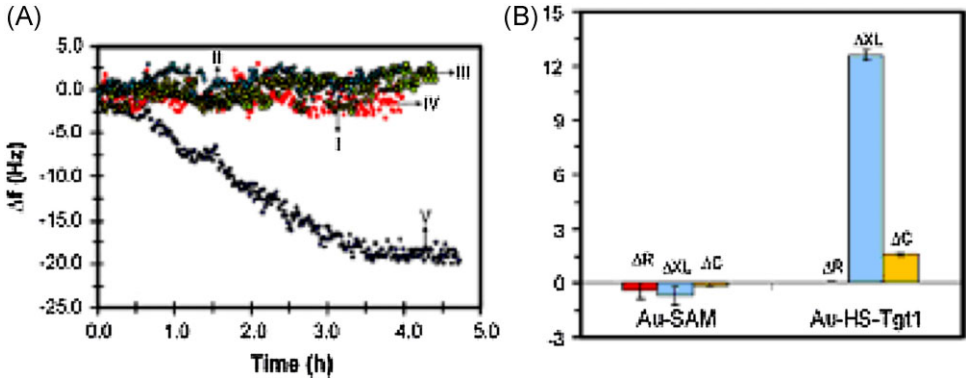

Figure 5. Crystal sensor response to DNA hybridization. All crystal sensors used were functionalized with HS-Pr1 probe and blocked with 11-hydroxy-1-undecanothiol: (A) resonance frequency recorded for crystal sensors incubated with (I) PBS buffer, (II) 1 μM of Ctr1, (III) 1 μM of Tgt1, (IV) 1.7 nM of Au-SAM nanoparticles, (V) 1.7 nM of Au–HS-Tgt1 nanoparticles; (B) impedance data acquired for crystal sensors incubated with gold nanoparticles modified with 11-hydroxy-1-undecanothiol (Au-SAM) and gold nanoparticles functionalized with complementary target HS-Tgt1 (Au–HS-Tgt1). From (Encarnacao *et al.*, 2007), reprinted with permission.

surface (Lu *et al.*, 2007). Immobilization of DNA on a polyelectrolyte surface enabled the real-time monitoring of induced DNA damage (Rawle *et al.*, 2008). Hianik *et al.* carried out a comparative study for the immobilization of aptamers and found that immobilization by means of avidin-biotin technology revealed the best results in terms of sensitivity in comparison with immobilization utilizing first generation dendrimers or chemisorption to a gold surface (Hianik *et al.*, 2007).

Encarnada *et al.* looked at the influence of electrolytes on the detection of oligonucleotide sequences and found that the presence of electrolytes in solution generates desorption-like transients when the resonance frequency is measured. They were able to discriminate these influences and quantified them as 8.0 ± 0.5 Hz per pF of electrolytes to the sensor resonance frequency and used this factor to correct the data obtained by frequency counting measurements (Encarnacao *et al.*, 2007). The influence on DNA hybridization is shown in Figure 5.

Detection of hybridization

The high specificity of DNA hybridization, together with the sensitivity of QCM, allowed several research groups to identify genes with single base pair mutations. Feng *et al.* used the DNA ligase reaction combined with the biocatalysed deposition of an insoluble product for signal amplification to identify target DNA (Feng *et al.*, 2007). The DNA target hybridized with a capture probe tethered onto the gold electrode and then with a biotinylated allele-specific detection DNA sequence. The amplification of the signal was achieved by the detection of the biotinylated allele-matched probe via the binding to streptavidin-horseradish peroxide (SA-HRP), which catalysed the oxidative precipitation of 3,3-diaminobenzidine (DAB) by hydrogen peroxide on the electrode. The detection limit for this method was 0.1 nM.

Uludag *et al.* could show for a hybridization asay detecting HSV-1 DNA that without the use of nanoparticles but utilizing capture protein, a hybridization sensitivity of 10^{-11} M could be achieved (Uludag *et al.*, 2008). An optimized surface chemistry was combined with a simple signal amplification method using NeutrAvidin labelled RNA to enhance the limit of detection for HSV viral DNA recognition. The frequency changes during the course of the assay including the signal enhancement step and the results of the assay are shown in Figure 6.

Another method for the detection of single-base mutations relied on the use of nanogold-labeled DNA probes (Pang *et al.*, 2006). A capture probe was designed with the potential point mutation site located at the 3′-end and immobilized via a thiol on the 5′-end. Successive hybridization with the target DNA and detection probe of nanogold-labeled DNA followed by DNA ligase reaction and denaturing at an elevated temperature led to a return of the QCM frequency to the original value for the target with single-base mismatch, whereas a reduced frequency response would be obtained for the case of the perfect match target. A detection limit of 2.6 nM was achieved (Nie *et al.*, 2007). A different approach used single-base-coded CdS nanoparticle

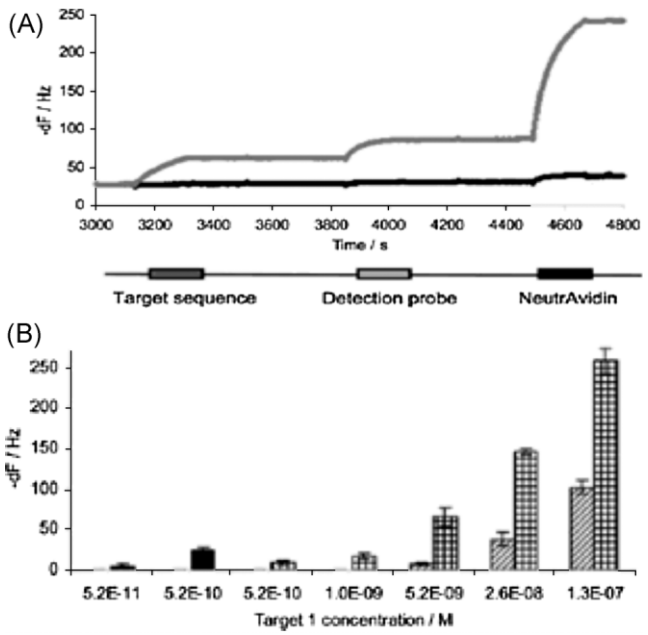

Figure 6. (A) Sequential injections of 1 μg/ml target sequence, 1 μg/ml detection probe and 5 μg/ml NeutrAvidin to enhance the hybridization signal. Grey: active flow cell; black: control flow cell; (B) Diagonally striped columns: VP16 target sequence hybridization onto the surface probe. Crossed columns: NeutrAvidin capture onto the VP16 detection probe. Black columns: NA capture after the injection of solution-hybridized VP16 target sequence and VP16 detection probe ($n = 4$ for all results). From (Uludag *et al.*, 2008), reprinted with permission.

probes and target DNA immobilized on core/shell Fe_3O_4/Au magnetic nanoparticles (Ye *et al.*, 2009). It was also demonstrated that the structure of the streptavidin film used to immobilize biotinylated DNA plays a role in target DNA hybridization (Su *et al.*, 2005). A biotinylated probe and classic PCR amplification were used with wild type and mutated cells in the analysis of the TP53 gene involved in a number of different tumors (Dell'Atti *et al.*, 2006). In another study single nucleotide exchanges or deletions were distinguished reliably from the wild-type sequences, on the basis of differences in their dissociation or association rates starting at low nanomolar concentration (Gronewold *et al.*, 2006). Both the mass and viscosity signals were measured allowing discriminating between mass effects resulting from hybridization of short DNA strands and viscosity effects due to increasing amounts of DNA deposited on the sensor.

Although not strictly a QCM a film-bulk-acoustic-resonator (FBAR) is closely related and works on the same principles but at a higher frequency (0.8–1.5 GHz). Its mass-sensitivity is about tens times higher than a typical quartz crystal microbalance and Zhang *et al.* were able to demonstrate its usefulness be creating a sensor that is capable of distinguishing a complementary DNA that is mismatched to a probe DNA by a single nucleotide (Figure 7). A 15-mer probe nucleotide was functionalized at the 5′-end with a thiol for immobilization on a gold surface (Zhang *et al.*, 2007b).

Oligonucleotide-protein interactions

Oligonucleotide aptamers have the ability to selectively bind to certain proteins and this ability can be used to develop QCM-based assays for the detection of such proteins. Using this principle interferon-γ could be detected down to a 10 pM level by a DNA aptamer in fetal bovine serum (Min *et al.*, 2008). QCM was also used to study the interaction of DNA aptamers with estrogen receptor α (Su *et al.*, 2006; Peh *et al.*, 2007), an investigation of enzymatic digestion with a type IIP restriction endonuclease EcoRV (Takahashi *et al.*, 2007b) and the influence of ultrasound irradiation on the DNA polymerase reaction (Hoshino *et al.*, 2006). One of the most widely studied oligonucleotide-protein interactions undoubtedly is in the context of the cellular translation machinery and the ribosome. QCM with immobilized mRNA proved useful in the study of the initial binding events between mRNA and the bacterial 70S ribosome (Takahashi *et al.*, 2006; Takahashi *et al.*, 2007a). A similar approach was used to study the binding of Tat protein to RNA which leads to translation of the HIV-1 virus and the inhibition of translation though PAMAM dendrimers (Wang *et al.*, 2006b).

Clinical applications

DNA detection assays have a number of clinical applications and QCM-based assays have been developed that show comparable results to existing PCR-based assays but with shorter analysis time. Traditional PCR and gel electrophoresis could be replaced by QCM in a DNA-based diagnosis of α-thalassemia (Vattanaviboon *et al.*, 2008). A QCM biosensor was used to assay 18 blinded specimens and could accurately discriminate between normal and Southeast Asian α-thalassemic genotypes. A peptide nucleic acid (PNA) piezoelectric sensor was developed for the detection of hepatitis B virus DNA (Yao *et al.*, 2008). The PNA probe was immobilized on the surface of the biosensor to substitute the conventional DNA probe for the direct detection of HBV genomic DNA without previous amplification by PCR. The hybridization assay was completed in 50 min, with a detection limit of 8.6 fg/mL and a clinical specificity was 94.44% compared with real time-PCR. Detection assays for the DNA of *E. coli* (Sun *et al.*, 2006) and a microalgae that produces neurotoxins responsible for paralytic shellfish poisoning, *Alexandrium minutum,* have also been reported (Lazerges *et al.*, 2006).

CELLS

For most normal eukaryotic cells adhesion is a pre-requisite for proliferation and growth, with detachment only occurring with the onset of apoptosis. Here QCM sensing can be used in the study of cellular films, cell adhesion, attachment, growth and cell-substrate interactions. Many of the latter applications once again exploit the ability of acoustic biosensors to detect changes in the viscoelastic properties of an entity adhered to a surface with real-time resolution and without reporter labels.

Attachment, adhesion and proliferation

Although QCM is generally considered to be non-invasive, the shear oscillation at the centre of the resonator could potentially impact on the ability of cultured cells to adhere to and spread on the sensor surface. This putative effect has been examined recently (Heitmann and Wegener, 2007) with three mammalian cell lines and variant elevated lateral oscillation amplitudes. Effects on the adhesion kinetics and the formation of stable cell-substrate contacts was retarded or blocked only when the

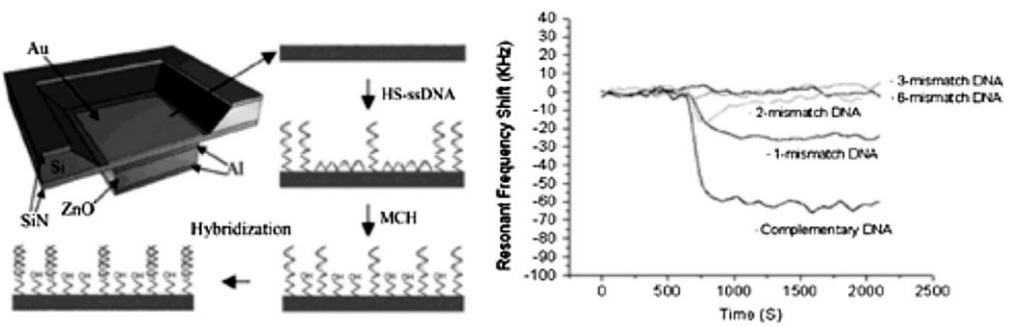

Figure 7. Illustration of FBAR device being treated with HS-ssDNA and MCH for mixed monolayer formation and hybridized with a target DNA sequence. The resonant frequency of the HS-DNA immoblized FBAR decreases when hybridized with the target DNA complement [left]. The resonant frequency shift of the FBAR on whose surface is immobolized DNA [right]. From (Zhang *et al.*, 2007b), reprinted with permission.

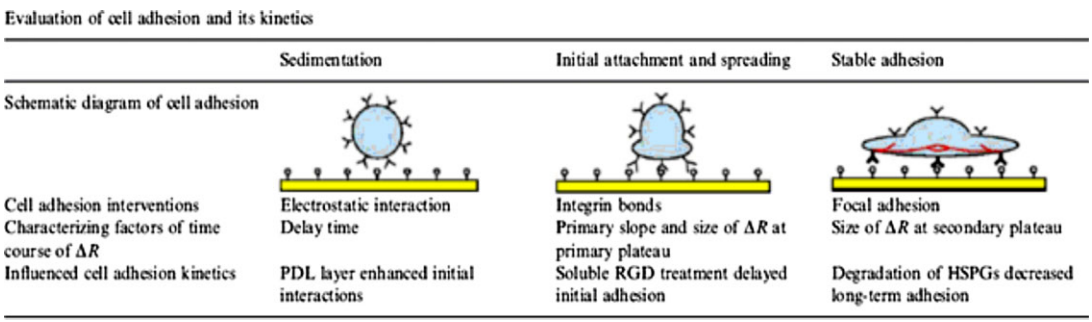

Figure 8. Evaluation of cell adhesion and it's kinetics. From (Hong *et al.*, 2006), reprinted with permission.

lateral oscillation amplitude exceeded values higher than 20 nm (typical lateral displacements for commercial QCM system driven at 100 mV are in the order of 1–3 nm). However, even shear displacements of 20 nm were found to be insufficient to displace attached cells from the surface. The experimental data suggest that the normal QCM mode of operation with low oscillation amplitudes is, indeed, non-invasive with respect to mammalian cells.

The cell adhesion process and the molecular interactions that determine its kinetics were investigated by Hong *et al.* (2006) (Figure 8). They were able to correlate sensor readings with the progression of cell adhesion and looked in detail at the specific effects of receptor-mediated adhesion, the glycocalyx and surface charge on initial cell-surface attachment and steady-state adhesion of endothelial cells (Hong *et al.*, 2006).

In addition to the requisite surface chemical properties conducive to cell adhesion, surface topology also has an impact on the adhesion, spreading and proliferation of cells. In a study with MCF-7 human mammary cancer cells on two gold electrodes with different surface roughness, it was shown that the analysis of the QCM resonant frequency (dF) and motional resistance changes (dR_1) revealed a significant surface-stress effect in addition to a viscodensity effect, and a comparitively small mass effect (Tan *et al.*, 2009b). Fluorescence microscopy, cyclic voltammetry and electrochemical impedance spectroscopy were used to further investigate and quantitatively correlate surface roughness and cell population resulting in a novel QCM method for dynamically measuring the surface stress on an electrode in cell-culture.

Depending on the type of cell used, differently modified sensor surfaces may need to be employed to ensure cell adhesion and cell survival. A number of studies have looked at different surface coatings presenting peptides or proteins. Extracellular matrix proteins pre-coated on a gold surface were used to facilitate QCM studies on the adhesion and spreading of WB F344 rat epithelial cells and B16F10 lung melanoma cells (Fohlerova *et al.*, 2007), and in a separate study with human embryonic stem cells (Kohen *et al.*, 2009). Surface coatings presenting the RGD peptide sequence were used in studies of rMSCs and 3T3-L1 fibroblasts (Knerr *et al.*, 2006), and human endothelial cells (Bodin *et al.*, 2007; Marx *et al.*, 2009). The adhesion of NIH3T3 fibroblasts to serum protein coated tantalum and oxidized polystyrene surfaces was investigated using QCM, and it was found that process of cell adhesion and spreading elicited different responses depending on both the protein coating composition and the influence of the underlying substrate (Lord *et al.*, 2006b; Lord *et al.*, 2008). Adsorption of serum proteins onto colloidal silica surfaces lead to a significantly reduced adhesion and proliferation of human endothelial cells compared to control silica surfaces (Lord *et al.*, 2006a). Polyelectrolyte multilayers can also facilitate cell adhesion and spreading onto surfaces. Human hepatoma cells (HepG2) were cultured on positively and negatively charged electrolytes and the adhesion and spreading monitored using QCM (Saravia and Toca-Herrera, 2009). Human fibroblast adhesion to multi-layers composed of heparin (an anionic glycosaminoglycan) and chitosan (a cationic biodegradable polysaccharide) was found to be highly pH-dependent, rendering the surfaces extremely cytophobic or moderately cytophilic (Kirchhof and Groth, 2008). Multi-layer films containing chitosan, hyaluronan and alginate and the impact of rigidification of the layers on cell binding were also investigated using MC3T3 pre-osteblastic and rat fibroblastic skin cells (Hillberg *et al.*, 2009). Finally, a polyporphorin film was successfully used to coat a gold sensor surface and enabled the real-time monitoring of MCF-7 human breast cancer cell growth and assessment of chemical cytotoxicity (Guo *et al.*, 2008).

A number of studies using QCM to monitor cell adhesion and spreading have been conducted in relation to transplant materials; here good cell adhesion is important to successfully facilitate the integration of the underlying substrate material, e.g. into bone structure and tissue. The initial cell adhesion of pre-osteoblastic MC3T3-E1 cells onto tantalum and chromium surfaces was investigated using QCM (Modin *et al.*, 2006). Biomimetic coatings containing fibronectin were tested for the growth of MG63 human osteoblast-like cells, in order to evaluate their potential for the treatment of materials employed in bone-tissue engineering (Soumetz *et al.*, 2008). Titanium surfaces covered with human fibronectin were investigated and several aspects of initial host/biomaterial interactions (keratinocyte adhesion, platelet interactions and pellicle formation) were studied (Scheideler *et al.*, 2007), as were titanium surfaces coated with peptides containing the RGD motif (Michael *et al.*, 2009).

Other studies relating to cell adhesion focused on the viscoelastic properties of the extracellular adhesives produced by marine diatoms *Amphora coffeaeformis* Cleve and *Craspedostauros australis* Cox (Molino *et al.*, 2008). The effect of mucin surface-shielding on activation of immobilized neutrophils (Sandberg *et al.*, 2009b), and other forms of surface grafting (Croll *et al.*, 2006; Chou *et al.*, 2009) involved integral use of the QCM.

Cellular responses to exogenous stimuli

An interesting study by Marx *et al.* demonstrated that QCM can be used to detect and study cell cytoskeleton alterations and dynamics (Marx *et al.*, 2007). The study utilized living endothelial cells and the metastatic human mammary cancer cell line MDA-MB-231, and probed the effect of the microtubule-binding drugs paclitaxel (taxol) and nocodazole in varying concentrations

by measuring changes in the QCM steady state frequency (dF) and motional resistance (dR) values. The authors observed the dF shift values to decrease significantly in magnitude to a limiting value, in a dose-dependent fashion after addition of nocodazole. This effect is consistent with nocodazole's known disruption of intracellular microtubules. Paclitaxel caused little alteration in dF over the same time period, consistent with its microtubule hyperstabilization effect. The data was confirmed by a fluorescence light microscopy investigation and indicated that the QCM biosensor can be used to detect and study endothelial cell cytoskeleton alterations and dynamics. Paclitaxel was also used in a study looking at disruption of adhesion and induction of apoptosis in HepG2 cells (Wei *et al.*, 2007). Another hepatic cancer cell line (Bel7402) and the apoptotic effects of doxorubicin were target of a different study (Tan *et al.*, 2009a). The discrimination between hepatic normal cells (L-02) and hepatic cancer (Bel7402) cells was possible using QCM in an agglutination assay (Tan *et al.*, 2009a). QCM was also useful in a study looking at the neural differentiation of PC12 cells (Washio *et al.*, 2009).

The reaction of mammalian MDCK-II to environmental changes such as osmotic stress, addition of fixation reagents, or the influence of drugs such as cytochalasin D was investigated in a comparative study using both QCM and electric cell-substrate impedance sensing (ECIS). The two techniques give substantially different results, indicating that both techniques may complement each other with respect to their biological information (Sapper *et al.*, 2006). Finally, a QCM system with a micro CCD camera that enabled microscopic observations simultaneously with the QCM measurements was developed (Kang and Muramatsu, 2009) and used in the investigation of chemical stressors to cultured cells.

SMALL MOLECULES

Detection of small molecular weight analytes is a pre-requisite for assays in a wide range of application areas: (i) environmental monitoring of low molecular weight analytes, (ii) interactions between receptors and small molecules that may be involved in ligand-receptor modulation of disease pathways, enzyme-substrate interactions and enzyme-cofactor interactions, (iii) pharmaceutical research where there is a growing need for binding-based assays that confirm putative 'hits' that result from high throughput functional screens and for information rich assays that can quantify target selectivity, affinity and kinetics during hit-to-lead and mode-of-action studies and finally (iv) in clinical diagnostics, where there are many low-molecular weight molecules that are important clinical biomarkers for disease risk, onset and response to therapy. There were relatively few representative examples relevant to the above for the period 2001–2005, and the publications in this area during the current review period grew by only 21%. In the following sections we highlight examples involving small molecule detection exploiting either: (a) direct binding, (b) competitive displacement assay, (c) small molecule as receptor (surface immobilized small molecule binding to a larger analyte in solution) or (d) molecularly imprinted polymers (Table 2).

Direct small molecule-receptor interactions

Low molecular weight β-amyloid fragment peptides such as the pentapeptide KLVFF were used as tools for detecting the specific aggregation of the amyloid-β peptides responsible for Alzheimer's disease in a QCM method (Okuno *et al.*, 2006; Okuno *et al.*, 2007). A QCM immunosensor was developed for the determination of the insecticides carbaryl, trichlopyr, and 3,5,6-trichloro-2-pyridinol (TCP), the main metabolite of the insecticide chlorpyrifos. The sensor showed detection limits (analyte concentrations producing 10% inhibition of the maximum signal) of 11 and 7 ng/mL for carbaryl and TCP respectively (March *et al.*, 2009). Acetylcholinesterase (AChE) was immobilized by chemisorption and cross-linking over the surface of a quartz crystal microbalance and an inhibition study with varying concentrations of a model organophosphorus pesticide EPN, a carbamate and one carbofuran was carried out. The limits of detection in these assays were 16 and 1.3 nM, respectively (Kim *et al.*, 2007b). A novel polymeric material for the detection of organophosphorous nerve agents was developed and used in a QCM sensor demonstrating a ten-fold higher sensitivity to the nerve agent simulant dimethyl methylphosphonate (DMMP) than to other interfering vapors (He *et al.*, 2008). DMMP was also detected with WO_3-nanoparticle functionalized quartz crystal microbalance sensors (Zhao *et al.*, 2009a).

Various approaches have been taken to develop heavy metal ion sensors based on QCM. Cross-linked melanin on a gold surface produced a sensor with a mercury ion sensitivity of 520 Hz/ppm with the limit of detection at 5 ppb (Huang *et al.*, 2007a). Other metal ions detected were Sn^{2+}, Ge^{4+}, Li^{+}, Zn^{2+}, Cu^{2+}, Bi^{3+}, Co^{2+}, Al^{3+}, Ni^{2+}, Ag^{+} and Fe^{3+}. Unexpectedly, binding of Mn^{7+}, Pb^{2+}, Cd^{2+} and Cr^{3+} led to an increase in resonant frequency, rather than the normal frequency decrease (Huang *et al.*, 2007a). Other approaches to heavy metal ion detections were reported (Sartore *et al.*, 2009), and a Pb^{2+} selective sensor using bovine serum albumin (BSA) showed a detection limit of 1 nM (Yin *et al.*, 2007). An ingenious way of detecting cyanide concentrations down to low ppb was developed by Timofeyenko *et al.* (2007). It relied on the ability of cyanide to form soluble gold complexes. Even very low concentrations of cyanide will lead to a slow ablation of the gold surface, which can be detected by QCM. The detection limits at pH 12 were 16.1 and 2.7 ppb using analysis times of 10 min and 1 h, respectively. The assay possessed excellent linearity over a variety of cyanide concentrations ranging from low ppb to hundreds of ppm (Timofeyenko *et al.*, 2007).

The binding processes and layer formation of some tea polyphenols to bovine serum albumin have been investigated: thearubigin (Chitpan *et al.*, 2007) and (-)-epigallocatechin gallate (Wang *et al.*, 2007a) both gave measurable signals indicative of binding to this serum protein. Ammonia in breath is an indicator of solute removal during dialysis and a QCM sensor has been used to continuously measure breath ammonia concentration of patients undergoing dialysis treatment. A strong correlation was observed between changes in the frequency of the QCM gas sensor and both the pre-dialysis blood urea nitrogen (BUN) level and the post-dialysis BUN level (Ishida *et al.*, 2008). Another gaseous analyte that a QCM sensor has been developed for is methane where cryptophane A has been used as a matrix for selective detection of methane (Sun *et al.*, 2009). Joo *et al.* designed a self-cleaning thiol sensor for natural gas fuel cells based on a ZnO nanorod-coated sensor surface. They could show that hexanethiol was adsorbed onto the nanorod-coated surface and that subsequent exposure of the surface to UV radiation led to a complete photodegradation and sensor surface free of adsorbed thiol (Joo *et al.*, 2009).

Table 2. Selected examples of QCM assays for small molecules

Analyte	Mwt (Da)	Detection limit (nM)	Assay type	Reference
Imidacloprid	256	10 000	MIP	(Bi and Yang, 2009)
Thiacloprid	253	10 000	MIP	(Bi and Yang, 2009)
8-hydroxy-2′-deoxyguanosine	283	8.3	MIP	(Ersoz *et al.*, 2008)
	283	7.5	MIP	(Say *et al.*, 2009)
EPN (ethyl p-nitrophenyl thionobenzenephosphonate)	323	15.5	Competition	(Kim *et al.*, 2007b)
Carbofuran	221	1.3	Competition	(Kim *et al.*, 2007b)
TCDD (2,3,7,8-tetrachlorodibenzo-pdioxin)	324	0.03	Direct	(Kurosawa *et al.*, 2006)
Carbaryl	201	50	Competition	(March *et al.*, 2009)
	201	62	MIP	(Yao *et al.*, 2009b)
TCP (3,5,6-trichloro-2-pyridinol)	198	35	Competition	(March *et al.*, 2009)
Histamine	101	5	MIP	(Pietrzyk *et al.*, 2009)
Bisphenol A	228	1.3	Direct	(Rahman *et al.*, 2007)
Pirimicarb	238	500	MIP	(Sun and Fung, 2006)
Cyanide	26	104	Direct	(Timofeyenko *et al.*, 2007)
γ-aminobutyric acid	103	42 000	Competition	(Wang and Muthuswamy, 2008)
Chloramphenicol	323	10 000	Direct	(Adányi *et al.*, 2006)
Daminozide	160	0.3	MIP	(Yan *et al.*, 2007)
Lead	207	1	Direct	(Yin *et al.*, 2007)
Mercury	201	25	Direct	(Huang *et al.*, 2007a)
Copper	64	0.8	MIP	(Yang and Zhang, 2009)

QCM and electrochemical impedance spectroscopic (EIS) techniques were used in an immunosensor for bisphenol A with a detection limit of 0.3 ng/mL (Rahman *et al.*, 2007). A more sensitive immunosensor for the detection of dioxins in fly ash was described by (Kurosawa *et al.*, 2006). The biointerface of QCM immunosensor was designed to immobilize antibodies and reduce non-specific binding using a self-assembled monolayer with subsequent blocking with a synthetic phospholipid polymer (2-methacryloyloxyethyl phosphorylcholine. The detection limits could be extended down to 10 pg/mL, which compares well with results obtained through other environmental monitoring methods such as ELISA and GC/MS. A similar dioxin immunosensor was described by Park *et al.* (2006).

Combination of a QCM sensor array with an artificial neural network led to the development of an 'E-nose' with various potential end-use applications. It was validated for the detection and anesthetic dose level predictions of the anesthetic sevoflurane (Saraoglu and Edin, 2007). Another sensor array system consisting of five QCM sensors (four active and one reference) and an artificial neural network for the on-line detection of volatile organic compounds was recently reported (Xu *et al.*, 2009). Three ionic liquids and a silicone oil, which are widely used as gas chromatographic stationary phases were selected as sensitive coatings on the quartz surface allowing the sensor array to effectively identify toluene, ethanol, acetone and dichloromethane. Incorporation of peptides selective for the binding to trinitrotoluene (TNT) in a polymeric matrix has led to the development of a selective sensor that can also discriminate between TNT and dinitrotoluene (DNT) (Cerruti *et al.*, 2009). Others TNT sensors are based on specific antibodies (Larsson *et al.*, 2006). The olfactory receptor protein of *Caenorhabditis elegans*, ODR-10, was expressed in *E. coli* and a QCM sensor then coated with crude membrane extracts, containing the expressed receptor protein and the interaction between the olfactory receptor and various odorant molecules examined (Sung *et al.*, 2006). An array consisting of nine sensor elements coated with different polymeric materials was developed for the analysis of odor emissions from a wastewater treatment facility (Ziya Ozturk *et al.*, 2009). Other areas where QCM was used to detect alcohols, esters and terpenes are in the continuous surveillance of composting processes (Lieberzeit *et al.*, 2008), volatile organic compounds in gas mixtures (Si *et al.*, 2007) (Filippov *et al.*, 2007), alcohols (Melegari *et al.*, 2008) (Koshets *et al.*, 2009), nonylphenol (Nabok *et al.*, 2007a), chloramphenicol (Adányi *et al.*, 2006), T-2 mycotoxin (Nabok *et al.*, 2007b), and paclitaxel (taxol), a natural anti-cancer agent providing a promising alternative to classical analytical methods for a fast and easy determination of paclitaxel (Pastorino *et al.*, 2006). QCM was also used to study the host–guest interaction between N,N-dimethylformamide or cholic acid and a cyclodextrin derivative (Schofield *et al.*, 2006), between heptaprenyl diphosphate synthase and the substrate farnesyl diphosphate (Suzuki *et al.*, 2006), and to determine drug binding to human serum albumin in a competition binding assay with bilirubin using flow injection analysis (Zhang *et al.*, 2008a). A QCM for low humidity detection was developed based on poly(l-lactide) stabilized gold nanoparticles (Sun *et al.*, 2007) and a hybrid humidity sensor was assembled using optical waveguides on a quartz crystal microbalance (Shinbo *et al.*, 2009).

In a thermochemical study on coronene Torres *et al*. were able to use QCM to reliably determine the enthalpy of sublimation for coronene (Torres *et al.*, 2009).

Recognition of chiral small molecules

An interesting application of QCM is the incorporation of chiral surfaces on the sensor to discriminate between different stereoisomers of small molecules. The immobilization of L-phenylalanine on the gold surface of a QCM sensor via a layer-by-layer assembly procedure led to a chiral surface that was able to discriminate between L- and D-mandelic acid. The chiral recognition ability of mandelic acid on the chiral surface was verified by sensing using the vapor diffused molecular assembly method with the QCM and the chiral discrimination factor between L- and D-mandelic acid compared to the racemic mixture was found to be about nine-fold (Guo *et al.*, a–c). Chiral HPLC stationary phases were immobilized onto a QCM sensor via a thiol monolayer to give a pseudo stationary phase, which could then be used to evaluate and predict chiral separation for different HPLC stationary phases with a reusable sensor and an analysis time of only a few minutes (Inagaki *et al.*, 2008). Molecularly imprinted polymers (MIPs) were used to discriminate between D- and L-tryptophan with a detection limit of 8.8 μM and the enantionmeric composition of the mixtures was determined by the degree of frequency shift (Liu *et al.*, 2006a). Molecularly imprinted nanoparticles were immobilized on the QCM transducers by physical entrapment in a thin poly(ethylene terephthalate) layer and (R)- and (S)-propranolol used as test compounds to exemplify chiral recognition capability.

A study on cyclodextrin derivatives (Xu *et al.*, 2008) investigated ten chiral sensors immobilized with mercaptyl perfunctionalized β-cyclodextrins with promising enantioselectivity. Proteins, which are made up from chiral amino acids and hence chiral themselves, can also be used to discriminate between different isomers. A method was developed for a chiral discrimination using a QCM biosensor with self-assembled bovine serum albumin (BSA) or human serum albumin (HSA) for chiral small molecules (Su *et al.*, 2009). (R,S)-1-(3-Methoxyphenyl) ethylamine and (R,S)-1-(4-methoxyphenyl)ethylamine could be easily differentiated by the BSA sensor, while the selectivity of the HSA sensor for (R,S) -tetrahydronaphthylamine, (R,S)-2- octanol and (R,S)-methyl lactate was higher than that of the BSA sensor.

Small molecules immobilized on a surface

Whilst most applications involve small molecules present in the bulk, or solution phase, several researchers have investigated surface-confined small molecules that interact with other ligands in free solution. When 2-[(4-hydroxyphenyl)azo]benzoic acid was immobilized onto a sensor surface it was shown to subsequently form a metastable complex with avidin (Deng *et al.*, 2006). Upon exposure to biotin a more stable complex was formed and the mass-loss of the desorbed avidin could be quantified in a competitive inhibition assay format. Various peptide probes were immobilized to assay their affinities to profilin, an actin-binding protein involved in the dynamic turnover and restructuring of the actin cytoskeleton (Okada *et al.*, 2007). The binding of vancomycin to peptide ligands immobilized on a sensor chip was investigated by QCM and showed that vancomycin specifically associated with the D-Ala-D-Ala-containing peptide with an affinity of 3.2 μM consistent with the value of 2.7 μM determined by surface plasmon resonance assay (Tseng *et al.*, 2007).

Real-time investigation of molecular recognition between protein and the low molecular weight photosensitizer (meso-tetrakis(4-hydroxyphenyl)porphyrin used in photodynamic therapy was carried out with the photosensitizer immobilized on the QCM surface and protein in solution (Yang *et al.*, 2009a). QCM and impedance analysis were used together to assess the activity and affinity of antibodies bound to the surface of a sensor coated with surface immobilized 2,4-dinitrophenyl (DNP)-ligands that bind specifically to anti-DNP antibodies (Senaratne *et al.*, 2006). The neurotransmitter γ-aminobutyric acid (GABA) was immobilized and GABA concentrations determined in a competition assay using QCM and a GABA antibody (Wang and Muthuswamy, 2008).

Molecularly imprinted polymers (MIPs)

QCM sensors for the detection of pesticides have been a focus of a number of different groups. A detection method that allowed the identification and quantification of two neonicotinoid pesticides (imidacloprid and thiacloprid) was developed by the preparation of molecularly imprinted monolayers of alkanethiols self-assembled on a QCM sensor chips with pre-adsorbed imidacloprid or thiacloprid templates (Bi and Yang, 2009). MIP-QCM sensors have been developed for the fast and on-site determination of the pesticide pirimicarb in contaminated vegetables (Sun and Fung, 2006), for carbaryl with a the detection limit of 12.5 ng/mL (Yao *et al.*, 2009b), and for the detection of daminozide, a plant regulator, where the detection limit was 50 pg/mL, which is lower than that of conventional methods (Yan *et al.*, 2007).

Molecularly imprinted polymers for QCM sensing were successfully used to build devices for the detection of explosives. MIPs were prepared as particulates or as thin coatings and used for the direct measurement of dinitrotoluene (2,4-DNT) and trinitrotoluene (2,4,6-TNT) with a TNT-uptake of about 150 pg per μg MIP per hour (Bunte *et al.*, 2007).

8-hydroxy-2′-deoxyguanosine (8-OHdG) has been used as a marker to quantify oxidative stress, but there is no cheap and easy determination method available. By using methacryloylamidohistidine-platinum(II), a novel metal-chelating monomer, and the generation of an imprinted polymer it was possible to manufacture a sensor with an average percentage recovery of 8-OHdG from plasma samples of 80% (Ersoz *et al.*, 2008; Say *et al.*, 2009). 8-OHdG levels in several clinical blood plasma samples were determined by this method. Imprinting techniques were combined with cyclodextrin to fabricate binding sites for aromatic compounds within TiO_2 ultrathin layers with a selectivity for bisphenol A (Yang *et al.*, 2006a). MIPs have also

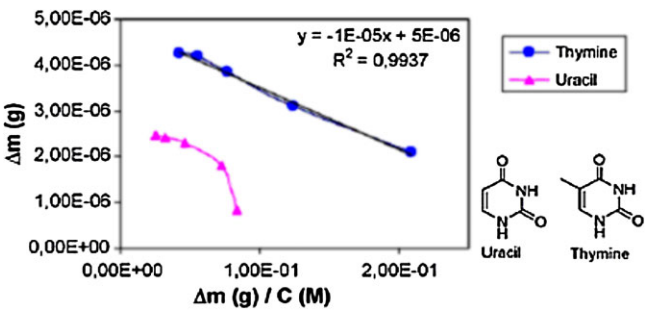

Figure 9. Linear Langmuir adsorption isotherm of thymine and uracil on thymine imprinted polymer. From (Diltemiz *et al.*, 2009), reprinted with permission.

been used in the detection of histamine with a detection limit of 5 nM (Pietrzyk *et al.*, 2009), toluene vapors (Matsuguchi and Uno, 2006), bilirubin (Wu and Syu, 2006) and thymine (Diltemiz *et al.*, 2009) (Figure 9). The molecular imprinting technique has also been successfully applied for the generation of sensors selective to Cu(II) ions with a short response time, wide linear range (1 nM to 50 μM) and a lower detection limit of 0.8 nM (Yang and Zhang, 2009).

LIPIDS AND MEMBRANES

The use of QCM to measure shear modulus and viscoelasticity in addition to mass adsorption and desorption has led researchers to apply QCM sensing in a varied study of lipid film formation, membrane morphology changes and interactions between an analyte and a membrane receptor or the membrane itself (Cooper, 2004).

Supported membranes and immobilized vesicles

The immobilization and characterization of intact liposomes via biotin-avidin interaction was the target of several QCM studies (Morita *et al.*, 2006; Brochu and Vermette, 2007). A hybrid bilayer membrane was used to immobilize avidin onto the sensor chip and sensitivity and stability of the resulting sensor chip was comparable to a sensor chip prepared by the conventional carbodiimide reaction (Mun and Choi, 2009). Another study using the amino-coupling method, found that intact liposomes could be immobilized on a solid surface and were stable for 10 h with frequency changes of less than 5% (Vu *et al.*, 2009). QCM monitoring and atomic force microscopy (AFM) were combined to evaluate the defects created by an ionic liquid anion and a cation in a supported phospholipid bilayer composed of zwitterionic lipids on a silica surface (Evans, 2008a). A real-time investigation of liposomal binding, under dynamic flow conditions, onto target proteins immobilized at the sensor with simultaneous damping analysis gave an insight into the nature of liposomal deformation or spreading at the target surface (Hopfner *et al.*, 2008). Ishizuka-Katsura *et al.* found that 1,2-dioleoyl-sn-glycero-3-phosphocholine (DOPC) vesicles rapidly adsorbed on a dithiobis(1-deoxy-glucitol-1-carbamoyl pentane) self-assembled monolayer to form a lipid layer of physisorbed intact vesicles (Ishizuka-Katsura *et al.*, 2008).

Bidirectional transfer of phospholipids between a charged, supported lipid bilayer on silica and oppositely charged, unilamellar vesicles was studied by means of QCM and optical reflectometry techniques with various possible mechanistic scenarios, including monomer insertion and hemifusion models (Kunze *et al.*, 2009a; Kunze *et al.*, 2009b). Liu *et al.* investigated the adsorption of poly(ethylene glycol) (PEG) with different end groups onto phospholipid membranes at the liquid/solid interface by use of a QCM with dissipation in real time. The experiments demonstrated that PEG chains with sufficient hydrophobic end groups (PEG-C(18)H(37)) can insert in the bilayer and form aggregates on the membrane surface (Liu *et al.*, 2009). Larger membrane constructs were produced and their formation observed with QCM by multilayer film assembly of polystyrene sulfonate, poly(allylamine hydrochloride) and 50 nm diameter 1,2-dioleoyl-sn-glycero-3-phosphocholine (DOPC) liposomes on planar substrates (Stadler *et al.*, 2009). The findings

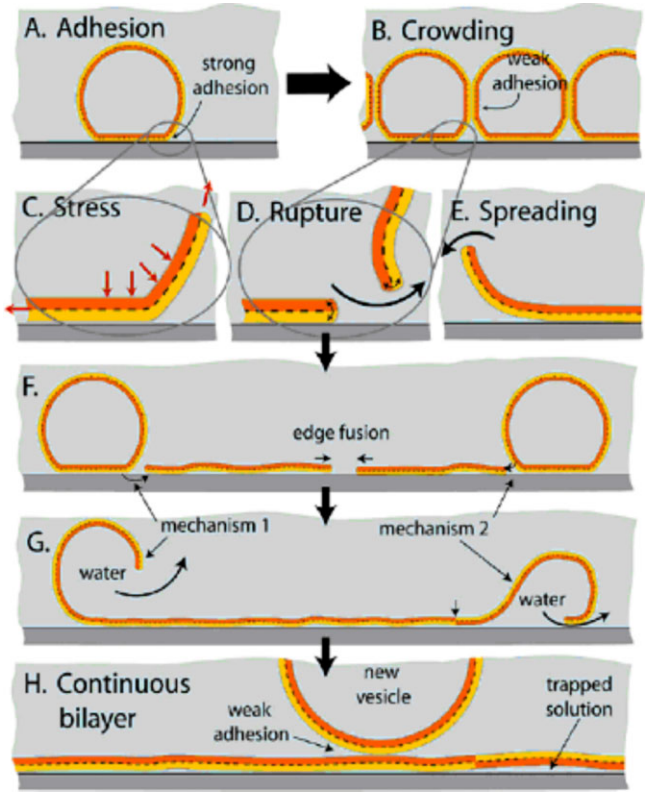

Figure 10. Different stages of vesicle adsorption: (A) adhesion, (B) crowding, (C–E) stress-induced rupture and spreading of bilayer patches that can expose either leaflet by either mechanism 1 or 2, (F,G) coalescence of high energy edges and and expulsion of water and excess lipid, and (H) growth of patches into a continous bilayer; further adsorption to the bilayer is weak and does not lead to their rupture or spreading. From (Anderson *et al.*, 2009), repinted with permission.

were then correlated to the film growth of the polyelectrolytes and structurally intact liposomes on silica particles. Upon removal of the silica template core, stable capsosomes containing one or two layers of intact liposomes as cargo were obtained.

Anderson *et al.* studied the deposition of dimyristoyl-phosphatidylcholine (DMPC) bilayers on various glass surfaces from vesicles in various aqueous solutions and temperatures using QCM (Anderson *et al.*, 2009) (Figure 10). A disposition study of different unsaturated fatty acids in alkane solution onto steel surfaces showed that depending on the fatty acid used either monolayers or multilayers were formed (Lundgren *et al.*, 2007). QCM with impedance analysis was used to monitor both the kinetics and viscoelastic properties of tether adsorption and vesicle fusion in tethered bilayer lipid membranes (tBLMs) (Dorvel *et al.*, 2007). Other applications of QCM in the area of artificial membranes and vesicles include the controlled radial distribution of nanoscale vesicles during binding to an oscillating QCM surface (Edvardsson *et al.*, 2007), deposition of vesicles on a hydrated cationic poly(diallyldimethylammonium chloride) layer as a function of phospholipid composition and sodium chloride concentration (Tang *et al.*, 2009), effect of docosahexaenoic acid on phosphocholine-supported lipid bilayers (Thid *et al.*, 2007), planar phospholipid bilayers supported on silicon dioxide surfaces with and without incorporation of glycolipids (Weng *et al.*, 2006), the adsorption of micelles or vesicles made from

polystyrene-β-poly(N-isopropylacrylamide) diblock copolymers onto gold surfaces (Yan *et al.*, 2006) and vesicles composed of DEPC and DMPG and their adsorption onto gold and silica sufaces (Evans, 2008b).

A layer-by-layer (LBL) assembly composed of liposomes and the membrane protein bacteriorhodopsin (bR) was fabricated by Nakane and Kubo (2009). The liposomes were found to be stacked regularly until the 8th layer of the liposome and the effect of nonylphenol on layer stability was investigated (Nakane and Kubo, 2009).

Membrane formation

Another detailed study of the mechanics of lipid bilayer formation via vesicle adsorption was carried out by Gromelski *et al.* who used QCM to show that depending on the chemical structure of the lipids, two different pathways are followed on SiO_2 surfaces: (i) vesicle adsorption occurs in a first step until a critical coverage is reached, followed by vesicle rupture and bilayer formation, or (ii) adsorption and vesicle rupture occur almost simultaneously (Gromelski *et al.*, 2009). In the case of polyelectrolyte cushions, both neutron reflectivity and quartz crystal microbalance experiments showed that the formation of homogeneous DMPC bilayers was significantly better on the negatively charged PSS surface compared to the positively charged PAH surface. Results obtained by Okazaki *et al.* indicated that the edges of polymeric bilayers catalyse the formation of substrate-supported planar lipid bilayers by destabilizing adsorbed vesicles, whereas polymeric bilayers and embedded fluid bilayers form a continuous hybrid bilayer membrane, sealing energetically unfavorable bilayer edges (Okazaki *et al.*, 2006).

SiO_2 particles with well-defined surface topology were used with 1-palmitoyl-2-oleoyl-sn-glycero-3-phosphocholine (POPC) lipid vesicles to examine effect of nanotopology on the adsorption and supported phospholipid bilayer formation (Pfeiffer *et al.*, 2008). Other studies looked at systems containing DPPC and monoolein, and the influence of lipid and solvent composition on membrane formation (Viitala *et al.*, 2007; Wang and Yang, 2008). Reimhult *et al.* used a setup for parallel QCM-D and SPR measurements to measure the kinetics of vesicle-to-bilayer transformation on SiO_2 and vesicle adsorption on Au, respectively. The combination of SPR and QCM, complemented by atomic force microscopy measurements, enabled a complete, time-resolved separation of vesicle and bilayer coverage, which allowed precise quantification of the critical surface coverage of vesicles needed for rupture (Reimhult *et al.*, 2006). Patel and Frank found evidence of a one-step mechanism for bilayer formation of tethered vesicles and monitored the subsequent adsorption and binding of streptavidin, biotinylated vesicles, and streptavidin-coated microspheres. For all three constructs a critical surface density was identified, above which a significant amount of coupled interstitial water contributed to the response of the quartz resonator in a phenomenon similar to dynamic coupling ascribed to surface roughness (Patel and Frank, 2006). The bilayer-tethered vesicle assembly was then used create an immunosensor with a model antibody-hapten system (Patel *et al.*, 2009a).

The structural transformation of lipid vesicles to a bilayer was also shown to be accompanied by significant changes in their physical properties (Cho *et al.*, 2007c). After the adsorption and saturation of intact vesicles onto a gold surface, the adsorbed vesicle layer exhibited a soft, water-rich, viscoelastic state. An amphipathic helix peptide, a vesicle-destabilizing agent, was then added to trigger the formation of a much thinner (approximately 5 nm), compact and rigid bilayer. The effect of monovalent and divalent cations on formation of supported phospholipid bilayers via deposition of palmitoyloleoyl phosphatidylcholine (POPC) vesicles on a SiO_2 support was investigated in a study by Seantier and Kasemo (2009). They found that very small concentrations of divalent cations could cause a strong reduction of the critical coverage, where conversion of intact, adsorbed vesicles to a bilayer occurs. This bilayer promoting effect increased in the order $Sr^{2+} < Ca^{2+} < Mg^{2+}$ (Seantier and Kasemo, 2009). In a similar manner, QCM was used in a study looking at the membrane destabilizing effects of ethylenediaminetetraacetic acid (EDTA) (Prachayasittikul *et al.*, 2007). Liposome deposition onto carboxylic acid-terminated self-assembled monolayers resulted in planar mono- and multilayer, vesicular and composite membranes, as a function of liposome size and composition. Quartz crystal microbalance data provided estimates for layer thicknesses and sheer moduli and were used for classification of the final structure (Mechler *et al.*, 2009). Sapper *et al.* used QCM to monitor the deformation of surface-bound giant liposomes by applying an electric field with small amplitudes. Changes in the apparent height of attached vesicles in the nanometer range were easily detected as a function of lipid composition (Sapper and Janshoff, 2006).

Membrane interactions

Wikstrom *et al.* (2008) investigated the interaction of positively and negatively charged lipid vesicles with supported lipid bilayers of opposite charge. The vesicle-bilayer interaction leads initially to adsorption of lipid vesicles on the bilayer; eventually, the vesicles (and possibly other lipid structures) desorb from the bilayer surface. This was explained in terms of initial strong electrostatic attraction between the added vesicles and the bilayer, forming a structure where lipid transfer between the two bilayers occurs on a time scale of 10–40 min. This lipid transfer causes a charge equilibration with an accompanying weakening of the attraction, and eventually repulsion, between the bilayer and vesicles, leading to desorption of vesicles from the bilayer (Wikstrom *et al.*, 2008). The interactions of unmodified versus PEGylated lectin-grafted liposomes with model glycolipids-containing membranes were studied reported (Bakowsky *et al.*, 2008). The interaction of chitosan with phospholipid monolayers as cell membrane model showed that chitosan was able to remove β-lactoglobulin from negatively charged dimyristoylphosphatidic acid and dipalmitoylphosphatidyl glycerol membranes (Caseli *et al.*, 2008). Using polyethersulfone as a model membrane surface Liu *et al.* studied the adsorption kinectics and viscoelastic behaviours of the adsorbed surfactant layers of sodium laureth sulfate, cocamidopropyl betaine and their mixed solution (Liu and Kim, 2009b).

Lee *et al.* studied water transport through stacked intercellular lipid membranes found in the stratum corneum is the outermost layer of the epidermis by using QCM and and a model SC membrane. (Lee *et al.*, 2009). Other systems studied by QCM include binding of F-actin to lipid bilayers containing ponticulin (Barfoot *et al.*, 2008), the interaction of chitosan and layers of dimyristoyl phosphatidic acid (Pavinatto *et al.*, 2007), and the interaction between phospholipid monolayers and water-soluble ethanol (Yamamoto *et al.*, 2006).

Membrane-protein interactions

QCM is a technology well suited for studying both the interaction between a protein and its target membrane and for screening for developing inhibitors of that interaction. Trepout *et al.* (2007) reported a method to reconstitute a membrane receptor into a lipid membrane in a selective orientation on a solid support. The membrane protein reconstitution process was carried out on silica nanoparticles and on planar silica surfaces, and was characterized by cryo-electron microscopy and QCM (Trepout *et al.*, 2007). QCM was used to demonstrate sequence specific immobilization of DNA modified liposomes created from the cellular membrane extracts of insect cells that were used to express transmembrane G-protein coupled receptors (GPCRs). Microarrays of GPCRs on a chip surface embedded in a membrane were generated this way (Bailey *et al.*, 2009). QCM with dissipation monitoring and SPR techniques were used to investigate new approach for surface immobilization of trans-membrane proteins where the proteins were immobilized on a surface in a proteoliposome multilayer structures (Graneli *et al.*, 2007).

To address the question of how annexins, which participate in various membrane-related processes, including endocytosis and exocytosis, bind to and aggregate membranes, the association of annexin A6 (Buzhynskyy *et al.*, 2009), annexin A5 (Garnier *et al.*, 2009) and annexin A1 (Kastl *et al.*, 2006; Faiss *et al.*, 2008) with model phospholipid membranes was studied using QCM and other techniques. Another important membrane-protein interaction probed by QCM was the membrane association of the hepatitis C virus NS5A protein, which is required for viral replication (Cho *et al.*, 2007a). The N-terminal amphipathic helix within NS5A was subsequently found to be able to lyse lipid vesicles that served as a model system for virus particles (Cho *et al.*, 2009). In a study investigating the effects of pulmonary surfactant protein B, QCM was found to provide a useful, simplified way to mimic the effect of surfactant protein on vesicle dynamics and permit a detailed characterization of the parameters governing the reorganization of surfactant layers (Cabre *et al.*, 2009). Similar results were obtained using phytase, a protein that also shows surface activity (Caseli *et al.*, 2006b).

The cytoplasmic peripheral membrane protein ezrin plays a key role in cell surface structure adhesion, migration, and organization. Its adsorption onto L-α-phosphatidylinositol-4,5 -bisphosphate (PIP(2)) containing solid-supported membranes was investigated using QCM (Herrig *et al.*, 2006). The lipid II binding kinetics of the natural peptide antibiotics gallidermin (Christ *et al.*, 2008) and nisin (Christ *et al.*, 2007) in model membranes were studied using QCM. Other antibacterial peptides that interact with bacterial membranes were also studied using QCM (Umeyama *et al.*, 2006; Mechler *et al.*, 2007), and a combined study using QCM and NMR found evidence of transmembrane pore formation (Sherman *et al.*, 2009).

The importance of membranes in the molecular recognition of membrane receptors could be demonstrated in a study looking at the binding between IgG and Staphylococcal Protein A oligo B domains with long trialkyl-tags immobilized in a lipid bilayer. IgG-LppB1 binding was found to be largely restricted because of steric hindrance on the lipid surfaces (Mitomo *et al.*, 2007). Nobre *et al.* immobilized a carbohydrate rich *Neurospora crassa* alkaline phosphatase in monolayers of the sodium salt of dihexadecylphosphoric acid, a synthetic phospholipid that provides very condensed Langmuir films. The binding of the alkaline phosphatase to Langmuir-Blodgett lipid films was mediated by the anionic polysaccharide iota-carrageenan, and the polysaccharide was found to be essential to promote the interaction between DHP and NCAP and also to increase the fluidity of the film (Nobre *et al.*, 2009).

Using QCM Turner *et al.* demonstrated that a molecular imprinting approach can be used to generate monolayers with enhanced affinity for specific proteins (Turner *et al.*, 2007). Monolayers consisting of cationic dioctadecyldimethylammonium bromide, non-ionic methyl stearate, and poly(ethylene glycol) bearing phospholipids were imprinted with ferritin at the air/water interface of a Langmuir-Blodgett trough and transferred hydrated to hydrophobic substrates for study. This immobilization was shown by fluorescence correlation spectroscopy to significantly hinder any further diffusion of lipids, while rebinding studies demonstrated up to a six-fold increase in ferritin adsorption to imprinted versus control monolayers.

VIRUSES

The versatility of QCM detection and the ability to sense particles in the order of 100–1000 nm diameter range has been exploited by a number of researchers in the field of viral detection and diagnosis, phage display and the interaction of virus particles with various surfaces.

Detection of viral particles

Peduru Hewa *et al.* used QCM for the rapid and sensitive detection of influenza A and B viruses (Peduru Hewa *et al.*, 2009). The limit for detection by QCM for stock preparations of both A/PR/8/34 and B/Lee/40 viruses was 10^4 pfu/mL. Conjugation of 13 nm gold nanoparticles to the detecting antibody improved the mass sensitivity, resulting in a ten-fold increase in sensitivity and a detection limit of 10^3 pfu/mL. A comparison of results obtained from 67 clinical samples using existing RT-PCR, shell vial, cell culture and ELISA methods showed that QCM techniques were comparable in sensitivity and specificity to the cell culture methods (Table 3). A QCM-based sensor for the direct detection of aerosolized influenza A virions utilizing surface-bound antibody with a limit of detection of 4 virus particles/mL was reported by Owen *et al.* (2007). A QCM DNA biosensing method using oligonucleotide-functionalized gold nanoparticles (AuNP) to amplify the detection signal for the detection of dengue virus was developed by Chen *et al.* (2009b). They were able to detect dengue viral RNA via RT-PCR amplification and QCM detection of the resultant amplified DNA in virus-contaminated serum. The sensitivity and specificity of this RT-PCR-QCM method with nanoparticle technology showed it to be comparable to the fluorescent real-time PCR methods.

Polyclonal and monoclonal antibodies developed against soluble ebola virus envelope glycoprotein were used to detect ebola virus in a study utilizing QCM as well as SPR and ELISA techniques (Yu *et al.*, 2006). Polyclonal and monoclonal antibodies were used in combination to identify and differentiate both human and non-human primate ebola virus glycoproteins. QCM was also used for real-time detection of airborne Vaccinia viruses (Lee *et al.*, 2008b). The capture rate varied linearly with the concentration of initial virus suspensions (8.5×10^8 to 8.5×10^{10} particles/mL) at flow rates of two and one L/min, respectively. This observation is consistent with mass transport-limited

Table 3. Results obtained for shell vial, standard cell culture, ELISA, Directigen Flu A and QCM methods in comparison with RT-PCR. (Data from Peduru Hewa *et al.*, 2009)

		No of specimens							
Test	TP[a]	TN[b]	FP[c]	FN[d]		Sensitivity[e]	Specificity[f]	PPV[g]	NPV[h]
Shell vial	*Influenza A*	*28*	*27*	*3*	*9*	76	90	80	75
	Influenza B	*12*	*52*	*0*	*3*	80	100	100	95
Cell culture	*Influenza A*	30	30	0	7	81	100	100	81
	Influenza B	15	52	0	0	100	100	100	100
ELISA	*Influenza A*	25	30	0	12	68	100	100	71
	Influenza B	9	52	0	6	60	100	100	90
Directigen Flu A	*Influenza A*	13	30	0	24	35	100	100	56
	Influenza B	NA	NA	NA	NA	NA	NA	NA	NA
QCM	*Influenza A*	28	30	0	9	76	100	100	77
	Influenza B	12	52	0	3	80	100	100	95
QCM (nanoparticles)	*Influenza A*	30	30	0	7	81	100	100	95
	Influenza B	13	52	0	2	87	100	100	96

A total of 67 nasal samples were compared with RT-PCR which was used as the reference method (gold standard).
Samples positive by shell vial, standard cell culture, ELISA, Directigen Flu A kit and QCM, but negative by RT-PCR, were considered FP. Samples that were identified by RT-PCR assays were considered as TP. Samples that were negative by shell vial, standard cell culture, ELISA, BD Directigen Flu A kit and QCM but positive by PCR were regarded as FN. A sample that was negative by RT-PCR was a TN.
[a] TP, true-positives;
[b] TN, true-negatives;
[c] FP, false-positives;
[d] FN, false-negatives;
[e] Sensitivity = number of TP specimens/(number of TP + number of FN specimens) × 100;
[f] Specificity = number of TN specimens/number of TN;specimens + number of FP specimens) × 100;
[g] PPV (positive predictive value) = TP/(TP + FP) × 100;
[h] NPV (negative predictive value) = TN/(TN + TN) × 100.

binding, most likely due to the dimensions of the flow cell used in this case. Other applications include a comparison study between QCM and carbon nanotube sensor detection of influenza virus hemagglutinin with randomly immobilized anti-hemagglutinin antibody (Takeda *et al.*, 2007), and the detection of M13 virus antibodies on a surface coated with M13 virus particles with a reusable detector and a limit of detection of 7 nM or 1.3 pmol of antibody (Yang *et al.*, 2008b).

Another very interesting area of virus detection using QCM is the use of molecular imprinting techniques to generate polymer surfaces with artificial binding sites for viruses. Tai *et al.* produced a QCM surface coated with molecularly imprinted polymers specific for dengue nonstructural protein 1 to develop a serologic technique for the diagnosis of early viremia in dengue (Tai *et al.*, 2006). Serum samples from patients with confirmed cases of dengue were compared with the results of monoclonal ELISA; QCM signals were >15 Hz in 18 of 21 (86%) of dengue samples and in 0 of 16 control samples. The correlation of the QCM response and the ELISA result was $R^2 = 0.73$ with CVs of between 4 and 28%. Jenik *et al.* used QCM and molecular imprinting techniques to created patterned polyurethane layers adapted to bind human rhinovirus (HRV) and the foot-and-mouth disease virus, two representatives of picornaviruses (Jenik *et al.*, 2009). The imprinted polymer was able to distinguish between different HRV serotypes (HRV1A, HRV2, HRV14, and HRV16, respectively) with a selectivity factor of three, regardless of the group (major/minor) to which the samples belonged. The same selectivity factor could be observed between HRV and foot-and-mouth disease virus.

Phages and phage display techniques

Immobilized phages have been used for the detection of β-galactosidase from *E. coli* with a detection limit of a few nanomoles (Nanduri *et al.*, 2007), and of prostate specific membrane antigen and antibody (Yang *et al.*, 2006b). A T7 phage display pool was screened for affinity towards the synthetic ligand for FK506-binding protein and irinotecan (Takakusagi *et al.*, 2008a), methotrexate (Takakusagi *et al.*, 2008b), and C10 biotinylated camptothectin (Takakusagi *et al.*, 2007). A similar approach using phage display also led to the identification of peptides with specific binding for SiO_2 and TiO_2 (Chen *et al.*, 2006).

Virus particles and surfaces

The binding of bacteriophage MS2 to bare silica and Suwannee River Natural Organic Matter was investigated (Yuan *et al.*, 2008; Pham *et al.*, 2009). Multilayers of viral nanoparticles (VNP) were generated using either alternating deposition of biotinylated cowpea mosaic virus (CPMV) and streptavidin (Steinmetz *et al.*, 2008a) or alternating layers of chemically modified CPMV and tobacco mosaic virus (Steinmetz *et al.*, 2008b). CPMV was also used together with poly(diallyldimethylammonium chloride) in a layer-by-layer assembly to generate biologically active surfaces for cell culture (Lin *et al.*, 2008). QCM was also used to monitor the directed platinum cluster deposition on a surface of genetically engineered TMV with the aim to construct nanoscaled platinum conductors (Lee *et al.*, 2006).

Journal of Molecular Recognition

PROTEIN INTERACTIONS

The interactions of proteins with one another and the adsorption of proteins onto solid surfaces are extremely important processes that have received increasing attention in medicine, biotechnology, diagnostics and food technology. QCM permits the monitoring of *in situ* adsorption, protein–protein interactions and can provide evidence of conformational effects in real time. Notably, acoustic sensing is not limited to the use of optically transmittive or reflective materials, as is the case with more traditional techniques. Consequently, QCM sensors devices have been widely employed to monitor biomolecule adsorption onto quartz, gold, self-assembled monolayers, graphite, polymer films, hydroxyapatite, lipid films and many other surfaces.

Protein adsorption: metal and metal oxides

Chen *et al.* studied the interaction between peptides and titanium oxide surfaces by using point mutants of a TiO_2-binding peptide. (Chen *et al.*, 2008). A comparison of Au and hydroxyapatite surfaces and their ability to bind fibronectin showed that the fibronectin uptake is larger on Au as compared with hydroxyapatite (Dolatshahi-Pirouz *et al.*, 2009). Fogel *et al.* examined the use of the QCM as a tool for fundamental analyses of a sensor for the enhanced detection of glucose constructed by the immobilization of cobalt(II) phthalocyanine and glucose oxidase (GOx) onto a Au-quartz electrode. The amount of GOx bound using the model system compared favourably to calculations derived from the maximal amperometric functioning of the electrochemical sensor but not to theoretical values derived from dimensions of GOx as established by crystallography (Fogel *et al.*, 2007). Hemmersam *et al.* studied the adsorption of fibronectin on gold, titanium, and tantalum oxide and found that the surface chemistry influenced the frequency shift observed during adsorption. The data was further analysed using the random sequential adsorption model, and the adsorption rate parameter k_{ass} was found to provide a means to determine the degree of hydration of the adsorbed protein layer (Hemmersam *et al.*, 2008). QCM in combination with electrochemical impedance spectroscopy has been utilized to monitor *in situ* anti-human IgG adsorption on several Au-based surfaces, bare Au, nanogold/4-aminothiophenol colloids, and multi-walled carbon nanotubes on Au, and succeeding human IgG reactions (Jia *et al.*, 2007).

A patterned two-dimensional hexagonally ordered array of ferritin molecules, the outer surfaces of which had been genetically modified by titanium specific binding peptides, was realized in a self-assembling manner on a hexagonal Ti thin film island made on a silicon substrate (Matsukawa *et al.*, 2009). Bare Si substrate and amino-modified Si substrates were the surfaces used in a QCM study of the adsorption kinetics and energy dissipation of poly(ethylene glycol)-modified ferritins with various molecular weights (Kumashiro *et al.*, 2008). Reimhult *et al.* report on a comparison of the ability of traditionally used blocking agents and poly(ethylene glycol) derivatives to prevent protein adsorption on both gold and polystyrene surfaces and showed that on pure gold the PEG-thiols are superior to the other blocking molecules tested (Reimhult *et al.*, 2008). Kacar *et al.* (2009) demonstrate the utilization of gold binding peptide as a molecular linker genetically fused to alkaline phosphatase and immobilized on gold substrate. The binding and enzymatic activities of the bi-functional fusion constructs were analysed using quartz QCM and biochemical assays. Self-immobilization of the bi-functional enzyme on micro-patterned substrates showed higher enzymatic activity per area compared to that of native alkaline phosphatase (Kacar *et al.*, 2009). The gold binding peptide itself and its adsorption kinetics were also studied (Tamerler *et al.*, 2006a; Tamerler *et al.*, 2006b).

Pillai *et al.* (2009) utilized an aqueous extract of fish proteins as a coating for minimizing the adsorption of fibrinogen and human serum albumin. The surfaces pre-treated this way included stainless steel, gold, silicon dioxide and polystyrene (Pillai *et al.*, 2009). The adsorption of albumin onto ceramic surfaces for biomedical applications (TiN, TiNbN, TiCN) was also studied (Serro *et al.*, 2009). Yang *et al.* studied the formation of apatite induced by negatively charged nanocrystalline TiO_2 coatings soaked in simulated body fluid; different stages were clearly observed in the process of apatite precipitation, indicating two different kinetic processes (Yang *et al.*, 2007). After fabrication of a hydroxyapatite ultra-thin layer on a gold surface the *in situ* adsorption mechanism and conformational changes of fibrinogen on gold, titanium and hydroxyapatite surfaces were investigated (Monkawa *et al.*, 2006). QCM and ellipsometry showed that during adsorption of fibrinogen on evaporated tantalum films the saturation uptake increases with increasing root-mean-square roughness (from 2.0 to 32.9 nm) beyond the accompanying increase in surface area. This increase was attributed to a change in the geometrical arrangement of the fibrinogen molecules on the surface. For comparison, the adsorption of a nearly globular protein, bovine serum albumin, was studied and it was found that the adsorption was less influenced by the roughness. Monte Carlo simulations taking into account surface roughness and the anisotropic shape of fibrinogen reproduced the experimentally observed trend (Rechendorff *et al.*, 2006). Hydrophobin, a small fungal protein that self-assembles on interfaces and significantly changes the surface wetability, was used to generate a self-assembled film on a gold surface. The protein film improved the surface hydrophilicity and the self-assembled film remained stable under different pH values ranging from 1 to 13. A hydrophilic protein such as choline oxidase was then successfully immobilized on the hydrophobin-modified gold surface (Zhao *et al.*, 2009b).

Other studies looked at different proteins and metal/metal oxide surfaces: bovine serum albumin adsorption on rough platinum surfaces (Dolatshahi-Pirouz *et al.*, 2008), the influence of roughness on the adsorption of fibronectin onto tantalum surfaces (Hovgaard *et al.*, 2008), adsorption of albumin, lysozyme and lactoferrin onto thin films of polyhydroxymethylsiloxane and SiO_x made by oxygen plasma treatment (Messina *et al.*, 2009), adsorption behaviours of lysozyme on Au, SiO_2, and TiO_2 surfaces (Nezu *et al.*, 2008), the influence of spacer length on heparin coupling efficiency and fibrinogen adsorption of modified titanium surfaces (Tebbe *et al.*, 2007), enamel matrix proteins on the enamel surface and their effect on the biomineralization of hydroxyapatite (Wang *et al.*, 2009), deposition kinetics of extracellular polymeric substances on silica (Zhu *et al.*, 2009), carboxylate coordination chemistry which relies on Zr^{4+} ion coordination chemistry that involves carboxyl terminal groups present on the protein (Mazur *et al.*, 2007).

Protein adsorption: quartz

Al-Jawad *et al.* used QCM to investigate the amount of fibronectin adsorbed, the layer density, thickness and structure of films

adsorbed to polished silicon oxide surfaces (Al-Jawad *et al.*, 2009). The adsorption of the amelogein protein mixture enamel matrix derivate (EMD) to silica surfaces has been studied. The protein was found to adsorb as nanospheres in mono- or multilayers, depending on the concentration of nanospheres available in solution (Halthur *et al.*, 2006). Sum frequency generation vibrational spectroscopy and QCM were employed by York *et al.* to study the interfacial structure and adsorbed amount of the amino acids L-lysine and L-proline and their corresponding homopeptides, poly-L-lysine and poly-L-proline, at two liquid-solid interfaces: hydrophobic d8-PS and the hydrophilic SiO_2 liquid-solid interface (York *et al.*, 2009).

Protein adsorption: self-assembled monolayers (SAMs) and polymer films

Belegrinou *et al.* studied the pH-dependent immobilization of bovine serum albumin, lysozyme, lactoferrin and fibronectin on surfaces functionalized by plasma-enhanced chemical vapor deposition of poly(acrylic acid)- and poly(ethylene oxide)-like films (Belegrinou *et al.*, 2008). Two antibody immobilization procedures were compared to set up an immunosensor for goat anti-rabbit immunoglobulin. Both cases used SAMs and the antibody was either covalently bound or immobilized via affinity to protein A. QCM measurements showed that the viscoelastic properties of the antibody layer were markedly modified during the antigen recognition when the antibody was bound by affinity to protein A (Briand *et al.*, 2007) and that the composition of the SAM played a part as well (Briand *et al.*, 2006). Hamlin *et al.* (2007) studied the immobilization of β-galactosidase onto polyelectrolyte multilayer assemblies of the polyanion poly[1-[4-(3-carboxy-4-hydroxyphenylazo)-benzenesulfonamido]-1,2-ethanediyl, sodium salt] and the polycation poly(ethylenimine) constructed by electrostatic self-assembly. Although comparable amounts of β-galactosidase were incorporated onto both surfaces, enzymatic activity was substantially inhibited when the β-galactosidase was immobilized on the polyanionic surface compared to the enzyme on the polycationic surface (Hamlin *et al.*, 2007).

Malmstrom *et al.* (2007) evaluated the capacity of QCM to be used as a quantitative technique on a nanostructured surface, where protein is adsorbed specifically in a nanopattern exploiting PLL-g-PEG as a protein-resistant background. They could show that laminin, an important cell adhesive protein that is central in developmental biology, forms a highly hydrated protein layer with different characteristics depending on the underlying substrate. Using a combination of QCM and atomic force microscopy data from nanostructured surfaces, they modeled laminin and antibody binding to nanometer-scale patches. A higher amount of laminin was found to adsorb in a thicker layer of a lower effective density in nanopatches compared to equivalent homogeneous surfaces. The results suggest that modeling of QCM data of soft viscoelastic layers arranged in nanopatterns may be applied where an independent measure of the 'dry' mass is known (Malmstrom *et al.*, 2007).

A highly sensitive biomolecule sensor using gold nanoparticles as signal amplification probes employed a streptavidin-biotin interaction as a model system and showed good linearity over a wide range from 1 ng/mL to 10 ug/mL for the quantitative streptavidin target molecule analysis (Kim *et al.*, 2007c). The adsorption characteristics of three proteins (bovine serum albumin, myoglobin and cytochrome c) onto self-assembled monolayers of mercaptoundecanoic acid on both gold nanoparticles and gold surfaces were described (Kaufman *et al.*, 2007). The incorporation of myoglobin into layer-by-layer assemblies together with hyaluronic acid and the resulting physico-chemical properties of the films have been studied using QCM and other techniques by a number of publications (Liu and Hu, 2006; Liu *et al.*, 2006b; Liu *et al.*, 2006d; Liu *et al.*, 2007; Lu and Hu, 2007).

Biocompatible and non-fouling poly(oligo(ethylene glycol) methacrylate) (pOEGMA) films with various thicknesses were formed on gold and Si/SiO_2 substrates by a combination of the formation of self-assembled monolayers and polymerization reactions and the surface biotinylated. These novel films gave enhanced signal-to-noise ratio (approximately ten-fold enhancement) for the bio-specific binding of streptavidin compared with the biotinylated substrate prepared from carboxylic acid-terminated SAMs (Lee *et al.*, 2007). Nonionic poly(ethylene glycol) and ZrO_2 nanoparticles were successfully assembled into layer-by-layer films on solid surfaces through coordination interaction between the ether oxygen groups in PEG and the Zr(IV) in ZrO_2 nanoparticles; the films were then loaded with myoglobin (Qiao and Hu, 2009). Mixed protein/dendrimer assemblies have been constructed with proteins differing in charge, nature of the prosthetic groups and sizes such as lysozyme, cytochrome c, polyhemic cytochrome c_3 or glucose oxidase. Generally, the stability of adsorbed films was limited to one dendrimer/protein bilayer (Lojou and Bianco, 2006).

Protein adsorbed from fetal bovine calf serum onto three oxygen-containing biomedical polymers: polycaprolactone, poly(ethylene glycol) and poly(methyl methacrylate) after Ar and He implantations using ion beam modification was studied using QCM and the resulting surfaces evaluated for the response of human mesenchymal stem cells (Manso *et al.*, 2007). Roach *et al.* (2006) described the use of 'Nano Orange', a fluorometric probe, to quantitatively assess the adsorption of bovine fibrinogen and albumin onto model hydrophilic and hydrophobic surfaces. Results obtained using this method allowed the calibration of data obtained on the same surfaces using quartz crystal microbalance measurements and an amido black protein assay (Roach *et al.*, 2006). Reisch *et al.* (2009) were able to demonstrate that protein adsorption can be strongly reduced or completely suppressed through the deposition of only one layer of polyelectrolyte modified with phosphorylcholine and/or $(ethylene\ oxide)_3$ groups. These moieties were grafted on poly(acrylic acid) and totally prevent protein adsorption for grafting ratios of 25% or more (Reisch *et al.*, 2009). Protein repellent surfaces were designed by using hydroxyethyl- and ethyl(hydroxyethyl) cellulose and hydrophobically modified analogues of these polymers. These were both found to completely hinder biofouling when deposited on the gold substrates (Volden *et al.*, 2009). Another protein repellent surface investigated by QCM is an organosilane self-assembled monolayer with perfluoroalkyl groups (Kira *et al.*, 2009). Modification of a surface with densely packed poly(ethylene glycol) brush layer was studied to improve the protein repellent ability of the surface. The density of the PEG brushed layer substantially increased with repetitive adsorption/rinse cycles of the PEG on the gold substrate, allowing significant reduction of nonspecific protein adsorption (Satomi *et al.*, 2007). The removal of proteins such as lysozyme from the solid-liquid interface has been investigated using a quartz crystal microbalance on both hydrophobic and hydrophilic surfaces. 'Nanobubbles', the common surfactant sodium dodecyl sulfate (SDS), and nanobubbles in combination with SDS were used as cleaning agents.

On hydrophobic surfaces SDS proved superior, whereas on hydrophilic surfaces the combination led to complete removal of the protein (Liu and Craig, 2009).

QCM has also been used in studies looking into the protein film structure of fibrinogen adsorbed to acrylic polymeric substrates with varying polymer chain flexibility (Berglin *et al.*, 2009) and various other polymeric surfaces (Osaki *et al.*, 2006; Weber *et al.*, 2007), to monitor the immobilization of tyrosinase on polycationic and polyanionic precursor assemblies (Gormally *et al.*, 2009), the adsorption of type I collagen (Gurdak *et al.*, 2006), interaction and adsorption of glucose oxidase on poly(methyl methacrylate)-bovine serum albumin particles (He *et al.*, 2009), adsorption of variants of the *Thermomyces lanuginosus* lipase onto a hydrophobic surface (Otzen, 2008), the adsorption profile and viscoelastic properties of bovine submaxillary gland mucin and bovine serum albumin (Feiler *et al.*, 2007), viscoelastic properties of the blue mussel, *Mytilus edulis*, foot protein 1 (Mefp-1) (Hedlund *et al.*, 2009), adsorption reversibility and viscoelastic properties of ribonuclease A adsorbed to hydrophobic self-assembled monolayers (Jordan and Fernandez, 2008), the adsorption process of β-lactoglobulin on a polyethersulfone-coated surface (Kim *et al.*, 2007a), the adsorption of whey protein onto a polyethersulfone membrane surface (Liu and Kim, 2009a), construction of nanosize gold hollow balls (NGB) with dendritic surface as the immobilized affinity support for aflatoxin B_1 antibody (Liao, 2007), the adsorption of lysozyme onto acrylic-based hydrogels (Lord *et al.*, 2006c), the adsorption of different proteins onto polyurethanes containing poly(ethylene glycol), poly(propylene glycol), or poly(dimethylsiloxane) soft segments (Ma *et al.*, 2009), immobilization of immunoglobulins specific to the human cytokine Transforming Growth Factor β1 and to paclitaxel (Pastorino *et al.*, 2007), reversible binding of the Anx5 protein onto PS-β-P(PEMA-co-HEMA) block copolymer micelles in the presence of Ca^{2+} ions (Schmidt *et al.*, 2008), inclusion of BSA into polyelectrolyte multilayers (Watanabe *et al.*, 2008), nonspecific hydrophobic interactions of a repressor protein, PhaR, with poly[(R)-3-hydroxybutyrate] films (Yamashita *et al.*, 2006), adsorption of the antimicrobial peptide histatin 5 on poly(methyl methacrylate) surfaces modified using a cold plasma technique (Yoshinari *et al.*, 2006), and the effect of hydrolysis of polyester surfaces for protein adsorption (Atthoff and Hilborn, 2007).

Conformational changes in protein films

The importance of the immobilization method in the ability of the QCM to track conformational changes in a protein bound to the sensor surface was demonstrated in a study by Baltus *et al.* (2007). Two different approaches were used to attach a genetically altered α-estrogen receptor to the gold electrode on the quartz surface: (i) the mutant receptor containing a single solvent-exposed cysteine was directly attached to the crystal via a sulfur to gold covalent bond, forming a self-assembled protein monolayer and (ii) the N-terminal histidine-tagged end was utilized to attach the receptor via a 3,3-dithiobis [N-(5-amino-5-carboxypentyl)-propionamide-N′,N′-diacetic acid] linker complexed with nickel. Both constructs have previously been shown to bind the substrate, but whereas exposure of the receptor directly attached to the piezoelectric crystal to the ligand 17-β-estradiol resulted in a measurable frequency response, consistent with a change in conformation of the receptor with ligand binding, no response was observed when the receptor immobilized via the linker was exposed to the same ligand (Baltus *et al.*, 2007). Azzaroni *et al.* investigated in detail the supramolecular bioconjugation of streptavidin on biotinylated self-assembled monolayers by using QCM. The biomolecular reorganization within the film at the early stage involved a significant increase in surface coverage followed by a second stage where the streptavidin layer slowly reached asymptotic coverage. Finally, a reorganization process takes place in the bioconjugated film. The kinetics of biomolecular reorganization could be described in terms of the Lifshitz-Slyozov law (Azzaroni *et al.*, 2007).

Real-time changes in viscoelasticity of adsorbed poly(L-lysine) and adsorbed histone (lysine rich fraction) due to cross-linking by glutaraldehyde and corresponding release of associated water were investigated by Dutta *et al.* The adsorbed mass estimated from the Sauerbrey equation (perfectly elastic) and the Voigt viscoelastic model differ appreciably prior to cross-linking whereas after cross-linking they converged. It was confirmed experimentally via ATR/FTIR measurements that this is due to trapped water molecules released during the cross-linking (Dutta *et al.*, 2008). Glomm *et al.* compared the adsorption of eight different proteins (α-lactalbumin (types I and III), bovine serum albumin, hemoglobin, myoglobin, cytochrome c, α-casein and lysozyme) under the same conditions onto citrate-coated gold surfaces of a QCM sensor. Protein surface coverage, layer thickness and flexibility could be tuned as a function of deposition method and has been correlated to native fold stability determined from near- and far-UV circular dichroism measurements (Glomm *et al.*, 2007). The adsorption and enzymatic cleavage of osteopontin on different surface chemistries was studied by Malmstrom *et al.* (2009). Thrombin was able to bind and cleave the surface bound osteopontin at the hydrophobic surface. The authors concluded that the altered levels of osteopontin binding, hydration of the layer, and susceptibility to thrombin cleavage suggestive of osteopontin adopting different conformations and/or orientations at the different material surfaces (Malmstrom *et al.*, 2009). Valiaev *et al.* used QCM together with AFM and microcantilever deflection measurements to investigate the conformational mechanics of stimulus-responsive elastin-like polypeptides in response to changes in solution pH and ionic strength (Valiaev *et al.*, 2007). QCM was used in to investigate the role of hydrodynamically coupled water in surface adsorbed amino acids and employed as a tool to study hydrated peptides. The data were used in the design of a hydropathy scale in surface adsorbed amino acid films on solid and this scale compared well with reported hydropathy scale reported in the literature and could be correlated with the solid/liquid interfacial tension and work of adhesion of the adsorbed amino acid films (Lakshmanan and Dhathathreyan, 2007). Protein hydration was also studied for human serum albumin (Lubarsky *et al.*, 2007).

Enzymatic reactions and enzyme kinetics

Sensor materials for the detection of proteases based on the thin film degradation of peptide cross-linked dextran hydrogels were developed by Stair *et al.* (2009). Hydrogel cross-links were formed via simple imine linkages between aldehyde groups in oxidized dextran and a peptide sequence susceptible to protease cleavage. Degradation of the hydrogel films was monitored by QCM (Stair *et al.*, 2009). In a similar approach peptide cross-linked polyacrylamide hydrogel films and their degradation by human

neutrophil elastase (HNE) were studied (Kamarun *et al.*, 2009). Another study on proteases used β-casein as a model protein, which was immobilized on the surface of a QCM sensor where its degradation caused shifts in the resonant frequency upon digestion with the peptidases pepsin or trypsin (Huenerbein *et al.*, 2007). To investigate the protease resistance of a surface-bound α-helix, Hardesty *et al.* designed an α-helical polypeptide, used it to form films of varying surface coverages and then measured responses of the films to serine protease exposure (Hardesty *et al.*, 2008). Furusawa *et al.* compared endo-type protease (subtilisin and α-chymotrypsin) and exo-type protease (carboxypeptidase P) reactions and characterized the enzymatic reaction mechanisms by determining all kinetic parameters, by following the mass change of the formation and the decay of the enzyme-substrate complex and the formation of the product (Furusawa *et al.*, 2008b; Furusawa *et al.*, 2008a). Numata *et al.* studied the reaction processes of poly[(R)-3-hydroxybutyric acid] (PHB) with two types of poly(-hydroxybutyric acid) depolymerases secreted from *Ralstonia pickettii* T1 and *Penicillium funiculosum*. QCM measurements clarified quantitatively the differences in detachment behaviour between two types of PHB depolymerases, namely the enzyme from *R. pickettii* T1 was hardly detached but the enzyme from *P. funiculosum* was released easily from the surface of P(3HB) crystals under an aqueous condition (Numata *et al.*, 2007).

The activity of gastric lipase was studied on a range of different solid substrates and at various pH values (Chahinian *et al.*, 2006). Potato amylopectin was immobilized on a QCM-D sensor surface by Sasaki *et al.* and enzymatic starch hydrolysis was monitored directly (Sasaki *et al.*, 2008). The specific interaction between tris(hydroxymethyl)aminomethane (Tris) and lysozyme were investigated by Quan *et al.* using QCM and confirmed by SPR and high-performance affinity chromatography. The low measured dissociation constant suggested that it was better to avoid using Tris buffers for a lysozyme ligand binding study when the ligands under study are weak binders (Quan *et al.*, 2008). QCM and *in vitro* motility assays have been employed to shed light on the interaction between myosin motor fragments (heavy meromyosin) and artificial surfaces in an effort to understand the principles of actomyosin function to be able to combine heavy meromyosin with nanostructuring techniques for the development of nanotechnological applications. QCM and assay data were found to be consistent with a model where the molecules are adsorbed either via their flexible C-terminal tail part of heavy meromyosin or via their positively charged N-terminal motor domain without other surface contact points (Albet-Torres *et al.*, 2007).

To investigate the reactions of protein translation, Takahashi *et al.* (2009) established a system that allowed real-time monitoring of protein synthesis using a cell-free translation mixture. Using an mRNA that encoded a fusion polypeptide comprising the streptavidin-binding peptide tag, a portion of Protein D as a spacer, and the SecM arrest sequence, they could follow the binding of the tag, while it was displayed on the 70S ribosome, to a streptavidin-modified QCM over time. From the results of this study, both the formation of the initiation complex from the 70S ribosome, mRNA, and fMet-tRNA (fMet) and the accommodation of the second aminoacyl-tRNA to the initiation complex were determined to be rate-limiting steps in protein synthesis (Takahashi *et al.*, 2009). QCM was the essential tool in a study aimed at elucidating the mechanism of the nuclease enzyme EcoRII. EcoRII is a homodimer with two domains consisting of a DNA-binding N-terminus and a catalytic C-terminus and recognizes two specific sequences on DNA. After binding to either recognition site, EcoRII cleaves the other recognition site of the same DNA (cis-binding) strand and/or the recognition site of the other DNA (trans-binding) strand. Takahashi *et al.* (2008) were able to obtain the binding and cleavage kinetics of only the cis-binding site by following the frequency (mass) changes of a DNA-immobilized QCM. It was determined from the kinetic analyses that the N-domain, which covers the catalytic C-domain in the absence of DNA, preferentially binds to the one DNA recognition site while transforming EcoRII into an active form allosterically, and then the secondary C-domain binds to and cleaves the other recognition site of the DNA strand (Takahashi *et al.*, 2008).

Protein–protein interactions

Most of the published work for protein–protein interactions involves antibody–antigen interactions, reports for which are covered separately in the immunoassay section of this review. The following papers are thus limited to the use of QCM in the studies involving proteins other than immunoglobulins.

A QCM study could demonstrate that cystatin C, an endogenous cysteine proteinase inhibitor that is often used as an indicator of glomerular filtration rate, binds directly to megalin, an endocytic receptor in proximal tubule cells, in a Ca(+)-dependent manner (Kaseda *et al.*, 2007). Pre-treatment of surfaces with casein as standard protocol for achieving optimal kinesin activity has been studied by QCM measurements and microtubule gliding to uncover the role that casein plays in enhancing the activity of surface-adsorbed kinesin (Ozeki *et al.*, 2009). Hovgaard *et al.* monitored the changes in layer thickness and viscoelastic properties accompanying multilayer amyloid deposition. The combination with AFM allowed the study of the temporal evolution of the interfacial fibrillation process as a first step to build up realistic models of amyloid plaque formation *in vitro* (Hovgaard *et al.*, 2007).

QCM was employed to analyse the real-time growth of amyloid-β protein (1–40) aggregation intermediates selectively immobilized on the crystal surface. Immobilization permitted quantitative evaluation of A-β(1–40) aggregation intermediate growth under controlled solution conditions. Elongation of A-β(1–40) aggregation intermediates via monomer addition proceeded in a non-saturable and reversible fashion (Kotarek *et al.*, 2008). The serine protease inhibitor, Kazal type 1 (SPINK1) is expressed in a variety of pancreatic ductal neoplasms. Ozaki *et al.* were able to show that SPINK1 co-precipitated with endothelial growth-factor receptor (EGFR) in an immunoprecipitation experiment and that the binding affinity of SPINK1 to EGFR was about half of that of EGF using quartz-crystal microbalance (Ozaki *et al.*, 2009). Fibroblast growth factor-1 (FGF1) was co-released with S100A13, a Ca^{2+}-binding protein that acts as an extracellular cargo molecule. QCM was used to determine affinities and kinetics in the presence of varying concentrations of Ca^{2+} or Cu^{2+} (Matsunaga and Ueda, 2008).

The kinetics of neurosteroid binding to recombinant human microtubule-associated protein 2C (rhMAP2C) and neurosteroid regulation of MAP2C-stimulated tubulin assembly were studied by QCM (Mizota and Ueda, 2008). A QCM biosensor for recombinant human interferon-β was constructed by utilizing antisense peptides adhered to the QCM gold surfaces (Luo *et al.*, 2007). Highly specific peptide aptamers were also used to detect

CDK2 protein from yeast cell lysate (Shu *et al.*, 2008). The ryanodine receptor 2 induces Ca^{2+} leak in failing hearts and K201 (JTV519) is a protein that inhibits the Ca^{2+} leak by correcting the defective interdomain interaction. QCM in conjunction with fluorescent labeling and digestion experiments was used to elucidate the binding fragments between the N-terminal and central regions of the ryanodine receptor 2 and K201 (JTV519) (Yamamoto *et al.*, 2008). The effect of ionic strength on the interfacial interactions between pectin and the bovine serum albumin surface were investigated using QCM (Wang *et al.*, 2007b).

THEORY

Background

The basic theory of signal dependence on adsorbed mass was first developed by Sauerbrey (1959), who showed that the frequency change of a quartz crystal TSM resonator was a linear function of the mass per area m_s, or absolute mass Δm:

$$\Delta f_m = -\frac{f_0^2}{F_q \rho_q} m_s = -\frac{f_0^2}{F_q \rho_q} \frac{\Delta m_s}{A_{el}} \quad (1)$$

where f_0 is the resonance frequency of the unperturbed quartz resonator, F_q the frequency constant of the crystal ($F_q = f_0.d_q$), d_q the thickness, ρ_q the quartz density, and A_{el} the electrode area. The above equation is only valid for thin, solid layers deposited on the resonator. This model for thin solid films was then further developed by various contributors: remarkably Kanazawa (1997), who expanded the model to Newtonian (viscous and lossy) liquids. The following equation gives the frequency shift for liquid loaded sensor surface in which the liquid is defined by its density ρ_l, and viscosity η_l:

$$\Delta f_l = -\sqrt{f_0^3 \frac{\eta_l \rho_l}{\pi \mu_q \rho_q}} = -f_0^{\frac{3}{2}} \sqrt{\frac{\eta_l \rho_l}{\pi \mu_q \rho_q}} \quad (2)$$

and in which μ_q is the shear module in x-direction, and ρ_q is the density of the crystal. This equation can be derived by calculation of an effective mass loading based on the penetration depth of the transversal wave propagated from the crystal surface into the liquid.

In a two layer system (i.e. a rigid mass layer and a viscous and lossy liquid) these frequency shifts simply add up to an overall shift:

$$\Delta f = \Delta f_m + \Delta f_l = -{f_0}^2 \left(\frac{\Delta m_s}{F_q \rho_q A_{el}} + \sqrt{\frac{\eta_l \rho_l}{f_0 \pi \mu_q \rho_q}} \right) \quad (3)$$

In addition to the frequency shift, there also exists a dampening of the resonator caused by the viscous liquid layer. Dampening due to liquid can be also be quantified in the measured series resistance in the equivalent electrical circuit.

$$\Delta R_l = 4 L_q \sqrt{f_0^3 \frac{\pi \eta_l \rho_l}{\mu_q \rho_q}} \quad (4)$$

This dampening factor allows the possibility to detect not only mass changes but also viscoelastic and conformational changes of interactions. This last equation contains the term L_q which describes the inductance due to the quartz (a constant). Note that there are several different methods of measuring the crystal load impedance and the acoustic or surface load impedance that are covered in more detail elsewhere (Johannsmann, 2006; Lucklum and Eichelbaum, 2006). Of note, however, is the measurement of the dissipation energy (D), which is realized as 'QCM-D' in commercially available instruments from Q-Sense AB (Rodahl *et al.*, 1995). Simplistically, a film that is viscoelastic or 'soft' will not fully couple to the oscillation of the crystal, and will dampen the crystal's oscillation. The damping or, dissipation (D), of the oscillation contains information on the film's viscoelasticity. D is defined by the ratio of energy lost (dissipated) during one oscillation cycle and the total energy stored in the oscillator:

$$D = \frac{E_{lost}}{2\pi E_{stored}} \quad (5)$$

The dissipation of the crystal is measured by recording the response of a freely oscillating crystal that has been vibrated at its resonant frequency. This also gives the opportunity to jump between the fundamental frequency and overtones. By measuring at multiple frequencies and applying a viscoelastic model (the so-called Voight model) an interfacial film can be characterized in detail, even for soft films when certain assumptions are made (Voinova *et al.*, 2002; Zhang *et al.*, 2009).

Advanced theory

As with any technology that possesses significant strengths in terms of versatility in measurement, there is also a corresponding weakness in terms of the number of possible interpretations of the sensor response. It is widely accepted that the QCM is not a simple 'mass balance', and can measure properties that are additional to mass coupled to the sensor surface. Despite this, it is surprising how many researchers publish papers that describe an interaction in which the signal is clearly not gravimetric in nature (non-Saubrey behaviour), but chose to simplistically ascribe any discrepancy to 'missing mass'. The detailed physical phenomena and various interpretations and models that can account for them are beyond the scope of this review and the remit of this journal; however, it should be noted that there are numerous effects other than mass addition that can lead to frequency changes on a QCM. In addition to liquid viscosity and density, temperature and pressure (Shen *et al.*, 2008), signals can be affected by electrode surface roughness and wetability (Cho *et al.*, 2007b; Roach *et al.*, 2007; Zhuang *et al.*, 2007), compressional wave reflection from a liquid meniscus in an open well or immersion configuration (Picard and Davoust, 2007; Shen *et al.*, 2007a), hydrostatic pressure in a flow system (Ogi *et al.*, 2008), liquid permittivity and conductivity (Yu and Janata, 2008), particularly if the electrode/circuit is not well grounded (Yoshimoto *et al.*, 2006), shear oscillation amplitutde (Edvardsson *et al.*, 2006; Encarnacao *et al.*, 2007; Yoshimoto *et al.*, 2007), and a variety of properties of the bound layer; shear modulus and elasticity(Jimenez *et al.*, 2006; Rojas *et al.*, 2008), homogeneity, topology and viscosity. Explanations for 'missing mass' centre on discussions of 'coupled water' (Lakshmanan *et al.*, 2006; Bingen *et al.*, 2008; Wang *et al.*, 2008a; Furusawa *et al.*, 2009b), the geometry and homogeneity of the attachmed mass on the surface (Konig *et al.*, 2006; Johannsmann *et al.*, 2008; Johannsmann *et al.*, 2009; Tellechea *et al.*, 2009), and various interpretations of the impact of the viscoelastic properties of the interfacial layer (Dutta *et al.*, 2008; Johannsmann, 2008; Zhu *et al.*, 2008; Zhuang *et al.*, 2008; Furusawa *et al.*, 2009a; Patel *et al.*, 2009b).

CONCLUSIONS AND OUTLOOK

The many references herein clearly illustrate that QCM can be used successfully to quantify many physical properties of molecules and molecular interactions. In addition to these fundamental capabilities, the technology possesses the additional advantages of being able to operate directly in a wide variety of complex liquids and detect interactions between molecules without the need to isolate and purify the analyte. This is because most liquids of interest to researchers in the field of molecular recognition possess very similar viscosities and densities, compared to their significantly variant refractive indices and optical transmission. In addition, there are a substantial number of reports that exemplify the use of QCM as a powerful analytical tool to monitor protein conformational changes in real time. Finally, the ability to 'overcoat' the quartz sensor with materials that may be optically opaque or incompatible with evanescent wave-based detection extends the range of applications beyond those possible with more conventional optical label-free detection platforms.

QCM sensors have traditionally been viewed as low-sensitivity devices; however, recent advances in the field together with innovative assay formats have enabled limits of detection and quantification that equal, and in some cases surpass, those achieved by more widely adopted optical techniques. Key advances in the field of acoustics and biophysics will continue to drive forward the sensitivity and specificity limits of piezoelectric assays. These include ultra-thin, high frequency 'inverted mesa' sensors formed by deep-reactive ion etching (Abe and Kato, 2007), novel sensors with both electrodes on one face of the quartz (Abe and Kato, 2007) or no electrodes (Ogi *et al.*, 2006; Ogi *et al.*, 2007; Larsson *et al.*, 2009; Ogi *et al.*, 2009a; Ogi *et al.*, 2009b), novel drive and electronic interface circuits (Arnau *et al.*, 2008; Torres *et al.*, 2008), multiplexed sensor arrays (Hsiao *et al.*, 2009), and systems capable of operating at multiple frequencies and oscillation amplitudes (Cooper *et al.*, 2001; Edvardsson *et al.*, 2005; Kankare *et al.*, 2006). More recently completely new micromechanical devices based on the principles of resonant acoustic biosensing have appeared involving torsional piezoelectric (Bucking *et al.*, 2007) and suspended piezoelectric resonators (Burg *et al.*, 2007). Ultra-high frequency film bulk acoustic resonator (FBAR) sensors are appearing with operating frequencies from 700 MHz up to 1.5 GHz (Wingqvist *et al.*, 2009), and multimode devices combining plasmon resonance and QCM (Dahlin *et al.*, 2008; Jonsson *et al.*, 2008; Zong *et al.*, 2008; Larsson *et al.*, 2009) or relectometry and QCM (Edvardsson *et al.*, 2009) into a single unit have been reported. Systems with integrated sample concentration involving paramagnetic nanoparticles (Tsai *et al.*, 2008) and even dielectrophoresis (Fatoyinbo *et al.*, 2007) have been reported, leading to further gains in sensitivity.

Finally, the emergence of a number of commercial organizations (Table 1) that are developing robust, reliable sensors, sample delivery and analysis systems will together push the technology more rapidly into the general laboratory and the field. The continued growth rate in published papers is indicative of considerable momentum gathering over the last four years leading to a general acceptance of acoustic biosensing as a mainstream research tool for the analysis of molecules and molecular recognition.

A NOTE ON NOMENCLATURE

All of the papers referenced in this review exploit the use of a piezoelectric sensor to analyse molecular interaction phenomena. As can be seen from many of these articles, this type of sensor can detect properties other than mass adsorption and desorption from a surface or receptor, implying that the most commonly used term to describe the technique: 'quartz crystal microbalance' or 'QCM', is not strictly accurate. Nevertheless, this term is still the most commonly invoked, and as such it should be taken to be used interchangeably with other nomenclatures: viz. 'quartz crystal resonant sensor, or QCRS', 'thickness shear mode, or TSM' and 'bulk acoustic wave, or BAW'.

Acknowledgements

Financial support for this review was provided by the National Health and Medical Research Council (NHMRC) grant AF 511105.

REFERENCES

Abe T, Kato H. 2007. Design and evaluation of an antiparallel coupled resonator for chemical sensor applications. *Anal. Chem.* **79**(17): 6804–6806.

Adányi N, Váradi M, Kim N, Szendrö I. 2006. Development of new immunosensors for determination of contaminants in food. *Curr. Appl. Phys.* **6**(2): 279–286.

Agmo Hernandez V, Niessen J, Harnisch F, Block S, Greinacher A, Kroemer HK, Helm CA, Scholz F. 2008. The adhesion and spreading of thrombocyte vesicles on electrode surfaces. *Bioelectrochemistry* **74**(1): 210–216.

Ahola S, Salmi J, Johansson LS, Laine J, Osterberg M. 2008a. Model films from native cellulose nanofibrils: preparation, swelling, and surface interactions. *Biomacromolecules* **9**(4): 1273–1282.

Ahola S, Turon X, Osterberg M, Laine J, Rojas OJ. 2008b. Enzymatic hydrolysis of native cellulose nanofibrils and other cellulose model films: effect of surface structure. *Langmuir* **24**(20): 11592–11599.

Aizawa H, Gokita Y, Park JW, Yoshimi Y, Kurosawa S. 2006. Antibody immobilization on functional monolayers using a quartz crystal microbalance. *IEEE Sens. J.* **6**(5): 1052–1056.

Albet-Torres N, O'Mahony J, Charlton C, Balaz M, Lisboa P, Aastrup T, Mansson A, Nicholls IA. 2007. Mode of heavy meromyosin adsorption and motor function correlated with surface hydrophobicity and charge. *Langmuir* **23**(22): 11147–11156.

Al-Jawad M, Fragneto G, Liu J, Chang SR, Clarkson B. 2009. Fibronectin adsorption studied using neutron reflectometry and complementary techniques. *Eur. Phys. J. E. Soft Matter.* **30**(2): 175–179.

Alves NM, Picart C, Mano JF. 2009. Self assembling and crosslinking of polyelectrolyte multilayer films of chitosan and alginate studied by QCM and IR spectroscopy. *Macromol. Biosci.* **9**(8): 776–785.

Amirkhani M, Volden S, Zhu K, Glomm WR, Nystrom B. 2008. Adsorption of cellulose derivatives on flat gold surfaces and on spherical gold particles. *J. Colloid. Interface. Sci.* **328**(1): 20–28.

Amstad E, Zurcher S, Mashaghi A, Wong JY, Textor M, Reimhult E. 2009. Surface functionalization of single superparamagnetic iron oxide nanoparticles for targeted magnetic resonance imaging. *Small* **5**(11): 1334–1342.

Anderson TH, Min Y, Weirich KL, Zeng H, Fygenson D, Israelachvili JN. 2009. Formation of supported bilayers on silica substrates. *Langmuir* **25**(12): 6997–7005.

Arnau A, Garcia JV, Jimenez Y, Ferrari V, Ferrari M. 2008. Improved electronic interfaces for AT-cut quartz crystal microbalance sensors under variable damping and parallel capacitance conditions. *Rev. Sci. Instrum.* **79**(7): 075110.

Atthoff B, Hilborn J. 2007. Protein adsorption onto polyester surfaces: is there a need for surface activation? *J. Biomed. Mater. Res. B Appl. Biomater.* **80**(1): 121–130.

Aulin C, Varga I, Claesson PM, Wagberg L, Lindstrom T. 2008. Buildup of polyelectrolyte multilayers of polyethyleneimine and microfibrillated cellulose studied by in situ dual-polarization interferometry and quartz crystal microbalance with dissipation. *Langmuir* **24**(6): 2509–2518.

Ayela C, Roquet F, Valera L, Granier C, Nicu L, Pugniere M. 2007. Antibody-antigenic peptide interactions monitored by SPR and QCM-D: a model for SPR detection of IA-2 autoantibodies in human serum. *Biosens. Bioelectron.* **22**(12): 3113–3119.

Azzaroni O, Mir M, Knoll W. 2007. Supramolecular architectures of streptavidin on biotinylated self-assembled monolayers. Tracking biomolecular reorganization after bioconjugation. *J. Phys. Chem. B* **111**(48): 13499–13503.

Bailey K, Bally M, Leifert W, Voros J, McMurchie T. 2009. G-protein coupled receptor array technologies: site directed immobilisation of liposomes containing the H1-histamine or M2-muscarinic receptors. *Proteomics* **9**(8): 2052–2063.

Bakowsky H, Richter T, Kneuer C, Hoekstra D, Rothe U, Bendas G, Ehrhardt C, Bakowsky U. 2008. Adhesion characteristics and stability assessment of lectin-modified liposomes for site-specific drug delivery. *Biochim. Biophys. Acta* **1778**(1): 242–249.

Balkenhohl T, Lisdat F. 2007. An impedimetric immunosensor for the detection of autoantibodies directed against gliadins. *Analyst* **132**(4): 314–322.

Baltus RE, Carmon KS, Luck LA. 2007. Quartz crystal microbalance (QCM) with immobilized protein receptors: comparison of response to ligand binding for direct protein immobilization and protein attachment via disulfide linker. *Langmuir* **23**(7): 3880–3885.

Barfoot RJ, Sheikh KH, Johnson BR, Colyer J, Miles RE, Jeuken LJ, Bushby RJ, Evans SD. 2008. Minimal F-actin cytoskeletal system for planar supported phospholipid bilayers. *Langmuir* **24**(13): 6827–6836.

Belegrinou S, Mannelli I, Lisboa P, Bretagnol F, Valsesia A, Ceccone G, Colpo P, Rauscher H, Rossi F. 2008. pH-dependent immobilization of proteins on surfaces functionalized by plasma-enhanced chemical vapor deposition of poly(acrylic acid)- and poly(ethylene oxide)-like films. *Langmuir* **24**(14): 7251–7261.

Berglin M, Pinori E, Sellborn A, Andersson M, Hulander M, Elwing H. 2009. Fibrinogen adsorption and conformational change on model polymers: novel aspects of mutual molecular rearrangement. *Langmuir* **25**(10): 5602–5608.

Bi X, Yang KL. 2009. On-line monitoring imidacloprid and thiacloprid in celery juice using quartz crystal microbalance. *Anal. Chem.* **81**(2): 527–532.

Bingen P, Wang G, Steinmetz NF, Rodahl M, Richter RP. 2008. Solvation effects in the quartz crystal microbalance with dissipation monitoring response to biomolecular adsorption: a phenomenological approach. *Anal. Chem.* **80**(23): 8880–8890.

Bitton R, Berglin M, Elwing H, Colin C, Delage L, Potin P, Bianco-Peled H. 2007. The influence of halide-mediated oxidation on algae-born adhesives. *Macromol. Biosci.* **7**(12): 1280–1289.

Bodin A, Ahrenstedt L, Fink H, Brumer H, Risberg B, Gatenholm P. 2007. Modification of nanocellulose with a xyloglucan-RGD conjugate enhances adhesion and proliferation of endothelial cells: implications for tissue engineering. *Biomacromolecules* **8**(12): 3697–3704.

Briand E, Salmain M, Herry JM, Perrot H, Compere C, Pradier CM. 2006. Building of an immunosensor: how can the composition and structure of the thiol attachment layer affect the immunosensor efficiency? *Biosens. Bioelectron.* **22**(3): 440–448.

Briand E, Salmain M, Compere C, Pradier CM. 2007. Anti-rabbit immunoglobulin G detection in complex medium by PM-RAIRS and QCM Influence of the antibody immobilisation method. *Biosens. Bioelectron.* **22**(12): 2884–2890.

Brochu H, Vermette P. 2007. Liposome layers characterized by quartz crystal microbalance measurements and multirelease delivery. *Langmuir* **23**(14): 7679–7686.

Bucking W, Du B, Turshatov A, Konig AM, Reviakine I, Bode B, Johannsmann D. 2007. Quartz crystal microbalance based on torsional piezoelectric resonators. *Rev. Sci. Instrum.* **78**(7): 074903.

Bunte G, Hurttlen J, Pontius H, Hartlieb K, Krause H. 2007. Gas phase detection of explosives such as 2,4,6-trinitrotoluene by molecularly imprinted polymers. *Anal. Chim. Acta* **591**(1): 49–56.

Burg TP, Godin M, Knudsen SM, Shen W, Carlson G, Foster JS, Babcock K, Manalis SR. 2007. Weighing of biomolecules, single cells and single nanoparticles in fluid. *Nature* **446**(7139): 1066–1069.

Buzhynskyy N, Golczak M, Lai-Kee-Him J, Lambert O, Tessier B, Gounou C, Berat R, Simon A, Granier T, Chevalier JM, Mazeres S, Bandorowicz-Pikula J, Pikula S, Brisson AR. 2009. Annexin-A6 presents two modes of association with phospholipid membranes: a combined QCM-D, AFM and cryo-TEM study. *J. Struct. Biol.* **168**(1): 107–116.

Cabre EJ, Malmstrom J, Sutherland D, Perez-Gil J, Otzen DE. 2009. Surfactant protein SP-B strongly modifies surface collapse of phospholipid vesicles: insights from a quartz crystal microbalance with dissipation. *Biophys. J.* **97**(3): 768–776.

Cabric S, Eich T, Sanchez J, Nilsson B, Korsgren O, Larsson R. 2008. A new method for incorporating functional heparin onto the surface of islets of Langerhans. *Tissue Eng. Part C Methods* **14**(2): 141–147.

Caruso F, Rodda E, Furlong DN. 1996. Orientational aspects of antibody immobilization and immunological activity on quartz crystal microbalance electrodes. *J. Colloid Interface Sci.* **178**(1): 104–115.

Caseli L, dos Santos DS Jr, Foschini M, Goncalves D, Oliveira ON Jr. 2006a. The effect of the layer structure on the activity of immobilized enzymes in ultrathin films. *J. Colloid Interface Sci.* **303**(1): 326–331.

Caseli L, Moraes ML, Zucolotto V, Ferreira M, Nobre TM, Zaniquelli ME, Rodrigues Filho UP, Oliveira ON Jr. 2006b. Fabrication of phytic acid sensor based on mixed phytase-lipid Langmuir–Blodgett films. *Langmuir* **22**(20): 8501–8508.

Caseli L, Pavinatto FJ, Nobre TM, Zaniquelli ME, Viitala T, Oliveira ON Jr. 2008. Chitosan as a removing agent of beta-lactoglobulin from membrane models. *Langmuir* **24**(8): 4150–4156.

Cerruti M, Jaworski J, Raorane D, Zueger C, Varadarajan J, Carraro C, Lee SW, Maboudian R, Majumdar A. 2009. Polymer-oligopeptide composite coating for selective detection of explosives in water. *Anal. Chem.* **81**(11): 4192–4199.

Chahinian H, Snabe T, Attias C, Fojan P, Petersen SB, Carriere F. 2006. How gastric lipase, an interfacial enzyme with a Ser-His-Asp catalytic triad, acts optimally at acidic pH. *Biochemistry* **45**(3): 993–1001.

Channasanon S, Graisuwan W, Kiatkamjornwong S, Hoven VP. 2007. Alternating bioactivity of multilayer thin films assembled from charged derivatives of chitosan. *J. Colloid Interface Sci.* **316**(2): 331–343.

Chayed S, Winnik FM. 2007. In vitro evaluation of the mucoadhesive properties of polysaccharide-based nanoparticulate oral drug delivery systems. *Eur. J. Pharm. Biopharm.* **65**(3): 363–370.

Chen ZG, Tang DY. 2007. Antigen-antibody interaction from quartz crystal microbalance immunosensors based on magnetic CoFe(2)O (4)/SiO (2) composite nanoparticle-functionalized biomimetic interface. *Bioprocess. Biosyst. Eng.* **30**(4): 243–249.

Chen H, Su X, Neoh KG, Choe WS. 2006. QCM-D analysis of binding mechanism of phage particles displaying a constrained heptapeptide with specific affinity to SiO2 and TiO2. *Anal. Chem.* **78**(14): 4872–4879.

Chen H, Jiang JH, Li YF, Deng T, Shen GL, Yu RQ. 2007a. A novel piezoelectric immunoagglutination assay technique with antibody-modified liposome. *Biosens. Bioelectron.* **22**(6): 993–999.

Chen X, Wang J, Paszti Z, Wang F, Schrauben JN, Tarabara VV, Schmaier AH, Chen Z. 2007b. Ordered adsorption of coagulation factor XII on negatively charged polymer surfaces probed by sum frequency generation vibrational spectroscopy. *Anal. Bioanal. Chem.* **388**(1): 65–72.

Chen H, Su X, Neoh KG, Choe WS. 2008. Probing the interaction between peptides and metal oxides using point mutants of a TiO2-binding peptide. *Langmuir* **24**(13): 6852–6857.

Chen HM, Huang TH, Tsai RM. 2009a. A biotin-hydrogel-coated quartz crystal microbalance biosensor and applications in immunoassay and peptide-displaying cell detection. *Anal. Biochem.* **392**(1): 1–7.

Chen SH, Chuang YC, Lu YC, Lin HC, Yang YL, Lin CS. 2009b. A method of layer-by-layer gold nanoparticle hybridization in a quartz crystal microbalance DNA sensing system used to detect dengue virus. *Nanotechnology* **20**(21): 215501.

Chitpan M, Wang X, Ho CT, Huang Q. 2007. Monitoring the binding processes of black tea thearubigin to the bovine serum albumin surface using quartz crystal microbalance with dissipation monitoring. *J. Agric Food Chem.* **55**(25): 10110–10116.

Cho NJ, Cheong KH, Lee C, Frank CW, Glenn JS. 2007a. Binding dynamics of hepatitis C virus' NS5A amphipathic peptide to cell and model membranes. *J. Virol.* **81**(12): 6682–6689.
Cho NJ, D'Amour JN, Stalgren J, Knoll W, Kanazawa K, Frank CW. 2007b. Quartz resonator signatures under Newtonian liquid loading for initial instrument check. *J. Colloid Interface Sci.* **315**(1): 248–254.
Cho NJ, Kanazawa KK, Glenn JS, Frank CW. 2007c. Employing two different quartz crystal microbalance models to study changes in viscoelastic behavior upon transformation of lipid vesicles to a bilayer on a gold surface. *Anal. Chem.* **79**(18): 7027–7035.
Cho NJ, Dvory-Sobol H, Xiong A, Cho SJ, Frank CW, Glenn JS. 2009. Mechanism of an amphipathic alpha-helical peptide's antiviral activity involves size-dependent virus particle lysis. *ACS Chem. Biol.* **4**(12): 1061–1067.
Chou HC, Yan TR, Chen KS. 2009. Detecting cells on the surface of a silver electrode quartz crystal microbalance using plasma treatment and graft polymerization. *Colloids Surf. B Biointerfaces* **73**(2): 244–249.
Christ K, Wiedemann I, Bakowsky U, Sahl HG, Bendas G. 2007. The role of lipid II in membrane binding of and pore formation by nisin analyzed by two combined biosensor techniques. *Biochim. Biophys. Acta* **1768**(3): 694–704.
Christ K, Al-Kaddah S, Wiedemann I, Rattay B, Sahl HG, Bendas G. 2008. Membrane lipids determine the antibiotic activity of the lantibiotic gallidermin. *J. Membr. Biol.* **226**(1–3): 9–16.
Chu X, Zhao Z-L, Shen G-L, Yu R-Q. 2006. Quartz crystal microbalance immunoassay with dendritic amplification using colloidal gold immunocomplex. *Sens. Actuators B Chem.* **114**(2): 696–704.
Cooper MA. 2002. Optical biosensors in drug discovery. *Nat. Rev. Drug Discov.* **1**(7): 515–528.
Cooper MA. 2003. Biosensor profiling of molecular interactions in pharmacology. *Curr. Opin. Pharmacol.* **3**(5): 557–562.
Cooper MA. 2004. Advances in membrane receptor screening and analysis. *J. Mol. Recognit.* **17**(4): 286–315.
Cooper MA. 2006a. Optical biosensors: where next and how soon? *Drug Discov. Today* **11**(23–24): 1061–1067.
Cooper MA. 2006b. Resonant acoustic profiling (RAP^{TM}) and rupture event scanning (REVS^{TM}). In Piezoelectric Sensors, Vol. 5, Steinem C, Janshoff A (eds). Springer-Verlag: Berlin Heidelberg, 449–481 and references cited therein.
Cooper MA, Singleton VT. 2007. A survey of the 2001 to 2005 quartz crystal microbalance biosensor literature: applications of acoustic physics to the analysis of biomolecular interactions. *J. Mol. Recognit.* **20**(3): 154–184.
Cooper MA, Dultsev FN, Minson T, Ostanin VP, Abell C, Klenerman D. 2001. Direct and sensitive detection of a human virus by rupture event scanning. *Nat. Biotechnol.* **19**(9): 833–837.
Corso CD, Stubbs DD, Lee S-H, Goggins M, Hruban RH, Hunt WD. 2006. Real-time detection of mesothelin in pancreatic cancer cell line supernatant using an acoustic wave immunosensor. *Cancer Detect. Prev.* **30**(2): 180–187.
Cote GL, Lec RM, Pishko MV. 2003. Emerging biomedical sensing technologies and their applications. *IEEE Sens. J.* **3**(3): 251–266.
Croll TI, O'Connor AJ, Stevens GW, Cooper-White JJ. 2006. A blank slate? Layer-by-layer deposition of hyaluronic acid and chitosan onto various surfaces. *Biomacromolecules* **7**(5): 1610–1622.
Dahlin AB, Jonsson P, Jonsson MP, Schmid E, Zhou Y, Hook F. 2008. Synchronized quartz crystal microbalance and nanoplasmonic sensing of biomolecular recognition reactions. *ACS Nano* **2**(10): 2174–2182.
Dell'Atti D, Tombelli S, Minunni M, Mascini M. 2006. Detection of clinically relevant point mutations by a novel piezoelectric biosensor. *Biosens. Bioelectron.* **21**(10): 1876–1879.
Deng T, Li JS, Huan SY, Yang HF, Wang H, Shen GL, Yu RQ. 2006. Quartz crystal microbalance bioaffinity sensor for biotin based on mixed self-assembled monolayers and metastable molecular complex receptor. *Biosens. Bioelectron.* **21**(8): 1545–1552.
Diltemiz SE, Hur D, Ersoz A, Denizli A, Say R. 2009. Designing of MIP based QCM sensor having thymine recognition sites based on biomimicking DNA approach. *Biosens. Bioelectron.* **25**(3): 599–603.
Ding Y, Liu J, Jin X, Lu H, Shen G, Yu R. 2008. Poly-L-lysine/hydroxyapatite/carbon nanotube hybrid nanocomposite applied for piezoelectric immunoassay of carbohydrate antigen 19–9. *Analyst* **133**(2): 184–190.
Dolatshahi-Pirouz A, Rechendorff K, Hovgaard MB, Foss M, Chevallier J, Besenbacher F. 2008. Bovine serum albumin adsorption on nanorough platinum surfaces studied by QCM-D. *Colloids Surf. B Biointerfaces* **66**(1): 53–59.
Dolatshahi-Pirouz A, Jensen T, Foss M, Chevallier J, Besenbacher F. 2009. Enhanced surface activation of fibronectin upon adsorption on hydroxyapatite. *Langmuir* **25**(5): 2971–2978.
Dorvel BR, Keizer HM, Fine D, Vuorinen J, Dodabalapur A, Duran RS. 2007. Formation of tethered bilayer lipid membranes on gold surfaces: QCM-Z and AFM study. *Langmuir* **23**(13): 7344–7355.
Drouvalakis KA, Bangsaruntip S, Hueber W, Kozar LG, Utz PJ, Dai H. 2008. Peptide-coated nanotube-based biosensor for the detection of disease-specific autoantibodies in human serum. *Biosens. Bioelectron.* **23**(10): 1413–1421.
Dubois J, Gaudreault C, Vermette P. 2009. Biofouling of dextran-derivative layers investigated by quartz crystal microbalance. *Colloids Surf. B Biointerfaces* **71**(2): 293–299.
Dutta AK, Nayak A, Belfort G. 2008. Viscoelastic properties of adsorbed and cross-linked polypeptide and protein layers at a solid-liquid interface. *J. Colloid Interface Sci.* **324**(1–2): 55–60.
Edvardsson M, Rodahl M, Kasemo B, Hook F. 2005. A dual-frequency QCM-D setup operating at elevated oscillation amplitudes. *Anal. Chem.* **77**(15): 4918–4926.
Edvardsson M, Rodahl M, Hook F. 2006. Investigation of binding event perturbations caused by elevated QCM-D oscillation amplitude. *Analyst* **131**(7): 822–828.
Edvardsson M, Zhdanov VP, Hook F. 2007. Controlled radial distribution of nanoscale vesicles during binding to an oscillating QCM surface. *Small* **3**(4): 585–589.
Edvardsson M, Svedhem S, Wang G, Richter R, Rodahl M, Kasemo B. 2009. QCM-D and reflectometry instrument: applications to supported lipid structures and their biomolecular interactions. *Anal. Chem.* **81**(1): 349–361.
Enarsson LE, Wagberg L. 2009. Polyelectrolyte adsorption on thin cellulose films studied with reflectometry and quartz crystal microgravimetry with dissipation. *Biomacromolecules* **10**(1): 134–141.
Encarnacao JM, Stallinga P, Ferreira GN. 2007. Influence of electrolytes in the QCM response: discrimination and quantification of the interference to correct microgravimetric data. *Biosens. Bioelectron.* **22**(7): 1351–1358.
Ergezen E, Appel M, Shah P, Kresh JY, Lec RM, Wootton DM. 2007. Real-time monitoring of adhesion and aggregation of platelets using thickness shear mode (TSM) sensor. *Biosens. Bioelectron.* **23**(4): 575–582.
Ersoz A, Diltemiz SE, Ozcan AA, Denizli A, Say R. 2008. Synergie between molecular imprinted polymer based on solid-phase extraction and quartz crystal microbalance technique for 8-OHdG sensing. *Biosens. Bioelectron.* **24**(4): 742–747.
Evans KO. 2008a. Supported phospholipid bilayer interaction with Components found in typical room-temperature ionic liquids: a QCM-D and AFM study. *Int. J. Mol. Sci.* **9**(4): 498–511.
Evans KO. 2008b. Supported phospholipid membrane interactions with 1-butyl-3-methylimidazolium chloride. *J. Phys. Chem. B* **112**(29): 8558–8562.
Evans-Nguyen KM, Fuierer RR, Fitchett BD, Tolles LR, Conboy JC, Schoenfisch MH. 2006. Changes in adsorbed fibrinogen upon conversion to fibrin. *Langmuir* **22**(11): 5115–5121.
Faiss S, Kastl K, Janshoff A, Steinem C. 2008. Formation of irreversibly bound annexin A1 protein domains on POPC/POPS solid supported membranes. *Biochim. Biophys. Acta* **1778**(7–8): 1601–1610.
Fatisson J, Merhi Y, Tabrizian M. 2008. Quantifying blood platelet morphological changes by dissipation factor monitoring in multilayer shells. *Langmuir* **24**(7): 3294–3299.
Fatoyinbo HO, Hoettges KF, Reddy SM, Hughes MP. 2007. An integrated dielectrophoretic quartz crystal microbalance (DEP-QCM) device for rapid biosensing applications. *Biosens. Bioelectron.* **23**(2): 225–232.
Feiler AA, Sahlholm A, Sandberg T, Caldwell KD. 2007. Adsorption and viscoelastic properties of fractionated mucin (BSM) and bovine serum albumin (BSA) studied with quartz crystal microbalance (QCM-D). *J. Colloid Interface Sci.* **315**(2): 475–481.
Feldoto Z, Pettersson T, Dedinaite A. 2008. Mucin-electrolyte interactions at the solid-liquid interface probed by QCM-D. *Langmuir* **24**(7): 3348–3357.
Feng K, Li J, Jiang JH, Shen GL, Yu RQ. 2007. QCM detection of DNA targets with single-base mutation based on DNA ligase reaction and biocatalyzed deposition amplification. *Biosens. Bioelectron.* **22**(8): 1651–1657.

Ferreira GN, da-Silva AC, Tome B. 2009. Acoustic wave biosensors: physical models and biological applications of quartz crystal microbalance. *Trends Biotechnol.* **27**(12): 689–697.
Filippov AP, Strizhak PE, Il'in VG. 2007. Quartz crystal microbalance modified with Cu(II) stearate and octadecylamine co-ordination chemical compounds for detection of volatile organic compounds. *Sens. Actuators B Chem.* **126**(2): 375–381.
Fogel R, Mashazi P, Nyokong T, Limson J. 2007. Critical assessment of the quartz crystal microbalance with dissipation as an analytical tool for biosensor development and fundamental studies: metallophthalocyanine-glucose oxidase biocomposite sensors. *Biosens. Bioelectron.* **23**(1): 95–101.
Fohlerova Z, Skladal P, Turanek J. 2007. Adhesion of eukaryotic cell lines on the gold surface modified with extracellular matrix proteins monitored by the piezoelectric sensor. *Biosens. Bioelectron.* **22**(9–10): 1896–1901.
Furusawa H, Takano H, Okahata Y. 2008a. Transient kinetic studies of pH-dependent hydrolyses by exo-type carboxypeptidase P on a 27-MHz quartz crystal microbalance. *Anal. Chem.* **80**(4): 1005–1011.
Furusawa H, Takano H, Okahata Y. 2008b. Transient kinetic studies of protein hydrolyses by endo- and exo-proteases on a 27MHz quartz-crystal microbalance. *Org. Biomol. Chem.* **6**(4): 727–731.
Furusawa H, Komatsu M, Okahata Y. 2009a. In situ monitoring of conformational changes of and peptide bindings to calmodulin on a 27MHz quartz-crystal microbalance. *Anal. Chem.* **81**(5): 1841–1847.
Furusawa H, Ozeki T, Morita M, Okahata Y. 2009b. Added mass effect on immobilizations of proteins on a 27 MHz quartz crystal microbalance in aqueous solution. *Anal. Chem.* **81**(6): 2268–2273.
Garnier B, Bouter A, Gounou C, Petry KG, Brisson AR. 2009. Annexin A5-functionalized liposomes for targeting phosphatidylserine-exposing membranes. *Bioconjug. Chem.* **20**(11): 2114–2122.
Glomm WR, Halskau O Jr, Hanneseth AM, Volden S. 2007. Adsorption behavior of acidic and basic proteins onto citrate-coated Au surfaces correlated to their native fold, stability, and pI. *J. Phys. Chem. B* **111**(51): 14329–14345.
Gormally MV, McKibben RK, Johal MS, Selassie CR. 2009. Controlling tyrosinase activity on charged polyelectrolyte surfaces: a QCM-D analysis. *Langmuir* **25**(17): 10014–10019.
Graneli A, Benkoski JJ, Hook F. 2007. Characterization of a proton pumping transmembrane protein incorporated into a supported three-dimensional matrix of proteoliposomes. *Anal. Biochem.* **367**(1): 87–94.
Gromelski S, Saraiva AM, Krastev R, Brezesinski G. 2009. The formation of lipid bilayers on surfaces. *Colloids Surf. B Biointerfaces* **74**(2): 477–483.
Gronewold TM, Baumgartner A, Quandt E, Famulok M. 2006. Discrimination of single mutations in cancer-related gene fragments with a surface acoustic wave sensor. *Anal. Chem.* **78**(14): 4865–4871.
Guo M, Chen J, Zhang Y, Chen K, Pan C, Yao S. 2008. Enhanced adhesion/spreading and proliferation of mammalian cells on electropolymerized porphyrin film for biosensing applications. *Biosens. Bioelectron.* **23**(6): 865–871.
Guo HS, Kim JM, Chang SM, Kim WS. 2009a. Chiral recognition of mandelic acid by L-phenylalanine-modified sensor using quartz crystal microbalance. *Biosens. Bioelectron.* **24**(9): 2931–2934.
Guo HS, Kim JM, Chang SM, Kim WS. 2009b. Chiral recognition of mandelic acid on quartz crystal microbalance by vapor diffused molecular assembly method. *J. Nanosci. Nanotechnol.* **9**(5): 2937–2943.
Guo HS, Kim JM, Kim SJ, Chang SM, Kim WS. 2009c. Versatile method for chiral recognition by the quartz crystal microbalance: chiral mandelic acid as the detection model. *Langmuir* **25**(2): 648–652.
Gurdak E, Booth J, Roberts CJ, Rouxhet PG, Dupont-Gillain CC. 2006. Influence of collagen denaturation on the nanoscale organization of adsorbed layers. *J. Colloid Interface Sci.* **302**(2): 475–484.
Halthur TJ, Bjorklund A, Elofsson UM. 2006. Self-assembly/aggregation behavior and adsorption of enamel matrix derivate protein to silica surfaces. *Langmuir* **22**(5): 2227–2234.
Hamlin RE, Dayton TL, Johnson LE, Johal MS. 2007. A QCM study of the immobilization of beta-galactosidase on polyelectrolyte surfaces: effect of the terminal polyion on enzymatic surface activity. *Langmuir* **23**(8): 4432–4437.
Han HC, Chang YR, Hsu WL, Chen CY. 2009. Application of parylene-coated quartz crystal microbalance for on-line real-time detection of microbial populations. *Biosens. Bioelectron.* **24**(6): 1543–1549.
Hao R, Wang D, Zhang X, Zuo G, Wei H, Yang R, Zhang Z, Cheng Z, Guo Y, Cui Z, Zhou Y. 2009. Rapid detection of Bacillus anthracis using monoclonal antibody functionalized QCM sensor. *Biosens. Bioelectron.* **24**(5): 1330–1335.
Hardesty JO, Cascao-Pereira L, Kellis JT, Robertson CR, Frank CW. 2008. Enzymatic proteolysis of a surface-bound alpha-helical polypeptide. *Langmuir* **24**(24): 13944–13956.
He W, Liu Z, Du X, Jiang Y, Xiao D. 2008. Analytical application of poly{methyl[3-(2-hydroxy-3,4-difluoro)phenyl]propyl siloxane} as a QCM coating for DMMP detection. *Talanta* **76**(3): 698–702.
He C, Liu J, Xie L, Zhang Q, Li C, Gui D, Zhang G, Wu C. 2009. Activity and thermal stability improvements of glucose oxidase upon adsorption on core-shell PMMA-BSA nanoparticles. *Langmuir* **25**(23): 13456–13460.
Hedin J, Lofroth JE, Nyden M. 2007. Adsorption behavior and cross-linking of EHEC and HM-EHEC at hydrophilic and hydrophobic modified surfaces monitored by SPR and QCM-D. *Langmuir* **23**(11): 6148–6155.
Hedin J, Isaksson D, Andersson M, Nyden M. 2009. Bi-layer formation of imidazole-modified ethyl(hydroxyethyl)cellulose at a hydrophobic surface as monitored by QCM-D. *J. Colloid Interface Sci.* **336**(2): 388–392.
Hedlund J, Andersson M, Fant C, Bitton R, Bianco-Peled H, Elwing H, Berglin M. 2009. Change of colloidal and surface properties of Mytilus edulis foot protein 1 in the presence of an oxidation (NaIO4) or a complex-binding (Cu2+) agent. *Biomacromolecules* **10**(4): 845–849.
Heitmann V, Wegener J. 2007. Monitoring cell adhesion by piezoresonators: impact of increasing oscillation amplitudes. *Anal. Chem.* **79**(9): 3392–3400.
Hemmersam AG, Rechendorff K, Foss M, Sutherland DS, Besenbacher F. 2008. Fibronectin adsorption on gold, Ti-, and Ta-oxide investigated by QCM-D and RSA modelling. *J. Colloid Interface Sci.* **320**(1): 110–116.
Herrig A, Janke M, Austermann J, Gerke V, Janshoff A, Steinem C. 2006. Cooperative adsorption of ezrin on PIP2-containing membranes. *Biochemistry* **45**(43): 13025–13034.
Hianik T, Ostatna V, Sonlajtnerova M, Grman I. 2007. Influence of ionic strength, pH and aptamer configuration for binding affinity to thrombin. *Bioelectrochemistry* **70**(1): 127–133.
Hillberg AL, Holmes CA, Tabrizian M. 2009. Effect of genipin cross-linking on the cellular adhesion properties of layer-by-layer assembled polyelectrolyte films. *Biomaterials* **30**(27): 4463–4470.
Hirlekar Schmid A, Stanca SE, Thakur MS, Thampi KR, Raman Suri C. 2006. Site-directed antibody immobilization on gold substrate for surface plasmon resonance sensors. *Sens. Actuators B Chem.* **113**(1): 297–303.
Hong S, Ergezen E, Lec R, Barbee KA. 2006. Real-time analysis of cell-surface adhesive interactions using thickness shear mode resonator. *Biomaterials* **27**(34): 5813–5820.
Hong SR, Choi SJ, Jeong HD, Hong S. 2009. Development of QCM biosensor to detect a marine derived pathogenic bacteria Edwardsiella tarda using a novel immobilisation method. *Biosens. Bioelectron.* **24**(6): 1635–1640.
Hook F, Kasemo B. 2006. The QCM-D technique. In Piezoelectric Sensors, Vol. 5, Steinem C, Janshoff A (eds). Springer-Verlag: Berlin Heidelberg, 425–449.
Hopfner M, Rothe U, Bendas G. 2008. Biosensor-based evaluation of liposomal behavior in the target binding process. *J. Liposome Res.* **18**(1): 71–82.
Hoshino Y, Kawasaki T, Okahata Y. 2006. Effect of ultrasound on DNA polymerase reactions: monitoring on a 27-MHz quartz crystal microbalance. *Biomacromolecules* **7**(3): 682–685.
Hovgaard MB, Dong M, Otzen DE, Besenbacher F. 2007. Quartz crystal microbalance studies of multilayer glucagon fibrillation at the solid-liquid interface. *Biophys. J.* **93**(6): 2162–2169.
Hovgaard MB, Rechendorff K, Chevallier J, Foss M, Besenbacher F. 2008. Fibronectin adsorption on tantalum: the influence of nanoroughness. *J. Phys. Chem. B* **112**(28): 8241–8249.
Hsiao HY, Chen RL, Cheng TJ. 2009. Single-scan measurement of conductance of a quartz crystal microbalance array coupled with resonant markers for biosensing in liquid phase. *Rev. Sci. Instrum.* **80**(4): 044301.
Hu G, Heitmann JA Jr, Rojas OJ. 2009a. In situ monitoring of cellulase activity by microgravimetry with a quartz crystal microbalance. *J. Phys. Chem. B* **113**(44): 14761–14768.
Hu G, Heitmann JA, Rojas OJ. 2009b. Quantification of cellulase activity using the quartz crystal microbalance technique. *Anal. Chem.* **81**(5): 1872–1880.

Huang GS, Wang MT, Su CW, Chen YS, Hong MY. 2007a. Picogram detection of metal ions by melanin-sensitized piezoelectric sensor. *Biosens. Bioelectron.* **23**(3): 319–325.
Huang M, Shen Z, Zhang Y, Zeng X, Wang PG. 2007b. Alkanethiol containing glycopolymers: a tool for the detection of lectin binding. *Bioorg. Med. Chem. Lett.* **17**(19): 5379–5383.
Huenerbein A, Schmelzer CE, Neubert RH. 2007. Real-time monitoring of peptic and tryptic digestions of bovine beta-casein using quartz crystal microbalance. *Anal. Chim. Acta* **584**(1): 72–77.
Hulander M, Hong J, Andersson M, Gerven F, Ohrlander M, Tengvall P, Elwing H. 2009. Blood interactions with noble metals: coagulation and immune complement activation. *ACS Appl. Mater. Interfaces* **1**(5): 1053–1062.
Hunter AC. 2009. Application of the quartz crystal microbalance to nanomedicine. *J. Biomed. Nanotechnol.* **5**(6): 669–675.
Ignatova M, Voccia S, Gilbert B, Markova N, Cossement D, Gouttebaron R, Jerome R, Jerome C. 2006. Combination of electrografting and atom-transfer radical polymerization for making the stainless steel surface antibacterial and protein antiadhesive. *Langmuir* **22**(1): 255–262.
Inagaki S, Min JZ, Toyo'oka T. 2008. Prediction for the separation efficiency of a pair of enantiomers during chiral high-performance liquid chromatography using a quartz crystal microbalance. *Anal. Chem.* **80**(5): 1824–1828.
Indest T, Laine J, Ribitsch V, Johansson LS, Stana-Kleinschek K, Strnad S. 2008. Adsorption of chitosan on PET films monitored by quartz crystal microbalance. *Biomacromolecules* **9**(8): 2207–2214.
Indest T, Laine J, Johansson LS, Stana-Kleinschek K, Strnad S, Dworczak R, Ribitsch V. 2009. Adsorption of fucoidan and chitosan sulfate on chitosan modified PET films monitored by QCM-D. *Biomacromolecules.* **10**(3): 630–637.
Inomata T, Eguchi H, Matsumoto K, Funahashi Y, Ozawa T, Masuda H. 2007. Adsorption of microorganisms onto an artificial siderophore-modified Au substrate. *Biosens. Bioelectron.* **23**(5): 751–755.
Ishida H, Satou T, Tsuji K, Kawashima N, Takemura H, Kosaki Y, Shiratori S, Agishi T. 2008. The breath ammonia measurement of the hemodialysis with a QCM-NH3 sensor. *Biomed. Mater. Eng.* **18**(2): 99–106.
Ishizuka-Katsura Y, Wazawa T, Ban T, Morigaki K, Aoyama S. 2008. Biotin-containing phospholipid vesicle layer formed on self-assembled monolayer of a saccharide-terminated alkyl disulfide for surface plasmon resonance biosensing. *J Biosci. Bioeng.* **105**(5): 527–535.
Janshoff A, Galla H-J, Steinem C. 2000. Piezoelectric mass-sensing devices as biosensors: an alternative to optical biosensors? *Angewandte Chemie* **39**(22): 4004–4032.
Jenik M, Schirhagl R, Schirk C, Hayden O, Lieberzeit P, Blaas D, Paul G, Dickert FL. 2009. Sensing picornaviruses using molecular imprinting techniques on a quartz crystal microbalance. *Anal. Chem.* **81**(13): 5320–5326.
Jia X, Xie Q, Zhang Y, Yao S. 2007. Simultaneous quartz crystal microbalance-electrochemical impedance spectroscopy study on the adsorption of anti-human immunoglobulin G and its immunoreaction at nanomaterial-modified Au electrode surfaces. *Anal. Sci.* **23**(6): 689–696.
Jimenez Y, Fernandez R, Torres R, Arnau A. 2006. A contribution to solve the problem of coating properties extraction in quartz crystal microbalance applications. *IEEE Trans. Ultrason. Ferroelectr. Freq. Control* **53**(5): 1057–1072.
Jin X, Liu X, Chen L, Jiang J, Shen G, Yu R. 2009. Biocatalyzed deposition amplification for detection of aflatoxin B1 based on quartz crystal microbalance. *Anal. Chim. Acta* **645**(1–2): 92–97.
Johannsmann D. 2006. Studies of contact mechanics with the QCM. In Piezoelectric Sensors, Vol. 5, Steinem C, Janshoff A (eds). Springer-Verlag: Berlin Heidelberg, 151–173.
Johannsmann D. 2008. Viscoelastic, mechanical, and dielectric measurements on complex samples with the quartz crystal microbalance. *Phys. Chem. Chem. Phys.* **10**(31): 4516–4534.
Johannsmann D, Reviakine I, Rojas E, Gallego M. 2008. Effect of sample heterogeneity on the interpretation of QCM(-D) data: comparison of combined quartz crystal microbalance/atomic force microscopy measurements with finite element method modeling. *Anal. Chem.* **80**(23): 8891–8899.
Johannsmann D, Reviakine I, Richter RP. 2009. Dissipation in films of adsorbed nanospheres studied by quartz crystal microbalance (QCM). *Anal. Chem.* **81**(19): 8167–8176.
Jonsson MP, Jonsson P, Hook F. 2008. Simultaneous nanoplasmonic and quartz crystal microbalance sensing: analysis of biomolecular conformational changes and quantification of the bound molecular mass. *Anal. Chem.* **80**(21): 7988–7995.
Joo J, Lee D, Yoo M, Jeon S. 2009. ZnO nanorod-coated quartz crystals as self-cleaning thiol sensors for natural gas fuel cells. *Sens. Actuators B Chem.* **138**(2): 485–490.
Jordan JL, Fernandez EJ. 2008. QCM-D sensitivity to protein adsorption reversibility. *Biotechnol. Bioeng.* **101**(4): 837–842.
Josefsson P, Henriksson G, Wagberg L. 2008. The physical action of cellulases revealed by a quartz crystal microbalance study using ultrathin cellulose films and pure cellulases. *Biomacromolecules* **9**(1): 249–254.
Jung H, Kim JY, Kim Y, Tae G, Kim YH, Johannsmann D. 2009a. QCM and AFM analysis of anticoagulant activities of sulfonated polymers against fibrin formation. *Langmuir* **25**(12): 7032–7041.
Jung H, Tae G, Kim YH, Johannsmann D. 2009b. Change of viscoelastic property and morphology of fibrin affected by antithrombin III and heparin: QCM-Z and AFM study. *Colloids Surf. B Biointerfaces* **68**(1): 111–119.
Kacar T, Zin MT, So C, Wilson B, Ma H, Gul-Karaguler N, Jen AK, Sarikaya M, Tamerler C. 2009. Directed self-immobilization of alkaline phosphatase on micro-patterned substrates via genetically fused metal-binding peptide. *Biotechnol. Bioeng.* **103**(4): 696–705.
Kamarun D, Zheng X, Milanesi L, Hunter CA, Krause S. 2009. A peptide cross-linked polyacrylamide hydrogel for the detection of human neutrophil elastase. *Electrochim. Acta* **54**(22): 4985–4990.
Kanazawa KK. 1997. Mechanical behaviour of films on the quartz microbalance. *Faraday Discuss.* **(107)**: 77–90.
Kang HW, Muramatsu H. 2009. Monitoring of cultured cell activity by the quartz crystal and the micro CCD camera under chemical stressors. *Biosens. Bioelectron.* **24**(5): 1318–1323.
Kankare J, Loikas K, Salomaki M. 2006. Method for measuring the losses and loading of a quartz crystal microbalance. *Anal. Chem.* **78**(6): 1875–1882.
Kaseda R, Iino N, Hosojima M, Takeda T, Hosaka K, Kobayashi A, Yamamoto K, Suzuki A, Kasai A, Suzuki Y, Gejyo F, Saito A. 2007. Megalin-mediated endocytosis of cystatin C in proximal tubule cells. *Biochem. Biophys. Res. Commun.* **357**(4): 1130–1134.
Kastl K, Menke M, Luthgens E, Faiss S, Gerke V, Janshoff A, Steinem C. 2006. Partially reversible adsorption of annexin A1 on POPC/POPS bilayers investigated by QCM measurements, SFM, and DMC simulations. *Chembiochem* **7**(1): 106–115.
Kaufman ED, Belyea J, Johnson MC, Nicholson ZM, Ricks JL, Shah PK, Bayless M, Pettersson T, Feldoto Z, Blomberg E, Claesson P, Franzen S. 2007. Probing protein adsorption onto mercaptoundecanoic acid stabilized gold nanoparticles and surfaces by quartz crystal microbalance and zeta-potential measurements. *Langmuir* **23**(11): 6053–6062.
Kida T, Minabe T, Nakano S, Akashi M. 2008. Fabrication of novel multilayered thin films based on inclusion complex formation between amylose derivatives and guest polymers. *Langmuir* **24**(17): 9227–9229.
Kim JT, Weber N, Shin GH, Huang Q, Liu SX. 2007a. The study of beta-lactoglobulin adsorption on polyethersulfone thin film surface using QCM-D and AFM. *J. Food Sci.* **72**(4): E214–221.
Kim N, Park IS, Kim DK. 2007b. High-sensitivity detection for model organophosphorus and carbamate pesticide with quartz crystal microbalance-precipitation sensor. *Biosens. Bioelectron.* **22**(8): 1593–1599.
Kim NH, Baek TJ, Park HG, Seong GH. 2007c. Highly sensitive biomolecule detection on a quartz crystal microbalance using gold nanoparticles as signal amplification probes. *Anal. Sci.* **23**(2): 177–181.
Kim N, Kim D-K, Cho Y-J. 2009. Development of indirect-competitive quartz crystal microbalance immunosensor for C-reactive protein. *Sens. Actuators B Chem.* **143**(1): 444–448.
Kira A, Okano K, Hosokawa Y, Naito A, Fuwa K, Yuyama J, Masuhara H. 2009. Micropatterning of perfluoroalkyl self-assembled monolayers for arraying proteins and cells on chips. *Appl. Surf. Sci.* **255**(17): 7647–7651.
Kirchhof K, Groth T. 2008. Surface modification of biomaterials to control adhesion of cells. *Clin. Hemorheol. Microcirc.* **39**(1–4): 247–251.
Knerr R, Weiser B, Drotleff S, Steinem C, Gopferich A. 2006. Measuring cell adhesion on RGD-modified, self-assembled PEG monolayers using

the quartz crystal microbalance technique. *Macromol. Biosci.* **6**(10): 827–838.

Kohen NT, Little LE, Healy KE. 2009. Characterization of Matrigel interfaces during defined human embryonic stem cell culture. *Biointerphases* **4**(4): 69–79.

Konig AM, Duwel M, Du B, Kunze M, Johannsmann D. 2006. Measurements of interfacial viscoelasticity with a quartz crystal microbalance: influence of acoustic scattering from a small crystal-sample contact. *Langmuir* **22**(1): 229–233.

Kontturi KS, Tammelin T, Johansson LS, Stenius P. 2008. Adsorption of cationic starch on cellulose studied by QCM-D. *Langmuir* **24**(9): 4743–4749.

Koshets IA, Kazantseva ZI, Belyaev AE, Kalchenko VI. 2009. Sensitivity of resorcinarene films towards aliphatic alcohols. *Sens. Actuators B Chem.* **140**(1): 104–108.

Kotarek JA, Johnson KC, Moss MA. 2008. Quartz crystal microbalance analysis of growth kinetics for aggregation intermediates of the amyloid-beta protein. *Anal. Biochem.* **378**(1): 15–24.

Kumashiro Y, Ikezoe Y, Tamada K, Hara M. 2008. Dynamic interfacial properties of poly(ethylene glycol)-modified ferritin at the solid/liquid interface. *J. Phys. Chem. B* **112**(28): 8291–8297.

Kunze A, Sjovall P, Kasemo B, Svedhem S. 2009a. In situ preparation and modification of supported lipid layers by lipid transfer from vesicles studied by QCM-D and TOF-SIMS. *J. Am. Chem. Soc.* **131**(7): 2450–2451.

Kunze A, Svedhem S, Kasemo B. 2009b. Lipid transfer between charged supported lipid bilayers and oppositely charged vesicles. *Langmuir* **25**(9): 5146–5158.

Kurosawa S, Park JW, Aizawa H, Wakida S, Tao H, Ishihara K. 2006. Quartz crystal microbalance immunosensors for environmental monitoring. *Biosens. Bioelectron.* **22**(4): 473–481.

Kwon KD, Green H, Bjoorn P, Kubicki JD. 2006. Model bacterial extracellular polysaccharide adsorption onto silica and alumina: quartz crystal microbalance with dissipation monitoring of dextran adsorption. *Environ. Sci. Technol.* **40**(24): 7739–7744.

Lakshmanan M, Dhathathreyan A. 2007. Hydrodynamically coupled water in surface adsorbed amino acids as a tool to study hydrated peptides. *Biochim. Biophys. Acta* **1774**(1): 138–145.

Lakshmanan M, Parthasarathi R, Dhathathreyan A. 2006. Do properties of bovine serum albumin at fluid/electrolyte interface follow the Hofmeister series? An analysis using Langmuir and Langmuir-Blodgett films. *Biochim. Biophys. Acta* **1764**(11): 1767–1774.

Larsson A, Angbrant J, Ekeroth J, Månsson P, Liedberg B. 2006. A novel biochip technology for detection of explosives—TNT: synthesis, characterisation and application. *Sens. Actuators B Chem.* **113**(2): 730–748.

Larsson EM, Edvardsson ME, Langhammer C, Zoric I, Kasemo B. 2009. A combined nanoplasmonic and electrodeless quartz crystal microbalance setup. *Rev. Sci. Instrum.* **80**(12): 125105.

Lazerges M, Perrot H, Antoine E, Defontaine A, Compere C. 2006. Oligonucleotide quartz crystal microbalance sensor for the microalgae Alexandrium minutum (Dinophyceae). *Biosens. Bioelectron.* **21**(7): 1355–1358.

Lebed K, Kulik AJ, Forro L, Lekka M. 2006. Lectin-carbohydrate affinity measured using a quartz crystal microbalance. *J. Colloid Interface Sci.* **299**(1): 41–48.

Lee SY, Choi J, Royston E, Janes DB, Culver JN, Harris MT. 2006. Deposition of platinum clusters on surface-modified Tobacco mosaic virus. *J. Nanosci. Nanotechnol.* **6**(4): 974–9981.

Lee BS, Chi YS, Lee KB, Kim YG, Choi IS. 2007. Functionalization of poly(oligo(ethylene glycol) methacrylate) films on gold and Si/SiO2 for immobilization of proteins and cells: SPR and QCM studies. *Biomacromolecules* **8**(12): 3922–3929.

Lee DY, Choi WS, Kafi AK, Park SH, Kwon YS. 2008a. Immobilization, hybridization and amperometric detection of DNA sensor using quartz crystal microbalance. *J. Nanosci. Nanotechnol.* **8**(9): 4553–4556.

Lee J, Jang J, Akin D, Savran CA, Bashir R. 2008b. Real-time detection of airborne viruses on a mass-sensitive device. *Appl. Phys. Lett.* **93**(1): 13901.

Lee D, Ashcraft JN, Verploegen E, Pashkovski E, Weitz DA. 2009. Permeability of model stratum corneum lipid membrane measured using quartz crystal microbalance. *Langmuir* **25**(10): 5762–5766.

Liao JY. 2007. Construction of nanogold hollow balls with dendritic surface as immobilized affinity support for protein adsorption. *Colloids Surf. B Biointerfaces* **57**(1): 75–80.

Lieberzeit PA, Rehman A, Najafi B, Dickert FL. 2008. Real-life application of a QCM-based e-nose: quantitative characterization of different plant-degradation processes. *Anal. Bioanal. Chem.* **391**(8): 2897–2903.

Lin Y, Su Z, Niu Z, Li S, Kaur G, Lee LA, Wang Q. 2008. Layer-by-layer assembly of viral capsid for cell adhesion. *Acta Biomater.* **4**(4): 838–843.

Liu G, Craig VS. 2009. Improved cleaning of hydrophilic protein-coated surfaces using the combination of Nanobubbles and SDS. *ACS Appl. Mater. Interfaces* **1**(2): 481–487.

Liu H, Hu N. 2006. Interaction between myoglobin and hyaluronic acid in their layer-by-layer assembly: quartz crystal microbalance and cyclic voltammetry studies. *J. Phys. Chem. B* **110**(29): 14494–14502.

Liu SX, Kim J-T. 2009a. Application of Kevin-Voigt model in quantifying whey protein adsorption on polyethersulfone using QCM-D. *JALA* **14**(4): 213–220.

Liu SX, Kim J-T. 2009b. Study of adsorption kinetics of surfactants onto polyethersulfone membrane surface using QCM-D. *Desalination* **247**(1–3): 355–361.

Liu F, Liu X, Ng SC, Chan HSO. 2006a. Enantioselective molecular imprinting polymer coated QCM for the recognition of l-tryptophan. *Sens. Actuators B Chem.* **113**(1): 234–240.

Liu Y, Lu H, Zhong W, Song P, Kong J, Yang P, Girault HH, Liu B. 2006b. Multilayer-assembled microchip for enzyme immobilization as reactor toward low-level protein identification. *Anal. Chem.* **78**(3): 801–808.

Liu Y, Tang X, Pei J, Zhang L, Liu F, Li K. 2006c. Gastrodin interaction with human fibrinogen: anticoagulant effects and binding studies. *Chemistry* **12**(30): 7807–7815.

Liu Y, Zhong W, Meng S, Kong J, Lu H, Yang P, Girault HH, Liu B. 2006d. Assembly-controlled biocompatible interface on a microchip: strategy to highly efficient proteolysis. *Chemistry* **12**(25): 6585–6591.

Liu Y, Xue Y, Ji J, Chen X, Kong J, Yang P, Girault HH, Liu B. 2007. Gold nanoparticle assembly microfluidic reactor for efficient on-line proteolysis. *Mol. Cell. Proteomics* **6**(8): 1428–1436.

Liu Y, Meng S, Mu L, Jin G, Zhong W, Kong J. 2008. Novel renewable immunosensors based on temperature-sensitive PNIPAAm bioconjugates. *Biosens. Bioelectron.* **24**(4): 710–715.

Liu G, Fu L, Zhang G. 2009. Role of hydrophobic interactions in the adsorption of poly(ethylene glycol) chains on phospholipid membranes investigated with a quartz crystal microbalance. *J. Phys. Chem. B* **113**(11): 3365–3369.

Lojou E, Bianco P. 2006. Assemblies of dendrimers and proteins on carbon and gold electrodes. *Bioelectrochemistry* **69**(2): 237–247.

Long G, Zhu P, Shen Y, Tong M. 2009. Influence of extracellular polymeric substances (EPS) on deposition kinetics of bacteria. *Environ. Sci. Technol.* **43**(7): 2308–2314.

Lord MS, Cousins BG, Doherty PJ, Whitelock JM, Simmons A, Williams RL, Milthorpe BK. 2006a. The effect of silica nanoparticulate coatings on serum protein adsorption and cellular response. *Biomaterials* **27**(28): 4856–4862.

Lord MS, Modin C, Foss M, Duch M, Simmons A, Pedersen FS, Milthorpe BK, Besenbacher F. 2006b. Monitoring cell adhesion on tantalum and oxidised polystyrene using a quartz crystal microbalance with dissipation. *Biomaterials* **27**(26): 4529–4537.

Lord MS, Stenzel MH, Simmons A, Milthorpe BK. 2006c. The effect of charged groups on protein interactions with poly(HEMA) hydrogels. *Biomaterials* **27**(4): 567–575.

Lord MS, Modin C, Foss M, Duch M, Simmons A, Pedersen FS, Besenbacher F, Milthorpe BK. 2008. Extracellular matrix remodelling during cell adhesion monitored by the quartz crystal microbalance. *Biomaterials* **29**(17): 2581–2587.

Lu H, Hu N. 2007. Salt-induced swelling and electrochemical property change of hyaluronic acid/myoglobin multilayer films. *J. Phys. Chem. B* **111**(8): 1984–1993.

Lu W, Lin L, Jiang L. 2007. Nanogold hollow balls with dendritic surface for hybridization of DNA. *Biosens. Bioelectron.* **22**(6): 1101–1105.

Lubarsky GV, Davidson MR, Bradley RH. 2007. Hydration-dehydration of adsorbed protein films studied by AFM and QCM-D. *Biosens. Bioelectron.* **22**(7): 1275–1281.

Lucklum R, Eichelbaum F. 2006. Interface circuits for QCM sensors. In Piezoelectric Sensors, Vol. 5, Steinem C, Janshoff A (eds). Springer-Verlag: Berlin Heidelberg, 3–49.

Lundgren SM, Persson K, Mueller G, Kronberg B, Clarke J, Chtaib M, Claesson PM. 2007. Unsaturated fatty acids in alkane solution: adsorption to steel surfaces. *Langmuir* **23**(21): 10598–10602.

Luo Y, Chen M, Wen Q, Zhao M, Zhang B, Li X, Wang F, Huang Q, Yao C, Jiang T, Cai G, Fu W. 2006. Rapid and simultaneous quantification of 4 urinary proteins by piezoelectric quartz crystal microbalance immunosensor array. *Clin. Chem.* **52**(12): 2273–2280.
Luo J, Zhang Q, Huang Y, Liu G, Zhao R. 2007. Quartz crystal microbalance biosensor for recombinant human interferon-beta detection based on antisense peptide approach. *Anal. Chim. Acta* **590**(1): 91–97.
Ma C, Hou Y, Liu S, Zhang G. 2009. Effect of microphase separation on the protein resistance of a polymeric surface. *Langmuir* **25**(16): 9467–9472.
Malmstrom J, Agheli H, Kingshott P, Sutherland DS. 2007. Viscoelastic modeling of highly hydrated laminin layers at homogeneous and nanostructured surfaces: quantification of protein layer properties using QCM-D and SPR. *Langmuir* **23**(19): 9760–9768.
Malmstrom J, Shipovskov S, Christensen B, Sorensen ES, Kingshott P, Sutherland DS. 2009. Adsorption and enzymatic cleavage of osteopontin at interfaces with different surface chemistries. *Biointerphases* **4**(3): 47–55.
Mangsbo SM, Sanchez J, Anger K, Lambris JD, Ekdahl KN, Loskog AS, Nilsson B, Totterman TH. 2009. Complement activation by CpG in a human whole blood loop system: mechanisms and immunomodulatory effects. *J. Immunol.* **183**(10): 6724–6732.
Manso M, Navas CR, Gilliland D, Ruiz PG, Rossi F. 2007. Cellular response to oxygen containing biomedical polymers modified by Ar and He implantation. *Acta Biomater.* **3**(5): 735–743.
Mao X, Yang L, Su XL, Li Y. 2006. A nanoparticle amplification based quartz crystal microbalance DNA sensor for detection of Escherichia coli O157:H7. *Biosens. Bioelectron.* **21**(7): 1178–1185.
March C, Manclus JJ, Jimenez Y, Arnau A, Montoya A. 2009. A piezoelectric immunosensor for the determination of pesticide residues and metabolites in fruit juices. *Talanta* **78**(3): 827–833.
Marx KA. 2003. Quartz crystal microbalance: a useful tool for studying thin polymer films and complex biomolecular systems at the solution–surface interface. *Biomacromolecules* **4**(5): 1099–1120.
Marx KA. 2006. The quarz crystal microbalance and the electrochemical QCM: applications to studies of thin polymer films, electron transfer systems, biological macromolecules, biosensors, and cells. In Piezoelectric Sensors, Vol. 5, Steinem C, Janshoff A (eds). Springer-Verlag: Berlin Heidelberg, 371–425.
Marx KA, Zhou T, Montrone A, McIntosh D, Braunhut SJ. 2007. A comparative study of the cytoskeleton binding drugs nocodazole and taxol with a mammalian cell quartz crystal microbalance biosensor: different dynamic responses and energy dissipation effects. *Anal. Biochem.* **361**(1): 77–92.
Marx KA, Zhou T, McIntosh D, Braunhut SJ. 2009. Electropolymerized tyrosine-based thin films: selective cell binding via peptide recognition to novel electropolymerized biomimetic tyrosine RGDY films. *Anal. Biochem.* **384**(1): 86–95.
Matsuda Y, Osaki T, Hashii T, Koshiba T, Kawabata S. 2007. A cysteine-rich protein from an arthropod stabilizes clotting mesh and immobilizes bacteria at injury sites. *J. Biol. Chem.* **282**(46): 33545–33552.
Matsuguchi M, Uno T. 2006. Molecular imprinting strategy for solvent molecules and its application for QCM-based VOC vapor sensing. *Sens. Actuators B Chem.* **113**(1): 94–99.
Matsukawa N, Nishio K, Sano K, Shiba K, Yamashita I. 2009. Hexagonal close-packed array formed by selective adsorption onto hexagonal patterns. *Langmuir* **25**(6): 3327–3330.
Matsunaga H, Ueda H. 2008. Synergistic Ca2+ and Cu2+ requirements of the FGF1-S100A13 interaction measured by quartz crystal microbalance: an initial step in amlexanox-reversible non-classical release of FGF1. *Neurochem. Int.* **52**(6): 1076–1085.
Matsusaki M, Omichi M, Maruyama I, Akashi M. 2008. Physical adsorption of human thrombomodulin (ART-123) onto polymeric biomaterials for developing an antithrombogenic blood-contacting material. *J. Biomed. Mater. Res. A* **84**(1): 1–9.
Mazur M, Krysinski P, Michota-Kaminska A, Bukowska J, Rogalski J, Blanchard GJ. 2007. Immobilization of laccase on gold, silver and indium tin oxide by zirconium-phosphonate-carboxylate (ZPC) coordination chemistry. *Bioelectrochemistry* **71**(1): 15–22.
Mechler A, Praporski S, Atmuri K, Boland M, Separovic F, Martin LL. 2007. Specific and selective peptide-membrane interactions revealed using quartz crystal microbalance. *Biophys. J.* **93**(11): 3907–3916.
Mechler A, Praporski S, Piantavigna S, Heaton SM, Hall KN, Aguilar MI, Martin LL. 2009. Structure and homogeneity of pseudo-physiological phospholipid bilayers and their deposition characteristics on carboxylic acid terminated self-assembled monolayers. *Biomaterials* **30**(4): 682–689.
Melegari M, Suman M, Pirondini L, Moiani D, Massera C, Ugozzoli F, Kalenius E, Vainiotalo P, Mulatier JC, Dutasta JP, Dalcanale E. 2008. Supramolecular sensing with phosphonate cavitands. *Chemistry* **14**(19): 5772–5779.
Messina GM, Satriano C, Marletta G. 2009. A multitechnique study of preferential protein adsorption on hydrophobic and hydrophilic plasma-modified polymer surfaces. *Colloids Surf. B Biointerfaces* **70**(1): 76–83.
Michael J, Schonzart L, Israel I, Beutner R, Scharnweber D, Worch H, Hempel U, Schwenzer B. 2009. Oligonucleotide-RGD peptide conjugates for surface modification of titanium implants and improvement of osteoblast adhesion. *Bioconjug. Chem.* **20**(4): 710–718.
Min K, Cho M, Han SY, Shim YB, Ku J, Ban C. 2008. A simple and direct electrochemical detection of interferon-gamma using its RNA and DNA aptamers. *Biosens. Bioelectron.* **23**(12): 1819–1824.
Mitomo H, Shigematsu H, Kobatake E, Furusawa H, Okahata Y. 2007. IgG binding kinetics to oligo B protein A domains on lipid layers immobilized on a 27MHz quartz-crystal microbalance. *J. Mol. Recognit.* **20**(2): 83–89.
Mizota K, Ueda H. 2008. N-terminus of MAP2C as a neurosteroid-binding site. *Neuroreport* **19**(15): 1529–1533.
Modin C, Stranne AL, Foss M, Duch M, Justesen J, Chevallier J, Andersen LK, Hemmersam AG, Pedersen FS, Besenbacher F. 2006. QCM-D studies of attachment and differential spreading of pre-osteoblastic cells on Ta and Cr surfaces. *Biomaterials* **27**(8): 1346–1354.
Molino PJ, Hodson OM, Quinn JF, Wetherbee R. 2008. The quartz crystal microbalance: a new tool for the investigation of the bioadhesion of diatoms to surfaces of differing surface energies. *Langmuir* **24**(13): 6730–6737.
Monkawa A, Ikoma T, Yunoki S, Yoshioka T, Tanaka J, Chakarov D, Kasemo B. 2006. Fabrication of hydroxyapatite ultra-thin layer on gold surface and its application for quartz crystal microbalance technique. *Biomaterials* **27**(33): 5748–5754.
Mori T, Toyoda M, Ohtsuka T, Okahata Y. 2009. Kinetic analyses for bindings of concanavalin A to dispersed and condensed mannose surfaces on a quartz crystal microbalance. *Anal. Biochem.* **395**(2): 211–216.
Morita S, Nukui M, Kuboi R. 2006. Immobilization of liposomes onto quartz crystal microbalance to detect interaction between liposomes and proteins. *J. Colloid Interface Sci.* **298**(2): 672–678.
Mun S, Choi SJ. 2009. Optimization of the hybrid bilayer membrane method for immobilization of avidin on quartz crystal microbalance. *Biosens. Bioelectron.* **24**(8): 2522–2527.
Myszka DG, Rich RL. 2000. Implementing surface plasmon resonance biosensors in drug discovery. *Pharm. Sci. Tech. Today* **3**(9): 310–317.
Nabok A, Tsargorodskaya A, Holloway A, Starodub NF, Demchenko A. 2007a. Specific binding of large aggregates of amphiphilic molecules to the respective antibodies. *Langmuir* **23**(16): 8485–8490.
Nabok AV, Tsargorodskaya A, Holloway A, Starodub NF, Gojster O. 2007b. Registration of T-2 mycotoxin with total internal reflection ellipsometry and QCM impedance methods. *Biosens. Bioelectron.* **22**(6): 885–890.
Nakane Y, Kubo I. 2009. Layer-by-layer of liposomes and membrane protein as a recognition element of biosensor. *Thin Solid Films* **518**(2): 678–681.
Nakano K, Matsunaga H, Sai K, Soh N, Imato T. 2006. Photoactive, covalent attachment of deoxyribonucleic acid on gold with double-strand specificity using self-assembled monolayers containing psoralen. *Anal. Chim. Acta* **578**(1): 93–99.
Nanduri V, Sorokulova IB, Samoylov AM, Simonian AL, Petrenko VA, Vodyanoy V. 2007. Phage as a molecular recognition element in biosensors immobilized by physical adsorption. *Biosens. Bioelectron.* **22**(6): 986–992.
Nezu T, Masuyama T, Sasaki K, Saitoh S, Taira M, Araki Y. 2008. Effect of pH and addition of salt on the adsorption behavior of lysozyme on gold, silica, and titania surfaces observed by quartz crystal microbalance with dissipation monitoring. *Dent. Mater. J.* **27**(4): 573–580.
Nguyen TH, Chen KL. 2007. Role of divalent cations in plasmid DNA adsorption to natural organic matter-coated silica surface. *Environ. Sci. Technol.* **41**(15): 5370–5375.
Nguyen TH, Elimelech M. 2007a. Adsorption of plasmid DNA to a natural organic matter-coated silica surface: kinetics, conformation, and reversibility. *Langmuir* **23**(6): 3273–3279.

Nguyen TH, Elimelech M. 2007b. Plasmid DNA adsorption on silica: kinetics and conformational changes in monovalent and divalent salts. *Biomacromolecules* **8**(1): 24–32.
Nie L, Yang Y, Li S, Wang J, Hou Q. 2007. QCM detection of oligonucleotide by quiescent mode and flowing mode. *J. Nanosci. Nanotechnol.* **7**(8): 2927–2929.
Nishiyama K, Takakusagi Y, Kusayanagi T, Matsumoto Y, Habu S, Kuramochi K, Sugawara F, Sakaguchi K, Takahashi H, Natsugari H, Kobayashi S. 2009. Identification of trimannoside-recognizing peptide sequences from a T7 phage display screen using a QCM device. *Bioorg. Med. Chem.* **17**(1): 195–202.
Nobre TM, de Sousa H, Silva e, Furriel RP, Leone FA, Miranda PB, Zaniquelli ME. 2009. Molecular view of the interaction between iota-carrageenan and a phospholipid film and its role in enzyme immobilization. *J. Phys. Chem. B* **113**(21): 7491–7497.
Nomura T, Okuhara M. 1982. Frequency-shifts of piezoelectric quartz crystals immersed in organic liquids. *Anal. Chim. Acta* **142**: 281–284.
Norberg O, Deng L, Yan M, Ramstrom O. 2009. Photo-click immobilization of carbohydrates on polymeric surfaces–a quick method to functionalize surfaces for biomolecular recognition studies. *Bioconjug. Chem.* **20**(12): 2364–2370.
Notley SM. 2008. Effect of introduced charge in cellulose gels on surface interactions and the adsorption of highly charged cationic polyelectrolytes. *Phys. Chem. Chem. Phys.* **10**(13): 1819–1825.
Notley SM, Norgren M. 2006. Measurement of interaction forces between lignin and cellulose as a function of aqueous electrolyte solution conditions. *Langmuir* **22**(26): 11199–11204.
Numata K, Yamashita K, Fujita M, Tsuge T, Kasuya K, Iwata T, Doi Y, Abe H. 2007. Adsorption and hydrolysis reactions of poly(hydroxybutyric acid) depolymerases secreted from Ralstonia pickettii T1 and Penicillium funiculosum onto poly[(R)-3-hydroxybutyric acid]. *Biomacromolecules* **8**(7): 2276–2281.
Ogi H, Motoshisa K, Matsumoto T, Hatanaka K, Hirao M. 2006. Isolated electrodeless high-frequency quartz crystal microbalance for immunosensors. *Anal. Chem.* **78**(19): 6903–6909.
Ogi H, Motohisa K, Hatanaka K, Ohmori T, Hirao M, Nishiyama M. 2007. Concentration dependence of IgG-protein A affinity studied by wireless-electrodeless QCM. *Biosens. Bioelectron.* **22**(12): 3238–3242.
Ogi H, Fukunishi Y, Omori T, Hatanaka K, Hirao M, Nishiyama M. 2008. Effects of flow rate on sensitivity and affinity in flow injection biosensor systems studied by 55-MHz wireless quartz crystal microbalance. *Anal. Chem.* **80**(14): 5494–5500.
Ogi H, Naga H, Fukunishi Y, Hirao M, Nishiyama M. 2009a. 170-MHz electrodeless quartz crystal microbalance biosensor: capability and limitation of higher frequency measurement. *Anal. Chem.* **81**(19): 8068–8073.
Ogi H, Okamoto K, Nagai H, Fukunishi Y, Hirao M. 2009b. Replacement-free electrodeless quartz crystal microbalance biosensor using non-specific-adsorption of streptavidin on quartz. *Anal. Chem.* **81**(10): 4015–4020.
Okada T, Yamamoto Y, Miyachi H, Karube I, Muramatsu H. 2007. Application of peptide probe for evaluating affinity properties of proteins using quartz crystal microbalance. *Biosens. Bioelectron.* **22**(7): 1480–1486.
Okazaki T, Morigaki K, Taguchi T. 2006. Phospholipid vesicle fusion on micropatterned polymeric bilayer substrates. *Biophys. J.* **91**(5): 1757–1766.
Okuno H, Mori K, Jitsukawa T, Inoue H, Chiba S. 2006. Convenient method for monitoring Abeta aggregation by quartz-crystal microbalance. *Chem. Biol. Drug Des.* **68**(5): 273–275.
Okuno H, Mori K, Okada T, Yokoyama Y, Suzuki H. 2007. Development of aggregation inhibitors for amyloid-beta peptides and their evaluation by quartz-crystal microbalance. *Chem. Biol. Drug Des.* **69**(5): 356–361.
Olsen EV, Sorokulova IB, Petrenko VA, Chen IH, Barbaree JM, Vodyanoy VJ. 2006. Affinity-selected filamentous bacteriophage as a probe for acoustic wave biodetectors of Salmonella typhimurium. *Biosens. Bioelectron.* **21**(8): 1434–1442.
Olsson AL, van der Mei HC, Busscher HJ, Sharma PK. 2009. Influence of cell surface appendages on the bacterium-substratum interface measured real-time using QCM-D. *Langmuir* **25**(3): 1627–1632.
Osaki T, Renner L, Herklotz M, Werner C. 2006. Hydrophobic and electrostatic interactions in the adsorption of fibronectin at maleic acid copolymer films. *J. Phys. Chem. B* **110**(24): 12119–12124.
Otzen D. 2008. Differential adsorption of variants of the Thermomyces lanuginosus lipase on a hydrophobic surface suggests a role for local flexibility. *Colloids Surf. B Biointerfaces* **64**(2): 223–228.
Owen TW, Al-Kaysi RO, Bardeen CJ, Cheng Q. 2007. Microgravimetric immunosensor for direct detection of aerosolized influenza A virus particles. *Sens. Actuators B Chem.* **126**(2): 691–699.
Ozaki N, Ohmuraya M, Hirota M, Ida S, Wang J, Takamori H, Higashiyama S, Baba H, Yamamura K. 2009. Serine protease inhibitor Kazal type 1 promotes proliferation of pancreatic cancer cells through the epidermal growth factor receptor. *Mol. Cancer Res.* **7**(9): 1572–1581.
Ozeki T, Verma V, Uppalapati M, Suzuki Y, Nakamura M, Catchmark JM, Hancock WO. 2009. Surface-bound casein modulates the adsorption and activity of kinesin on SiO2 surfaces. *Biophys. J.* **96**(8): 3305–3318.
Pang L, Li J, Jiang J, Shen G, Yu R. 2006. DNA point mutation detection based on DNA ligase reaction and nano-Au amplification: a piezoelectric approach. *Anal. Biochem.* **358**(1): 99–103.
Park JW, Kurosawa S, Aizawa H, Hamano H, Harada Y, Asano S, Mizushima Y, Higaki M. 2006. Dioxin immunosensor using anti-2,3,7,8-TCDD antibody which was produced with mono 6-(2,3,6,7-tetrachloroxanthene-9-ylidene) hexyl succinate as a hapten. *Biosens. Bioelectron.* **22**(3): 409–414.
Pastorino L, Caneva Soumetz F, Giacomini M, Ruggiero C. 2006. Development of a piezoelectric immunosensor for the measurement of paclitaxel. *J. Immunol. Methods* **313**(1–2): 191–198.
Pastorino L, Soumetz FC, Ruggiero C. 2007. Nanostructured thin films for the development of piezoelectric immunosensors. *Conf. Proc. IEEE Eng. Med. Biol. Soc.* **1**: 2257–2260.
Patel AR, Frank CW. 2006. Quantitative analysis of tethered vesicle assemblies by quartz crystal microbalance with dissipation monitoring: Binding dynamics and bound water content. *Langmuir* **22**(18): 7587–7599.
Patel AR, Kanazawa KK, Frank CW. 2009a. Antibody binding to a tethered vesicle assembly using QCM-D. *Anal. Chem.* **81**(15): 6021–6029.
Patel AR, Kerwin BA, Kanapuram SR. 2009b. Viscoelastic characterization of high concentration antibody formulations using quartz crystal microbalance with dissipation monitoring. *J. Pharm. Sci.* **98**(9): 3108–3116.
Pavinatto FJ, Caseli L, Pavinatto A, dos Santos DS Jr, Nobre TM, Zaniquelli ME, Silva HS, Miranda PB, de Oliveira ON Jr. 2007. Probing chitosan and phospholipid interactions using Langmuir and Langmuir-Blodgett films as cell membrane models. *Langmuir* **23**(14): 7666–7671.
Peduru Hewa TM, Tannock GA, Mainwaring DE, Harrison S, Fecondo JV. 2009. The detection of influenza A and B viruses in clinical specimens using a quartz crystal microbalance. *J. Virol. Methods* **162**(1–2): 14–21.
Peh WY, Reimhult E, Teh HF, Thomsen JS, Su X. 2007. Understanding ligand binding effects on the conformation of estrogen receptor alpha-DNA complexes: a combinational quartz crystal microbalance with dissipation and surface plasmon resonance study. *Biophys. J.* **92**(12): 4415–4423.
Pei ZC, Larsson R, Aastrup T, Anderson H, Lehn JM, Ramstrom O. 2006. Quartz crystal microbalance bioaffinity sensor for rapid identification of glycosyldisulfide lectin inhibitors from a dynamic combinatorial library. *Biosens. Bioelectron.* **22**(1): 42–48.
Pei Y, Yu H, Pei Z, Theurer M, Ammer C, Andre S, Gabius HJ, Yan M, Ramstrom O. 2007. Photoderivatized polymer thin films at quartz crystal microbalance surfaces: sensors for carbohydrate-protein interactions. *Anal. Chem.* **79**(18): 6897–6902.
Pfeiffer I, Seantier B, Petronis S, Sutherland D, Kasemo B, Zach M. 2008. Influence of nanotopography on phospholipid bilayer formation on silicon dioxide. *J. Phys. Chem. B* **112**(16): 5175–5181.
Pham M, Mintz EA, Nguyen TH. 2009. Deposition kinetics of bacteriophage MS2 to natural organic matter: role of divalent cations. *J. Colloid Interface Sci.* **338**(1): 1–9.
Picard C, Davoust L. 2007. Resonance frequencies of meniscus waves as a physical mechanism for a DNA biosensor. *Langmuir* **23**(3): 1394–1402.
Pietrzyk A, Suriyanarayanan S, Kutner W, Chitta R, D'Souza F. 2009. Selective histamine piezoelectric chemosensor using a recognition film of the molecularly imprinted polymer of bis(bithiophene) derivatives. *Anal. Chem.* **81**(7): 2633–2643.
Pillai S, Arpanaei A, Meyer RL, Birkedal V, Gram L, Besenbacher F, Kingshott P. 2009. Preventing protein adsorption from a range of surfaces using an aqueous fish protein extract. *Biomacromolecules* **10**(10): 2759–2766.

Poitras C, Tufenkji N. 2009. A QCM-D-based biosensor for E. coli O157:H7 highlighting the relevance of the dissipation slope as a transduction signal. *Biosens. Bioelectron.* **24**(7): 2137–2142.
Poitras C, Fatisson J, Tufenkji N. 2009. Real-time microgravimetric quantification of Cryptosporidium parvum in the presence of potential interferents. *Water Res.* **43**(10): 2631–2638.
Prachayasittikul V, Isarankura-Na-Ayudhya C, Tantimongcolwat T, Nantasenamat C, Galla HJ. 2007. EDTA-induced membrane fluidization and destabilization: biophysical studies on artificial lipid membranes. *Acta Biochim. Biophys. Sin. (Shanghai)* **39**(11): 901–913.
Pribyl J, Skládal P. 2006. Development of a combined setup for simultaneous detection of total and glycated haemoglobin content in blood samples. *Biosens. Bioelectron.* **21**(10): 1952–1959.
Qiao K, Hu N. 2009. Direct electron transfer and electrocatalysis of myoglobin loaded in layer-by-layer films assembled with nonionic poly(ethylene glycol) and ZrO(2) nanoparticles. *Bioelectrochemistry* **75**(1): 71–76.
Quan L, Wei D, Jiang X, Liu Y, Li Z, Li N, Li K, Liu F, Lai L. 2008. Resurveying the Tris buffer solution: the specific interaction between tris(hydroxymethyl)aminomethane and lysozyme. *Anal. Biochem.* **378**(2): 144–150.
Rahman MA, Shiddiky MJ, Park JS, Shim YB. 2007. An impedimetric immunosensor for the label-free detection of bisphenol A. *Biosens. Bioelectron.* **22**(11): 2464–2470.
Rawle RJ, Selassie CR, Johal MS. 2007. Creation of mammalian single- and double-stranded DNA surfaces: a real-time QCM-D study. *Langmuir* **23**(19): 9563–9566.
Rawle RJ, Johal MS, Selassie CR. 2008. A real-time QCM-D approach to monitoring mammalian DNA damage using DNA adsorbed to a polyelectrolyte surface. *Biomacromolecules* **9**(1): 9–12.
Razumovitch J, de Franca K, Kehl F, Wiki M, Meier W, Vebert C. 2009. Optimal hybridization efficiency upon immobilization of oligonucleotide double helices. *J. Phys. Chem. B* **113**(24): 8383–8390.
Rechendorff K, Hovgaard MB, Foss M, Zhdanov VP, Besenbacher F. 2006. Enhancement of protein adsorption induced by surface roughness. *Langmuir* **22**(26): 10885–10888.
Reimhult E, Zach M, Hook F, Kasemo B. 2006. A multitechnique study of liposome adsorption on Au and lipid bilayer formation on SiO2. *Langmuir* **22**(7): 3313–3319.
Reimhult K, Petersson K, Krozer A. 2008. QCM-D analysis of the performance of blocking agents on gold and polystyrene surfaces. *Langmuir* **24**(16): 8695–8700.
Reipa V, Almeida J, Cole KD. 2006. Long-term monitoring of biofilm growth and disinfection using a quartz crystal microbalance and reflectance measurements. *J. Microbiol. Methods* **66**(3): 449–459.
Reisch A, Voegel JC, Gonthier E, Decher G, Senger B, Schaaf P, Mesini PJ. 2009. Polyelectrolyte multilayers capped with polyelectrolytes bearing phosphorylcholine and triethylene glycol groups: parameters influencing antifouling properties. *Langmuir* **25**(6): 3610–3617.
Rich RL, Myszka DG. 2006. Survey of the year 2005 commercial optical biosensor literature. *J. Mol. Recognit.* **19**(6): 478–534.
Rich RL, Myszka DG. 2007. Higher-throughput, label-free, real-time molecular interaction analysis. *Anal. Biochem.* **361**(1): 1–6.
Roach P, Shirtcliffe NJ, Farrar D, Perry CC. 2006. Quantification of surface-bound proteins by fluorometric assay: Comparison with quartz crystal microbalance and amido black assay. *J. Phys. Chem. B* **110**(41): 20572–20579.
Roach P, McHale G, Evans CR, Shirtcliffe NJ, Newton MI. 2007. Decoupling of the liquid response of a superhydrophobic quartz crystal microbalance. *Langmuir* **23**(19): 9823–9830.
Rodahl M, Hook F, Krozer A, Brzezinski P, Kasemo B. 1995. Quartz-crystal microbalance setup for frequency and Q-factor measurements in gaseous and liquid environments. *Rev. Sci. Instrum.* **66**(7): 3924–3930.
Rojas E, Gallego M, Reviakine I. 2008. Effect of sample heterogeneity on the interpretation of quartz crystal microbalance data: impurity effects. *Anal. Chem.* **80**(23): 8982–8990.
Sai VV, Mahajan S, Contractor AQ, Mukherji S. 2006. Immobilization of antibodies on polyaniline films and its application in a piezoelectric immunosensor. *Anal. Chem.* **78**(24): 8368–8373.
Sandberg T, Karlsson Ott M, Carlsson J, Feiler A, Caldwell KD. 2009a. Potential use of mucins as biomaterial coatings. II. Mucin coatings affect the conformation and neutrophil-activating properties of adsorbed host proteins: toward a mucosal mimic. *J. Biomed. Mater. Res. A.* **91**(3): 773–785.
Sandberg T, Carlsson J, Karlsson Ott M. 2009b. Interactions between human neutrophils and mucin-coated surfaces. *J. Mater. Sci. Mater. Med.* **20**(2): 621–631.
Sapper A, Janshoff A. 2006. Electrically induced deformation of giant liposomes monitored by thickness shear mode resonators. *Langmuir* **22**(26): 10869–10873.
Sapper A, Wegener J, Janshoff A. 2006. Cell motility probed by noise analysis of thickness shear mode resonators. *Anal. Chem.* **78**(14): 5184–5191.
Saraoglu HM, Edin B. 2007. E-nose system for anesthetic dose level detection using artificial neural network. *J. Med. Syst.* **31**(6): 475–482.
Saravia V, Toca-Herrera JL. 2009. Substrate influence on cell shape and cell mechanics: HepG2 cells spread on positively charged surfaces. *Microsc. Res. Tech.* **72**(12): 957–964.
Sartore L, Barbaglio M, Penco M, Bergese P, Bontempi E, Colombi P, Depero LE. 2009. Polymer-coated quartz crystal microbalance chemical sensor for heavy cations in water. *J. Nanosci. Nanotechnol.* **9**(2): 1164–1168.
Sasaki T, Noel TR, Ring SG. 2008. Study on alpha-amylase hydrolysis of potato amylopectin by a quartz crystal microbalance. *J. Agric. Food Chem.* **56**(3): 1091–1096.
Sato S, Ohtsuka K, Takenaka S. 2009. Immobilization of a naphthalene diimide-DNA complex on the gold through dithiolane moieties. *Nucleic. Acids Symp. Ser. (Oxf.)* **53**(3): 147–148.
Satomi T, Nagasaki Y, Kobayashi H, Tateishi T, Kataoka K, Otsuka H. 2007. Physicochemical characterization of densely packed poly(ethylene glycol) layer for minimizing nonspecific protein adsorption. *J. Nanosci. Nanotechnol.* **7**(7): 2394–2399.
Sauerbrey G. 1959. Verwendung von Schwingquarzen zur Wagung dunner Schichten und zur Microwagang. *Z. Phys.* **155**: 206–212.
Say R, Gultekin A, Ozcan AA, Denizli A, Ersoz A. 2009. Preparation of new molecularly imprinted quartz crystal microbalance hybride sensor system for 8-hydroxy-2'-deoxyguanosine determination. *Anal. Chim. Acta* **640**(1–2): 82–86.
Scheideler L, Rupp F, Wendel HP, Sathe S, Geis-Gerstorfer J. 2007. Photocoupling of fibronectin to titanium surfaces influences keratinocyte adhesion, pellicle formation and thrombogenicity. *Dent. Mater.* **23**(4): 469–478.
Schmidt V, Giacomelli C, Gounou C, Lai-Kee-Him J, Brisson AR, Borsali R. 2008. Formation of annexin-a5 protein/block copolymer micelle complexes: QCM-D and PAGE experiments. *Langmuir* **24**(21): 12189–12195.
Schmidt TF, Pavinatto FJ, Caseli L, Gonzaga ML, Soares SA, Ricardo NM, Oliveira ON Jr. 2009. Interaction of polysaccharide-protein complex from Agaricus blazei with Langmuir and Langmuir-Blodgett films of phospholipids. *J. Colloid Interface Sci.* **330**(1): 84–89.
Schofield WC, McGettrick JD, Badyal JP. 2006. A substrate-independent approach for cyclodextrin functionalized surfaces. *J. Phys. Chem. B* **110**(34): 17161–17166.
Schofield AL, Rudd TR, Martin DS, Fernig DG, Edwards C. 2007. Real-time monitoring of the development and stability of biofilms of Streptococcus mutans using the quartz crystal microbalance with dissipation monitoring. *Biosens. Bioelectron.* **23**(3): 407–413.
Seantier B, Kasemo B. 2009. Influence of mono- and divalent ions on the formation of supported phospholipid bilayers via vesicle adsorption. *Langmuir* **25**(10): 5767–5772.
Senaratne W, Takada K, Das R, Cohen J, Baird B, Abruna HD, Ober CK. 2006. Dinitrophenyl ligand substrates and their application to immunosensors. *Biosens. Bioelectron.* **22**(1): 63–70.
Serizawa T, Nagasaka Y, Matsuno H, Shimoyama M, Kurita K. 2007. A stereocomplex platform efficiently detecting antigen-antibody interactions. *Bioconjug. Chem.* **18**(2): 355–362.
Serra B, Gamella M, Reviejo AJ, Pingarron JM. 2008. Lectin-modified piezoelectric biosensors for bacteria recognition and quantification. *Anal. Bioanal. Chem.* **391**(5): 1853–1860.
Serro AP, Completo C, Colaço R, dos Santos F, da Silva CL, Cabral JMS, Araújo H, Pires E, Saramago B. 2009. A comparative study of titanium nitrides, TiN, TiNbN and TiCN, as coatings for biomedical applications. *Surface Coatings Technol.* **203**(24): 3701–3707.
Shen D, Kang Q, Li X, Cai H, Wang Y. 2007a. Different experimental results for the influence of immersion angle on the resonant frequency of a quartz crystal microbalance in a liquid phase: with a comment. *Anal. Chim. Acta* **593**(2): 188–195.
Shen G, Wang H, Shen G, Yu R. 2007b. Au nanoparticle network-type thin films formed via mixed assembling and cross-linking route for

biosensor application: quartz crystal microbalance study. *Anal. Biochem.* **365**(1): 1–6.

Shen Z, Huang M, Xiao C, Zhang Y, Zeng X, Wang PG. 2007c. Nonlabeled quartz crystal microbalance biosensor for bacterial detection using carbohydrate and lectin recognitions. *Anal. Chem.* **79**(6): 2312–2319.

Shen Z, Yan H, Parl FF, Mernaugh RL, Zeng X. 2007d. Recombinant antibody piezoimmunosensors for the detection of cytochrome P450 1B1. *Anal. Chem.* **79**(4): 1283–1289.

Shen D, Kang Q, Wang YE, Hu Q, Du J. 2008. New cut angle quartz crystal microbalance with low frequency-temperature coefficients in an aqueous phase. *Talanta* **76**(4): 803–808.

Sherman PJ, Jackway RJ, Gehman JD, Praporski S, McCubbin GA, Mechler A, Martin LL, Separovic F, Bowie JH. 2009. Solution structure and membrane interactions of the antimicrobial peptide fallaxidin 4.1a: an NMR and QCM study. *Biochemistry* **48**(50): 11892–11901.

Shinbo K, Otuki S, Kanbayashi Y, Ohdaira Y, Baba A, Kato K, Kaneko F, Miyadera N. 2009. A hybrid humidity sensor using optical waveguides on a quartz crystal microbalance. *Thin Solid Films* **518**(2): 629–633.

Shinmyouzu K, Takahashi T, Ariyoshi W, Ichimiya H, Kanzaki S, Nishihara T. 2007. Dermatan sulfate inhibits osteoclast formation by binding to receptor activator of NF-kappa B ligand. *Biochem. Biophys. Res. Commun.* **354**(2): 447–452.

Shu W, Laurenson S, Knowles TP, Ko Ferrigno P, Seshia AA. 2008. Highly specific label-free protein detection from lysed cells using internally referenced microcantilever sensors. *Biosens. Bioelectron.* **24**(2): 233–237.

Si P, Mortensen J, Komolov A, Denborg J, Moller PJ. 2007. Polymer coated quartz crystal microbalance sensors for detection of volatile organic compounds in gas mixtures. *Anal. Chim. Acta* **597**(2): 223–230.

Simonis D, Christ K, Alban S, Bendas G. 2007a. Affinity and kinetics of different heparins binding to P- and L-selectin. *Semin Thromb Hemost* **33**(5): 534–539.

Simonis D, Fritzsche J, Alban S, Bendas G. 2007b. Kinetic analysis of heparin and glucan sulfates binding to P-selectin and its impact on the general understanding of selectin inhibition. *Biochemistry* **46**(20): 6156–6164.

Soumetz FC, Pastorino L, Ruggiero C. 2008. Human osteoblast-like cells response to nanofunctionalized surfaces for tissue engineering. *J. Biomed. Mater. Res. B Appl. Biomater.* **84**(1): 249–255.

Soumetz FC, Pastorino L, Ruggiero C. 2009. Development of a piezoelectric immunosensor for matrix metalloproteinase-1 detection. *Conf. Proc. IEEE Eng. Med. Biol. Soc.* **2009**: 2775–2778.

Sprung C, Wahlisch D, Huttl R, Seidel J, Meyer A, Wolf G. 2009. Detection and monitoring of biofilm formation in water treatment systems by quartz crystal microbalance sensors. *Water Sci. Technol.* **59**(3): 543–548.

Stadler B, Chandrawati R, Goldie K, Caruso F. 2009. Capsosomes: subcompartmentalizing polyelectrolyte capsules using liposomes. *Langmuir* **25**(12): 6725–6732.

Stair JL, Watkinson M, Krause S. 2009. Sensor materials for the detection of proteases. *Biosens. Bioelectron.* **24**(7): 2113–2118.

Steinem C, Janshoff A. 2006. Piezoelectric Sensors. Springer-Verlag: Berlin Heidelberg.

Steinmetz NF, Bock E, Richter RP, Spatz JP, Lomonossoff GP, Evans DJ. 2008a. Assembly of multilayer arrays of viral nanoparticles via biospecific recognition: a quartz crystal microbalance with dissipation monitoring study. *Biomacromolecules* **9**(2): 456–462.

Steinmetz NF, Findlay KC, Noel TR, Parker R, Lomonossoff GP, Evans DJ. 2008b. Layer-by-layer assembly of viral nanoparticles and polyelectrolytes: the film architecture is different for spheres versus rods. *Chembiochem* **9**(10): 1662–1670.

Su X, Wu YJ, Robelek R, Knoll W. 2005. Surface plasmon resonance spectroscopy and quartz crystal microbalance study of streptavidin film structure effects on biotinylated DNA assembly and target DNA hybridization. *Langmuir* **21**(1): 348–353.

Su X, Lin CY, O'Shea SJ, Teh HF, Peh WY, Thomsen JS. 2006. Combinational application of surface plasmon resonance spectroscopy and quartz crystal microbalance for studying nuclear hormone receptor-response element interactions. *Anal. Chem.* **78**(15): 5552–5558.

Su WC, Zhang WG, Zhang S, Fan J, Yin X, Luo ML, Ng SC. 2009. A novel strategy for rapid real-time chiral discrimination of enantiomers using serum albumin functionalized QCM biosensor. *Biosens. Bioelectron.* **25**(2): 488–492.

Sultan Y, Walsh R, Monreal C, DeRosa MC. 2009. Preparation of functional aptamer films using layer-by-layer self-assembly. *Biomacromolecules* **10**(5): 1149–1154.

Sun H, Fung Y. 2006. Piezoelectric quartz crystal sensor for rapid analysis of pirimicarb residues using molecularly imprinted polymers as recognition elements. *Anal. Chim. Acta* **576**(1): 67–76.

Sun H, Zhang YY, Fung YS. 2006. Flow analysis coupled with PQC/DNA biosensor for assay of E-coli based on detecting DNA products from PCR amplification. *Biosens. Bioelectron.* **22**(4): 506–512.

Sun Y-L, Chen Y-Z, Wu R-J, Chavali M, Huang Y-C, Su P-G, Lin C-C. 2007. Poly(l-lactide) stabilized gold nanoparticles based QCM sensor for low humidity detection. *Sens. Actuators B Chem.* **126**(2): 441–446.

Sun P, Jiang Y, Xie G, Du X, Hu J. 2009. A room temperature supramolecular-based quartz crystal microbalance (QCM) methane gas sensor. *Sens. Actuators B Chem.* **141**(1): 104–108.

Sung JH, Ko HJ, Park TH. 2006. Piezoelectric biosensor using olfactory receptor protein expressed in Escherichia coli. *Biosens. Bioelectron.* **21**(10): 1981–1986.

Suzuki T, Zhang YW, Koyama T, Sasaki DY, Kurihara K. 2006. Direct observation of substrate-enzyme complexation by surface forces measurement. *J. Am. Chem. Soc.* **128**(47): 15209–15214.

Tai DF, Lin CY, Wu TZ, Huang JH, Shu PY. 2006. Artificial receptors in serologic tests for the early diagnosis of dengue virus infection. *Clin. Chem.* **52**(8): 1486–1491.

Takahashi S, Akita R, Furusawa H, Shimizu Y, Ueda T, Okahata Y. 2006. Kinetic analysis of ribosome binding process onto mRNA using a quartz-crystal microbalance. *Nucleic Acids Symp. Ser. (Oxf.) (50) (1):* 49–50.

Takahashi S, Furusawa H, Shimizu Y, Ueda T, Okahata Y. 2007a. Kinetic analysis of the effects of translation enhancers in translation initiation. *Nucleic Acids Symp. Ser. (Oxf.) (51) (1):* 45–46.

Takahashi S, Matsuno H, Furusawa H, Okahata Y. 2007b. Kinetic analyses of divalent cation-dependent EcoRV digestions on a DNA-immobilized quartz crystal microbalance. *Anal. Biochem.* **361**(2): 210–217.

Takahashi S, Matsuno H, Furusawa H, Okahata Y. 2008. Direct monitoring of allosteric recognition of type IIE restriction endonuclease EcoRII. *J. Biol. Chem.* **283**(22): 15023–15030.

Takahashi S, Iida M, Furusawa H, Shimizu Y, Ueda T, Okahata Y. 2009. Real-time monitoring of cell-free translation on a quartz-crystal microbalance. *J. Am. Chem. Soc.* **131**(26): 9326–9332.

Takakusagi Y, Takakusagi K, Kuramochi K, Kobayashi S, Sugawara F, Sakaguchi K. 2007. Identification of C10 biotinylated camptothecin (CPT-10-B) binding peptides using T7 phage display screen on a QCM device. *Bioorg. Med. Chem.* **15**(24): 7590–7598.

Takakusagi Y, Kuramochi K, Takagi M, Kusayanagi T, Manita D, Ozawa H, Iwakiri K, Takakusagi K, Miyano Y, Nakazaki A, Kobayashi S, Sugawara F, Sakaguchi K. 2008a. Efficient one-cycle affinity selection of binding proteins or peptides specific for a small-molecule using a T7 phage display pool. *Bioorg. Med. Chem.* **16**(22): 9837–9846.

Takakusagi Y, Kuroiwa Y, Sugawara F, Sakaguchi K. 2008b. Identification of a methotrexate-binding peptide from a T7 phage display screen using a QCM device. *Bioorg. Med. Chem.* **16**(15): 7410–7414.

Takatani M, Ito Y. 2006. Facile synthesis of oligosaccharide probes for the analysis of protein-carbohydrate interactions. *Chem. Asian J.* **1**(1–2): 64–75.

Takeda S, Ozaki H, Hattori S, Ishii A, Kida H, Mukasa K. 2007. Detection of influenza virus hemagglutinin with randomly immobilized anti-hemagglutinin antibody on a carbon nanotube sensor. *J. Nanosci. Nanotechnol.* **7**(3): 752–756.

Tam K, Kinsinger N, Ayala P, Qi F, Shi W, Myung NV. 2007. Real-time monitoring of Streptococcus mutans biofilm formation using a quartz crystal microbalance. *Caries Res.* **41**(6): 474–483.

Tamerler C, Duman M, Oren EE, Gungormus M, Xiong X, Kacar T, Parviz BA, Sarikaya M. 2006a. Materials specificity and directed assembly of a gold-binding peptide. *Small* **2**(11): 1372–1378.

Tamerler C, Oren EE, Duman M, Venkatasubramanian E, Sarikaya M. 2006b. Adsorption kinetics of an engineered gold binding peptide by surface plasmon resonance spectroscopy and a quartz crystal microbalance. *Langmuir* **22**(18): 7712–7718.

Tan L, Jia X, Jiang X, Zhang Y, Tang H, Yao S, Xie Q. 2009a. In vitro study on the individual and synergistic cytotoxicity of adriamycin and selenium nanoparticles against Bel7402 cells with a quartz crystal microbalance. *Biosens. Bioelectron.* **24**(7): 2268–2272.

Tan L, Xie Q, Jia X, Guo M, Zhang Y, Tang H, Yao S. 2009b. Dynamic measurement of the surface stress induced by the attachment and

growth of cells on Au electrode with a quartz crystal microbalance. *Biosens. Bioelectron.* **24**(6): 1603–1609.
Tang DQ, Zhang DJ, Tang DY, Ai H. 2006. Amplification of the antigen-antibody interaction from quartz crystal microbalance immunosensors via back-filling immobilization of nanogold on biorecognition surface. *J. Immunol. Methods* **316**(1–2): 144–152.
Tang D, Yuan R, Chai Y. 2008. Quartz crystal microbalance immunoassay for carcinoma antigen 125 based on gold nanowire-functionalized biomimetic interface. *Analyst* **133**(7): 933–938.
Tang Y, Wang Z, Xiao J, Yang S, Wang YJ, Tong P. 2009. Studies of phospholipid vesicle deposition/transformation on a polymer surface by dissipative quartz crystal microbalance and atomic force microscopy. *J. Phys. Chem. B* **113**(45): 14925–14933.
Tatami A, Hon YS, Matsuo I, Takatani M, Koshino H, Ito Y. 2007. Analyses of carbohydrate binding property of lectin-chaperone calreticulin. *Biochem. Biophys. Res. Commun.* **364**(2): 332–337.
Tebbe D, Thull R, Gbureck U. 2007. Influence of spacer length on heparin coupling efficiency and fibrinogen adsorption of modified titanium surfaces. *Biomed. Eng. Online* **6**: 31.
Tellechea E, Johannsmann D, Steinmetz NF, Richter RP, Reviakine I. 2009. Model-independent analysis of QCM data on colloidal particle adsorption. *Langmuir* **25**(9): 5177–5184.
Thid D, Benkoski JJ, Svedhem S, Kasemo B, Gold J. 2007. DHA-induced changes of supported lipid membrane morphology. *Langmuir* **23**(11): 5878–5881.
Thompson M, Hayward GL. 1997. Mass response of the thickness-shear mode acoustic wave sensor in liquids as a central misleading dogma. *Proceedings of the 1997 IEEE International Frequency Control Symposium*. 114–119.
Timofeyenko YG, Rosentreter JJ, Mayo S. 2007. Piezoelectric quartz crystal microbalance sensor for trace aqueous cyanide ion determination. *Anal. Chem.* **79**(1): 251–255.
Torres R, Garcia JV, Arnau A, Perrot H, Kim LT, Gabrielli C. 2008. Improved frequency/voltage converters for fast quartz crystal microbalance applications. *Rev. Sci. Instrum.* **79**(4): 045113.
Torres LA, Campos M, Martínez M, Rojas A. 2009. The thermochemistry of coronene revisited. *J. Chem. Thermodyn.* **41**(8): 957–965.
Trepout S, Mornet S, Benabdelhak H, Ducruix A, Brisson AR, Lambert O. 2007. Membrane protein selectively oriented on solid support and reconstituted into a lipid membrane. *Langmuir* **23**(5): 2647–2654.
Tsai H, Lin Y, Chang HW, Fuh CB. 2008. Integrating the QCM detection with magnetic separation for on-line analysis. *Biosens. Bioelectron.* **24**(3): 485–488.
Tseng MC, Chang YP, Chu YH. 2007. Quantitative measurements of vancomycin binding to self-assembled peptide monolayers on chips by quartz crystal microbalance. *Anal. Biochem.* **371**(1): 1–9.
Turner NW, Wright BE, Hlady V, Britt DW. 2007. Formation of protein molecular imprints within Langmuir monolayers: a quartz crystal microbalance study. *J. Colloid Interface Sci.* **308**(1): 71–80.
Turon X, Rojas OJ, Deinhammer RS. 2008. Enzymatic kinetics of cellulose hydrolysis: a QCM-D study. *Langmuir* **24**(8): 3880–3887.
Uludag Y, Li X, Coleman H, Efstathiou S, Cooper MA. 2008. Direct acoustic profiling of DNA hybridisation using HSV type 1 viral sequences. *Analyst* **133**(1): 52–57.
Umeyama M, Kira A, Nishimura K, Naito A. 2006. Interactions of bovine lactoferricin with acidic phospholipid bilayers and its antimicrobial activity as studied by solid-state NMR. *Biochim. Biophys. Acta* **1758**(9): 1523–1528.
Valiaev A, Abu-Lail NI, Lim DW, Chilkoti A, Zauscher S. 2007. Microcantilever sensing and actuation with end-grafted stimulus-responsive elastin-like polypeptides. *Langmuir* **23**(1): 339–344.
Vattanaviboon P, Sangseekhiow K, Winichagoon P, Promptmas C. 2008. Detection and haplotype differentiation of Southeast Asian alpha-thalassemia using polymerase chain reaction and a piezoelectric biosensor immobilized with a single oligonucleotide probe. *Transl. Res.* **151**(5): 246–254.
Vidal JC, Duato P, Bonel L, Castillo JR. 2009. Use of polyclonal antibodies to ochratoxin A with a quartz-crystal microbalance for developing real-time mycotoxin piezoelectric immunosensors. *Anal. Bioanal. Chem.* **394**(2): 575–582.
Viitala T, Hautala JT, Vuorinen J, Wiedmer SK. 2007. Structure of anionic phospholipid coatings on silica by dissipative quartz crystal microbalance. *Langmuir* **23**(2): 609–618.
Voinova MV, Jonson M, Kasemo B. 2002. 'Missing mass' effect in biosensor's QCM applications. *Biosens. Bioelectron.* **17**(10): 835–841.
Volden S, Zhu K, Nystrom B, Glomm WR. 2009. Use of cellulose derivatives on gold surfaces for reduced nonspecific adsorption of immunoglobulin G. *Colloids Surf. B Biointerfaces* **72**(2): 266–271.
Vu TH, Shimanouchi T, Ishii H, Umakoshi H, Kuboi R. 2009. Immobilization of intact liposomes on solid surfaces: a quartz crystal microbalance study. *J. Colloid Interface Sci.* **336**(2): 902–907.
Wang L, Gan XX. 2009. Biomolecule-functionalized magnetic nanoparticles for flow-through quartz crystal microbalance immunoassay of aflatoxin B1. *Bioprocess Biosyst. Eng.* **32**(1): 109–116.
Wang T, Muthuswamy J. 2008. Immunosensor for detection of inhibitory neurotransmitter gamma-aminobutyric acid using quartz crystal microbalance. *Anal. Chem.* **80**(22): 8576–8582.
Wang Z, Yang S. 2008. Adsorption behaviors of DPPC/MO aggregates on SiO2 surfaces. *Langmuir* **24**(20): 11616–11624.
Wang H, Zhang Y, Yan B, Liu L, Wang S, Shen G, Yu R. 2006a. Rapid, simple, and sensitive immunoagglutination assay with SiO2 particles and quartz crystal microbalance for quantifying Schistosoma japonicum antibodies. *Clin. Chem.* **52**(11): 2065–2071.
Wang W, Guo Z, Chen Y, Liu T, Jiang L. 2006b. Influence of generation 2–5 of PAMAM dendrimer on the inhibition of Tat peptide/TAR RNA binding in HIV-1 transcription. *Chem. Biol. Drug Des.* **68**(6): 314–318.
Wang X, Ho CT, Huang Q. 2007a. Investigation of adsorption behavior of (-)-epigallocatechin gallate on bovine serum albumin surface using quartz crystal microbalance with dissipation monitoring. *J. Agric. Food Chem.* **55**(13): 4987–4992.
Wang X, Ruengruglikit C, Wang YW, Huang Q. 2007b. Interfacial interactions of pectin with bovine serum albumin studied by quartz crystal microbalance with dissipation monitoring: effect of ionic strength. *J. Agric. Food Chem.* **55**(25): 10425–10431.
Wang G, Rodahl M, Edvardsson M, Svedhem S, Ohlsson G, Hook F, Kasemo B. 2008a. A combined reflectometry and quartz crystal microbalance with dissipation setup for surface interaction studies. *Rev. Sci. Instrum.* **79**(7): 075107.
Wang LJ, Wu CS, Hu ZY, Zhang YF, Li R, Wang P. 2008b. Sensing Escherichia coli O157:H7 via frequency shift through a self-assembled monolayer based QCM immunosensor. *J. Zhejiang Univ. Sci. B* **9**(2): 121–131.
Wang ZW, Zhao YP, Zhou CR, Liao GW. 2009. [Role of enamel matrix proteins in inducing biomimetic mineralization of the enamel: a study with quartz crystal microbalance technique]. *Nan Fang Yi Ke Da Xue Xue Bao* **29**(5): 966–969.
Washio A, Kitamura C, Jimi E, Terashita M, Nishihara T. 2009. Mechanisms involved in suppression of NGF-induced neuronal differentiation of PC12 cells by hyaluronic acid. *Exp. Cell Res.* **315**(17): 3036–3043.
Watanabe J, Shen H, Akashi M. 2008. Polyelectrolyte droplets facilitate versatile layer-by-layer coating for protein loading interface. *Acta Biomater.* **4**(5): 1255–1262.
Weber N, Pesnell A, Bolikal D, Zeltinger J, Kohn J. 2007. Viscoelastic properties of fibrinogen adsorbed to the surface of biomaterials used in blood-contacting medical devices. *Langmuir* **23**(6): 3298–3304.
Wei XL, Mo ZH, Li B, Wei JM. 2007. Disruption of HepG2 cell adhesion by gold nanoparticle and Paclitaxel disclosed by in situ QCM measurement. *Colloids Surf. B Biointerfaces* **59**(1): 100–104.
Wen Y, Shan G, Pu J, Liu Z. 2009. [Research on piezoelectric protein sensor array for rapid detecting HIV(1+2) antibody]. *Sheng Wu Yi Xue Gong Cheng Xue Za Zhi* **26**(4): 883–885.
Weng KC, Kanter JL, Robinson WH, Frank CW. 2006. Fluid supported lipid bilayers containing monosialoganglioside GM1: a QCM-D and FRAP study. *Colloids Surf. B Biointerfaces* **50**(1): 76–84.
Wikstrom A, Svedhem S, Sivignon M, Kasemo B. 2008. Real-time QCM-D monitoring of electrostatically driven lipid transfer between two lipid bilayer membranes. *J. Phys. Chem. B* **112**(44): 14069–14074.
Wingqvist G, Anderson H, Lennartsson C, Weissbach T, Yantchev V, Spetz AL. 2009. On the applicability of high frequency acoustic shear mode biosensing in view of thickness limitations set by the film resonance. *Biosens. Bioelectron.* **24**(11): 3387–3390.
Wu AH, Syu MJ. 2006. Synthesis of bilirubin imprinted polymer thin film for the continuous detection of bilirubin in an MIP/QCM/FIA system. *Biosens. Bioelectron.* **21**(12): 2345–2353.
Wu Z, Wu J, Wang S, Shen G, Yu R. 2006. An amplified mass piezoelectric immunosensor for Schistosoma japonicum. *Biosens. Bioelectron.* **22**(2): 207–212.
Wu VC, Chen SH, Lin CS. 2007. Real-time detection of Escherichia coli O157:H7 sequences using a circulating-flow system of quartz crystal microbalance. *Biosens. Bioelectron.* **22**(12): 2967–2975.

Xing Q, Eadula SR, Lvov YM. 2007. Cellulose fiber-enzyme composites fabricated through layer-by-layer nanoassembly. *Biomacromolecules* **8**(6): 1987–1991.
Xu C, Ng SC, Chan HS. 2008. Self-assembly of perfunctionalized beta-cyclodextrins on a quartz crystal microbalance for real-time chiral recognition. *Langmuir* **24**(16): 9118–9124.
Xu X, Cang H, Li C, Zhao ZK, Li H. 2009. Quartz crystal microbalance sensor array for the detection of volatile organic compounds. *Talanta* **78**(3): 711–716.
Yamamoto Y, Taga K, Yoshida T, Kamaya H, Ueda I. 2006. Action mechanism of water soluble ethanol on phospholipid monolayers using a quartz crystal oscillator. *J. Colloid Interface Sci.* **298**(2): 529–534.
Yamamoto T, Yano M, Xu X, Uchinoumi H, Tateishi H, Mochizuki M, Oda T, Kobayashi S, Ikemoto N, Matsuzaki M. 2008. Identification of target domains of the cardiac ryanodine receptor to correct channel disorder in failing hearts. *Circulation* **117**(6): 762–772.
Yamasaki R, Ito M, Lee B, Jung H, Lee H, Kawai T. 2007. Single probe nucleic acid immobilization on chemically modified single protein by controlling ionic strength and pH. *Anal. Chim. Acta* **603**(1): 76–81.
Yamashita K, Yamada M, Numata K, Taguchi S. 2006. Nonspecific hydrophobic interactions of a repressor protein, PhaR, with poly [(R)-3-hydroxybutyrate] film studied with a quartz crystal microbalance. *Biomacromolecules* **7**(8): 2449–2454.
Yan Y, Zhou X, Ji J, Yan L, Zhang G. 2006. Adsorption of polymeric micelles and vesicles on a surface investigated by quartz crystal microbalance. *J. Phys. Chem. B* **110**(42): 21055–21059.
Yan S, Fang Y, Gao Z. 2007. Quartz crystal microbalance for the determination of daminozide using molecularly imprinted polymers as recognition element. *Biosens. Bioelectron.* **22**(6): 1087–1091.
Yang Z-P, Zhang C-J. 2009. Designing of MIP-based QCM sensor for the determination of Cu(II) ions in solution. *Sens. Actuators B Chem.* **142**(1): 210–215.
Yang DH, Ju MJ, Maeda A, Hayashi K, Toko K, Lee SW, Kunitake T. 2006a. Design of highly efficient receptor sites by combination of cyclodextrin units and molecular cavity in TiO2 ultrathin layer. *Biosens. Bioelectron.* **22**(3): 388–392.
Yang LM, Tam PY, Murray BJ, McIntire TM, Overstreet CM, Weiss GA, Penner RM. 2006b. Virus electrodes for universal biodetection. *Anal. Chem.* **78**(10): 3265–3270.
Yang Z, Si S, Zeng X, Zhang C, Dai H. 2007. Mechanism and kinetics of apatite formation on nanocrystalline TiO(2) coatings: a quartz crystal microbalance study. *Acta Biomater.* **5**(2): 191–197.
Yang AY, Rawle RJ, Selassie CR, Johal MS. 2008a. A quartz crystal microbalance study of polycation-supported single and double stranded DNA surfaces. *Biomacromolecules* **9**(12): 3416–3421.
Yang LM, Diaz JE, McIntire TM, Weiss GA, Penner RM. 2008b. Covalent virus layer for mass-based biosensing. *Anal. Chem.* **80**(4): 933–943.
Yang Y, Long Y, Li Z, Li N, Li K, Liu F. 2009a. Real-time molecular recognition between protein and photosensitizer of photodynamic therapy by quartz crystal microbalance sensor. *Anal. Biochem.* **392**(1): 22–27.
Yang Y, Zhu Y, Chen Q, Liu Y, Zeng Y, Xu F. 2009b. Carbon-nanotube-activated Pt quartz-crystal microbalance for the immunoassay of human IgG. *Small* **5**(3): 351–355.
Yao C, Zhu T, Tang J, Wu R, Chen Q, Chen M, Zhang B, Huang J, Fu W. 2008a. Hybridization assay of hepatitis B virus by QCM peptide nucleic acid biosensor. *Biosens. Bioelectron.* **23**(6): 879–885.
Yao C, Qi Y, Zhao Y, Xiang Y, Chen Q, Fu W. 2009a. Aptamer-based piezoelectric quartz crystal microbalance biosensor array for the quantification of IgE. *Biosens. Bioelectron.* **24**(8): 2499–2503.
Yao W, Gao Z, Cheng Y. 2009b. Quartz crystal microbalance for the detection of carbaryl using molecularly imprinted polymers as recognition element. *J. Sep. Sci.* **32**(19): 3334–3339.
Ye M, Zhang Y, Li H, Tan P, Tang H, Yao S. 2009. A novel method for the detection of point mutation in DNA using single-base-coded CdS nanoprobes. *Biosens. Bioelectron.* **24**(8): 2339–2345.
Yin J, Wei W, Liu X, Kong B, Wu L, Gong S. 2007. Immobilization of bovine serum albumin as a sensitive biosensor for the detection of trace lead ion in solution by piezoelectric quartz crystal impedance. *Anal. Biochem.* **360**(1): 99–104.
York RL, Holinga GJ, Somorjai GA. 2009. An investigation of the influence of chain length on the interfacial ordering of L-lysine and L-proline and their homopeptides at hydrophobic and hydrophilic interfaces studied by sum frequency generation and quartz crystal microbalance. *Langmuir* **25**(16): 9369–9374.
Yoshimoto M, Tokimura S, Kurosawa S. 2006. Characteristics of the series resonant-frequency shift of a quartz crystal microbalance in electrolyte solutions. *Analyst* **131**(10): 1175–1182.
Yoshimoto M, Maruyama Y, Kurosawa S, Kanazawa KK. 2007. Dependence on the electric power of the immersion-angle dependence of the resonant-frequency shift of a quartz crystal microbalance in a liquid. *Anal. Chim. Acta* **589**(1): 39–43.
Yoshinari M, Kato T, Matsuzaka K, Hayakawa T, Inoue T, Oda Y, Okuda K, Shimono M. 2006. Adsorption behavior of antimicrobial peptide histatin 5 on PMMA. *J. Biomed. Mater. Res. B Appl. Biomater.* **77**(1): 47–54.
Yu GY, Janata J. 2008. Proximity effect in quartz crystal microbalance. *Anal. Chem.* **80**(8): 2751–2755.
Yu JS, Liao HX, Gerdon AE, Huffman B, Scearce RM, McAdams M, Alam SM, Popernack PM, Sullivan NJ, Wright D, Cliffel DE, Nabel GJ, Haynes BF. 2006. Detection of Ebola virus envelope using monoclonal and polyclonal antibodies in ELISA, surface plasmon resonance and a quartz crystal microbalance immunosensor. *J. Virol. Methods* **137**(2): 219–228.
Yuan B, Pham M, Nguyen TH. 2008. Deposition kinetics of bacteriophage MS2 on a silica surface coated with natural organic matter in a radial stagnation point flow cell. *Environ. Sci. Technol.* **42**(20): 7628–7633.
Zhang Y, Luo S, Tang Y, Yu L, Hou KY, Cheng JP, Zeng X, Wang PG. 2006. Carbohydrate-protein interactions by 'clicked carbohydrate self-assembled monolayers'. *Anal. Chem.* **78**(6): 2001–2008.
Zhang B, Zhang X, Yan HH, Xu SJ, Tang DH, Fu WL. 2007a. A novel multi-array immunoassay device for tumor markers based on insert-plug model of piezoelectric immunosensor. *Biosens. Bioelectron.* **23**(1): 19–25.
Zhang H, Marma MS, Bahl SK, Eun Sok K, McKenna CE. 2007b. Sequence Specific Label-Free DNA Sensing Using Film-Bulk-Acoustic-Resonators. *Sensors J. IEEE* **7**(12): 1587–1588.
Zhang Q, Huang Y, Zhao R, Liu G, Chen Y. 2008a. Determining binding sites of drugs on human serum albumin using FIA-QCM. *Biosens. Bioelectron.* **24**(1): 48–54.
Zhang Q, Huang Y, Zhao R, Liu G, Chen Y. 2008b. In situ growth of nanogold on quartz crystal microbalance and its application in the interaction between heparin and antithrombin III. *J. Colloid Interface Sci.* **319**(1): 94–99.
Zhang Y, Du B, Chen X, Ma H. 2009. Convergence of dissipation and impedance analysis of quartz crystal microbalance studies. *Anal. Chem.* **81**(2): 642–648.
Zhao Y, He J, Yang M, Gao S, Zuo G, Yan C, Cheng Z. 2009a. Single crystal WO(3) nanoflakes as quartz crystal microbalance sensing layer for ultrafast detection of trace sarin simulant. *Anal. Chim. Acta* **654**(2): 120–126.
Zhao ZX, Wang HC, Qin X, Wang XS, Qiao MQ, Anzai J, Chen Q. 2009b. Self-assembled film of hydrophobins on gold surfaces and its application to electrochemical biosensing. *Colloids Surf. B Biointerfaces* **71**(1): 102–106.
Zhu DM, Fang J, Wu B, Du X. 2008. Viscoelastic response and profile of adsorbed molecules probed by quartz crystal microbalance. *Phys. Rev. E Stat. Nonlin. Soft Matter Phys.* **77**(3, Pt 1): 031605.
Zhu P, Long G, Ni J, Tong M. 2009. Deposition kinetics of extracellular polymeric substances (EPS) on silica in monovalent and divalent salts. *Environ. Sci. Technol.* **43**(15): 5699–5704.
Zhuang H, Lu P, Lim SP, Lee HP. 2007. Frequency response of a quartz crystal microbalance loaded by liquid drops. *Langmuir* **23**(13): 7392–7397.
Zhuang H, Lu P, Lim SP, Lee HP. 2008. Effects of interface slip and viscoelasticity on the dynamic response of droplet quartz crystal microbalances. *Anal. Chem.* **80**(19): 7347–7353.
Ziya Ozturk Z, Tasaltin C, Engin GO, Gurek AG, Atilla D, Ahsen V, Ince M. 2009. Evaluation of a fast wastewater odour characterisation procedure using a chemical sensor array. *Environ. Monit. Assess.* **151**(1–4): 369–375.
Zong Y, Xu F, Su X, Knoll W. 2008. Quartz crystal microbalance with integrated surface plasmon grating coupler. *Anal. Chem.* **80**(13): 5246–5250.

